Tissue-Engineered Skeletal Muscle Stimulator

Biomedical Engineering Major Qualifying Project

Syed Asaad Hussain, Spencer Ryan Keilich, Shreyas Renganathan, and Stephanie Jo Lindow

4/22/2015

Abstract

This project set out to mechanically stimulate *in vitro* skeletal muscle tissue to produce more accurate models of *in vivo* tissue for use in studying human muscular diseases. Active and passive contractions play a key role in the *in vivo* development of skeletal muscle. A device was produced in which tissue was cultured in fibrin gel to grow dogbone-shaped tissue around sets of posts in the device. The device is able to: statically or cyclically strain the tissue, control the amount of strain from -50% to +50%, allow for stimulation of up to 96 samples, and minimize the construct size of the tissues. Mechanical stimulation by the device led to greater myofiber alignment, higher fiber density, and overall a closer resemblance to *in vivo* tissue.

Executive Summary

Introduction

Clinical Significance

Significant research has been done to find treatments for muscular degenerative diseases such as muscular dystrophy and multiple sclerosis. New drugs are required to go through several approval phases before they can be tested on live animals or humans, and the approval process can be tedious and costly [1]. Even if the new drugs pass the approval process, most fail due to lack of homology between animal muscle models and human muscle. There is a need for a technology platform that can bridge researchers' need for, high throughput testing with an accurate muscle tissue model that utilizes human cells to recapitulate human tissue response. This also eliminates the time-consuming approval process necessary for animal testing.

In Vitro Mechanical Stimulation

Myoblasts fuse and align into multinucleated myotubes as the cell membranes between adjoining cells dissolve, as shown in Figure 8 [2]. During later *in vivo* development of muscle, following neonatal myogenesis, mechanical loading is responsible for many key aspects of mature muscle functionality, including increased number, diameter, length, and parallel alignment of muscle fibers, as well as regulation of cellular protein synthesis, protein localization, and insulin sensitivity [3].

The generation of mature, *in vitro* skeletal muscle seeks to mimic the mechanical stimuli found *in vivo* to direct native-like myogenesis, cell metabolism, fiber orientation, and muscle morphology by benchtop mechanical stimulation [4]. Several studies have been performed, showing that different mechanical stimulation regimens induce various alterations for *in vitro* skeletal muscle. Higher rates of muscle stimulation lead to more growth in these cultured tissues [5].
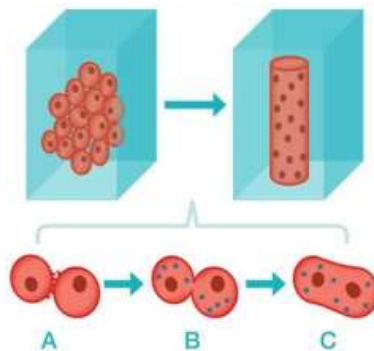

Figure 1: Cell fusion is a key characteristic of skeletal tissue, and myogenic cell fusion requires specific growth factors and an external load to dictate fiber alignment [6].

Design

Design Components

The final design consists of three major components:top and bottom plates, posts and wells, and a syringe pump system. Each well of the moveable top plate contains a post, with another, fixed, post extending upwards through a slot from the bottom plate, as shown in Figure 54. The material choosen was MED610 plastic, which is biocompatible.

Figure 2: 3D printed prototype of top and bottom plates is shown on left, close-up of wells and posts is shown on right.

The formed tissue wraps around each pair of posts. This system allows for optimal control of mechanical strain in the device. Between the syringes and the tubing, the enclosed system has a constant volume; thus as the plunger of the outside syringe is actuated by the syringe pump, the volume change in the outside syringe is the same as inside syringe. Based on the geometry of the inside syringe, the amount the plunger actuates is directly proportional to its volume change. Therefore, by controlling the fluid volume infused or withdrawn, the system directly controls the amount of strain delivered to the tissue.

Tissue Final Design

Tissue culture within the device uses a "cell-in-gel" technique, where myoblasts are seeded within a fibrin gel suspension, via a simple gelation process between fibrinogen and thrombin. NIPAAm was added first to the wells. Once the tissue-gel construct forms on the solid NIPAAm surface, the NIPAAm is removed by cooling the device, and then aspirating the now-liquid NIPAAm. The tissue construct is then suspended between the two posts, facilitating tissue organization solely around those two anchorage points. Such anchorage mimics myotendinous attachment to bone, which is critical in myogenesis. This suspension of the tissue construct also facilitates mechanical stimulation of the suspended tissue. The tissue culture process in the device is shown in Figure 3.
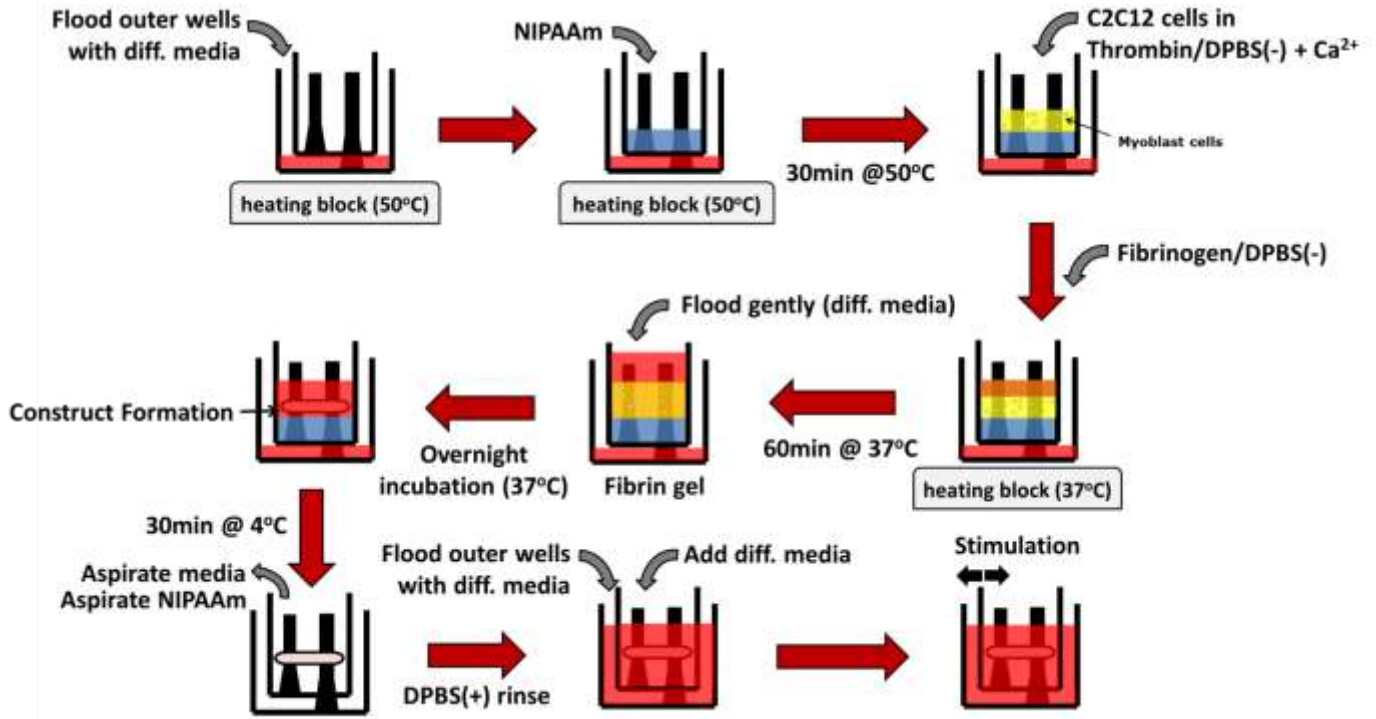
Figure 3: Flow diagram of thrombin/fibrinogen cellular seeding method

Results

Mechanical Testing

To verify the strain by volume change achieved by the device, the syringe was infused and withdrawn at several volume increments and the resultant strain was recorded.
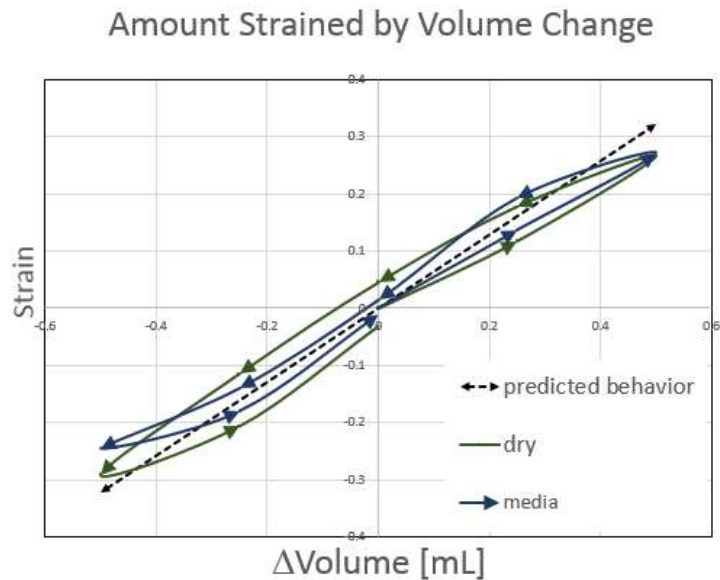

Figure 4: Strain resulting from volume change

Cellular Seeding

Mechanical strain tests were performed, exercising the tissue from 5-10% strain at 1 cycle/minute for 15 minutes a day, starting on day 4 after tissue formation and continuing to day 8.
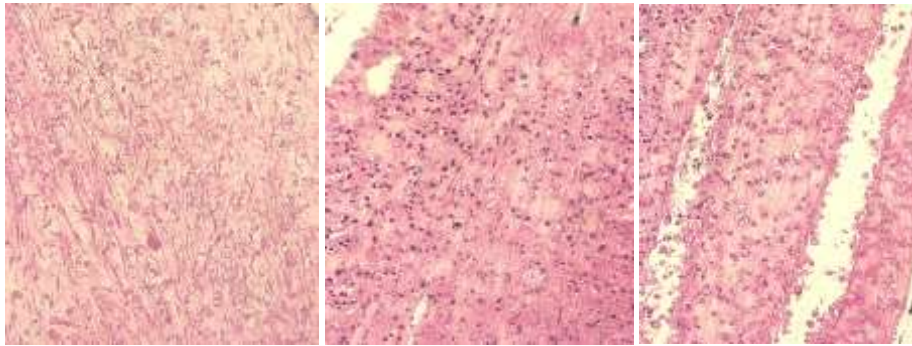

Figure 5: Histology of control tissue (left), and stimulated tissues (middle and right). Images shown at 200X magnification.

Discussion

Mechanical Testing: Analysis of Results

The final device was capable of operation within incubator conditions, and was reusable after sterilization between experiments. As shown in Figure 4, the device is capable of uniaxial positive and negative strain, matching both the recommended literature values of -5 to 15% strain and the user/client request for +/- 50% strain. Strain rates produced by the device are predictable, with the highest percent error being ~17% at maximum strain of 50%. However, between -5 and 15% strain the maximum error is 8%, indicating that the device will be accurate within the range that literature values indicate is best for forming muscle tissue.

Cellular Seeding: Analysis of Results

Histology results showed that mechanical stimulation using the device improved key muscle parameters, as seen in **Error! Reference source not found.** Lengthwise cross sections were made of stimulated and control tissues, and these were stained with hematoxylin and eosin. Compared to the controls, the stimulated tissues had greater fiber alignment, increased fiber length, and increased fiber density.

Future Recommendations

The final design accomplished many of the objectives set out originally for the project; however, not all objectives were covered due to time and financial constraints. Therefore, the team recommends the following for future work: seeding a cell co-culture for tissue growth with endogenous extracellular matrix, incorporating electrical stimulation to recapitulate muscle innervation, replacing the MED610 material, and using PDMS posts to enable force deflection measurements of muscle contractile force.

Acknowledgment

References

[1] T.M. St. John. (2013). *Degenerative Muscle Disease Symptoms* [Online]. Available:http://www.livestrong.com/article/117083-degenerative-muscle-disease-symptoms/

[2] M. Buckingham et al, "The formation of skeletal muscle: From somite ot limb," *Journal of Anatomy,* vol. 202, no. 1, pp. 59-68, 2003.

[3] S.F. Gilbert, "Myogenesis: The development of muscle," *Developmental Biology,* vol. 6, no. 1, 2000.

[4]   C. Powell, "Mechanical stimulation improves tissue-engineered human skeletal muscle," *American Journal of Physiology-Cell Physiology,* vol. 283, no. 1, pp. 1557-1565, 2002.

[5]   H.H. Vandenburgh, "Mechanically induced alterations in cutured skeletal muscle growth," *Journal of Biomechanics,* vol.24, no.1, pp. 91-99, 1991.

[6]   R. Brock, "NIH study uncovers details of early stages in muscle formation and regeneration," *Institute of Neurological Disordersand Stroke,* 2014.

Authorship

Chapter	Author(s)	Editor(s)
Chapter 1: Introduction	Everyone	Everyone
Chapter 2: Literature Review		
2.1 Clinical Significance	Spencer	Everyone
2.2 Disease	Spencer	Everyone
2.3 Injuries	Spencer	Everyone
2.4 Tissue Regeneration and Reconstruction	Spencer	Everyone
2.5 Need for an Enabling Tool	Spencer	Everyone
2.6 Muscle and Myoblast Physiology	Spencer	Everyone
2.7 In vitro Muscle Generation	Shreyas	Everyone
2.8 In vitro Mechanical and Electrical Stimulation	Asaad	Everyone
2.9 Tests for Myocyte Culture	Stephanie	Everyone
2.10 Existing Patents	Stephanie	Everyone
2.11 Mechanical and Electrical Design	Stephanie	Everyone
2.12 Limitations	Stephanie and Shreyas	Everyone
Chapter 3: Methodology:		
3.1 Initial Client Statement	Raymond Page	
3.2 Objectives and Constraints	Stephanie and Spencer	Everyone
3.3 Revised Client Statement	Asaad	Everyone
3.4 Project Approach	Stephanie and Shreyas	Everyone
Chapter 4: Alternative Designs		
4.1 Needs Analysis	Stephanie	Everyone
4.2 Functions and Means	Stephanie	Everyone
4.3 Conceptual Designs	Asaad	Everyone
4.4 Preliminary/Alternative Designs	Asaad and Spencer	Everyone
4.5 Tissue Formation Techniques	Spencer	Everyone
4.6 Comparison of Alternative Designs	Stephanie	Everyone
4.7 Experimental/Design Validation	Spencer and Shreyas	Everyone
4.8 Modeling of Alternative Designs	Asaad and Shreyas	Everyone
Chapter 5: Final Design		
5.1 Overall Design and Major Components	Asaad	Everyone
5.2 Posts and Slits	Stephanie	Everyone
5.3 Top and Bottom Sliding Plates	Asaad	Everyone
5.4 Syringe Pump System	Stephanie	Everyone
5.5 Tissue Final Design	Shreyas	Everyone
5.6 Device Operation (Flow Diagram)	Shreyas	Everyone
5.7 Limitations	Spencer	Everyone
Chapter 6: Device Verification Testing (DVT)		
6.1 Cytotoxicity Test	Spencer and Shreyas	Everyone
6.2 "Cell-in-gel" Seeding	Shreyas	Everyone
6.3 Mechanical Analysis	Asaad	Everyone

6.4 Stimulated Tissue Results	Spencer	Everyone
Chapter 7: Discussion of Results		
7.1 Mechanical Testing: Analysis of Results	Stephanie	Everyone
7.2 Cellular Seeding : Analysis of Results	Shreyas	Everyone
Chapter 8: Project Impact		
8.1 Benchmarks and Standards	Spencer	Everyone
8.2 Limitations in Data	Spencer	Everyone
8.3 Economics	Spencer	Everyone
8.4 Environmental Impact	Spencer	Everyone
8.5 Societal Influence	Spencer	Everyone
8.6 Ethical Concern	Spencer	Everyone
8.7 Manufacturability	Asaad and Steph	Everyone
8.8 Sustainability, Health and Safety Issues	Shreyas	Everyone
Chapter 9: Conclusions and Recommendations		
9.1 Conclusion	Shreyas	Everyone
9.2 Recommendations	Asaad	Everyone
References	Everyone	Everyone
Appendices	Everyone	Everyone

Table of Contents

Table of Figures

Table of Tables

Chapter 1: Introduction

Human skeletal muscle tissue has the ability to self-regenerate following small injuries; however, it is unable to functionally restore loss from congenital/systemic defects, myopathies, or large traumatic injuries (Ahadian, 2012) (Bach et al, 2007). Examples of degenerative skeletal muscle diseases include Muscular Dystrophy (MD) and Multiple Sclerosis (MS). Muscular Dystrophy affects 32,000 people between ages 5-24 annually in the United States, while Multiple Sclerosis affects 2.3 million people worldwide (Center for Disease Control and Prevention, 2014) (Campellone, 2014). Care for patients with these diseases is expensive, as the average cost of an MD patient is estimated at $4,600 annually (Center for Disease Control and Prevention, 2014). Currently no cure or effective treatments for MD exist, therefore tissue engineering, the mimicry of organogenesis in vitro, has recently emerged as a novel approach to engineer skeletal muscle tissue for in vitro applications (Rossi et al, 2010). Engineered skeletal muscle tissue (ESMT) also has numerous in vitro applications— as analogous models for drug screening and diagnostic testing (Vandenburgh, 2009), or as engineered biological actuators for microelectromechanical devices (Fujita et al, 2011).

Though mechanically-stimulated tissue constructs have been found to be more developed than non- stimulated constructs, they still remain morphologically dissimilar to the adult skeletal muscle found functional in vivo. The primary challenge of ESMT in vitro is to induce the differentiation of cultured cells into mature skeletal muscle – with morphology and functionality including contractile force production resembling in vivo tissue. The application of directed mechanical strain and electrical stimulation on engineering skeletal muscle tissue has been shown to promote maturation (native levels) that more closely resembles mature tissue (Bach et al, 2004).

In addition to creating tissue sub-native levels of skeletal muscle found in vivo, current mechanical stimulation methods for ESMTs are ineffective and inefficient. High-throughput testing is

limited because current testing methods only capable of producing 3-10 tissue samples at a time

(Vandenburgh et al, 1991). Current stimulation devices are not incubator compatible, which means

constructs are tested outside of in vivo conditions. Myofiber diameter and density are less in current

mechanically-stimulated ESMTs than in native skeletal muscle tissue (Collinsworth et al, 2000). Electrical

stimulation is typically applied to promote active contraction which helps in fiber alignment and fiber

density (Powell et al, 2002). Electrical Stimulation uses a pair of biologically inert electrodes inserted into

the culture with active current. This allows the observer to view muscle contraction and measure the

force of the pull. However, this method results in pH and temperature changes, culture contamination

from corrosion by-products, and surface fouling at electrodes (Ahadian et al, 2012).

This project's device is meant to improve the rate and quantity at which these tissue cultures

can be matured through mediated mechanical and electrical stimulation. Initial prototypes of such

mechanical stimulation devices have been developed by previous MQPs, but their prototypes were not

sufficiently tested. Therefore, the design task is to develop an efficient technology platform for growth

and stimulation of skeletal muscle tissue functional units in vitro. The proposed device will encompass

an ESMT incorporated into a device that mechanically and/or electrically stimulates ESMTs to more

precisely mimic in vivo myogenesis and generate a more clinically-relevant model of skeletal muscle in

vitro.

The overall aim of this project is to develop and test an *in vitro* technology platform that enables

high-throughput generation of ESMT constructs with functional and morphological properties that more

closely mimic native skeletal muscle tissue than current models. The specific goals of this project are as

follows: firstly, to optimize the myogenic tissue culture process to create an environment that accurately

simulates in vivo 3D anchorage and growth conditions; secondly, to maximize the efficiency of

generating and testing ESMTs by determining parameters required for generating a minimal functional

unit for optimum tissue size for skeletal muscle tissue formation, and then develop a high-throughput process to create this optimum tissue; and thirdly, to mechanically and electrically stimulate ESMTs to maximize *in vitro* maturation, resulting in ESMT more closely to that of native muscle function and structure, which will bridge the gap in skeletal muscle in vitro research.

The device will be considered successful if it meets the specific projects goals listed above by i) enabling processing and testing of more than 24 constructs at one time; ii) tissue exhibiting maturity closer to native muscle, versus current ESMTs created in the Page Lab; iii) all stimulation can be conducted without affecting growth conditions. Chapter 2 further explores the clinical significance of this work, the background on muscle and myoblast physiology, and muscle regeneration. The following chapter also details the current process for making ESMT's, including the limitations and potential efficiency improvements. The literature review will also review previous work in order to analyze their strengths and weaknesses.

Chapter 2: Literature Review

The following chapter outlines the aspects of background research relevant to the project. The clinical need underlying our problem statement was analyzed, along with aspects of skeletal muscle development in vivo that in vitro tissue culture seeks to recapitulate. The importance of mechanical stimulation to improve the resemblance of in vitro muscle to mature in vivo tissue is discussed, and existing systems that mechanically a stimulate in vitro muscle tissue are presented. Finally, validation tests for cell viability and intracellular organization are discussed, as well as limitations in generating in vitro muscle tissue.

2.1 Clinical Significance

Muscular degenerative diseases such as muscular dystrophy (MD) and multiple sclerosis (MS) cause progressive and rapid muscle degeneration, with early death and severe debilitation being common outcomes (Eagle et al, 2002). There is significant research being done to find treatments for these diseases. The approval process can be tedious and costly. Drugs developed for treatment are required to go through several regulatory approval phases, including live animal testing, before they can finally be tested on humans. The preferred drug screening method continues to be the in vivo murine model. Though muscle pathologies can be recreated to some extent in a mouse model, the disease phenotype is substantially different than in humans. Key differences in genetics and molecular mechanisms compared to human tissue limit the accuracy of the mouse as a model of human myopathy (Vandenburgh et al, 2008). Consequently, many drugs that appear to successfully treat disease in the murine model have minimal long-term benefits or adverse using side effects in humans (Vandenburgh et al, 2009).There is a need for a technology platform that can bridge the need for rapid drug development and approval with the need for a model of human disease that accurately recapitulates *in vivo* drug efficacy in humans.

2.2 Disease

There are several degenerative diseases affecting the muscles that do not have cures, specifically muscular dystrophy, muscular sclerosis, and amyotrophic lateral sclerosis that cause progressive loss and weakening of muscle tissue (St. John, 2013) (Campellone, 2014) (Amyotrophic Lateral Sclerosis, 2013). The current treatments of these diseases are to make the patient more comfortable by improving quality of life (St. John, 2013).

2.2.1 Muscular Dystrophy

Muscular dystrophy (MD) is a category of inherited genetic disorders that cause progressive muscle impairment and weakening ultimately causing fatal respiratory failure (Eagle et al, 2002). Duchenne muscular dystrophy causes progressive and relentless skeletal muscle wasting, and patients rarely survive even to age 20 years of age. Cardiomyopathy is the ultimate cause for death for about 10% of affected males, though cardiac arrhythmia and other abnormalities are common to all patients (Eagle et al, 2002). At present, no treatment is available to prevent or arrest the progressive muscle degeneration. Depending on the type of MD, symptoms can appear in childhood or adulthood (Emery et al, 1994). The most common symptoms of MD are delayed development of motor skills, eyelid drooping, frequent falls or loss of balance, problems walking, diminishing muscle mass, and loss of strength (Campellone, 2014).

Current diagnostic exams can identify the disorder through genetic testing via a blood or muscle biopsy test. Severe forms of MD such as duchenne muscular dystrophy become present in young children and degenerate muscle so expediently that, by age 12, the child is wheelchair-bound (St. John, 2013) (Mirski et al, 2014). Figure 6 depicts a direct comparison of a healthy eight year old boy and one with MD. Current treatments aim to control symptoms and maintain or increase muscle mass as long as possible. Keeping the patient active through physical therapy prolongs the strength of function of muscular groups, while braces can improve stability and mobility. Medications such as painkillers or

corticosteroids can be administered to ease pain and boost muscle mass to keep the person mobile as long as possible by slowing degradation (Campellone, 2014). After the disease onset (generally at about 10 years of age), quality of life diminishes significantly as loss of muscle/control of the body leads to death in the mid-twenties. Treatment generally cost $4,600 annually per patient (Center for Disease control and Prevention, 2014).
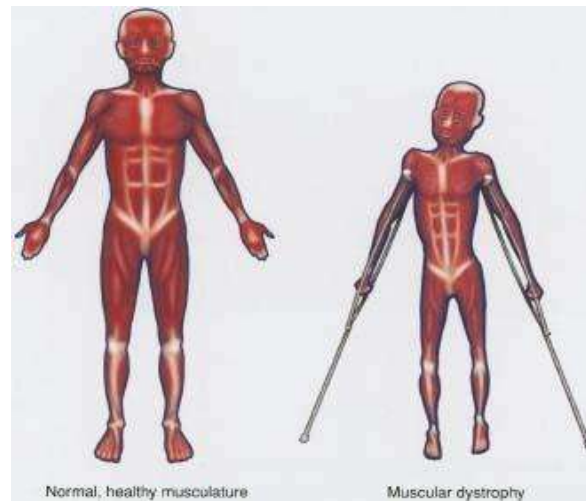
Figure 6: Compares a healthy 8 year old boy to an 8 year old boy with muscular dystrophy (Emery et al, 1994)

2.2.2 Multiple Sclerosis

One of the main differences between MD and MS is that MS is an autoimmune disease that leads to the destruction of the myelin sheath surrounding nerves, which leads pain and immobility from the destruction and disruption of the central nervous system. This disease most commonly begins to show symptoms between the ages of 20-40 (Campellone, 2013). Symptoms of MS include muscle spasms, loss of balance, numbness, weakness in limbs, and difficulty controlling fine motor movement. MS patients could benefit from this project through use of the device to create better muscle tissue models for testing new drugs and treatment methods.

MS can be difficult to diagnose because its symptoms are similar to other nervous system problems. The three main diagnostic tests are blood tests (which rule out similar conditions), lumbar

puncture (to test cerebrospinal fluid for abnormally high antibody levels and breakdown products of myelin), and MRI scans of the brain to diagnose and follow the natural degeneration and progression of the disease (Campellone, 2013). There is no cure for the disease, the medications slow progression of the disease and steroids help maintain muscle. The cost of MS treatment per patient averages at $19,500 annually.

2.2.3 Amyotrophic Lateral Sclerosis

Amyotrophic lateral sclerosis (ALS), also known as Lou Gehrig's disease, is classified as a fatal neurological disease which attacks motor neurons and muscles (Amyotrophic Lateral Sclerosis, 2013). The degeneration mainly occurs in lower motor neurons from the spinal cord to nearby muscles that are attached to the neurons. The disease is most common in Caucasian males between the ages of 60-69, and is usually fatal within 3-5 years from the onset of symptoms. Only 10% survive beyond 10 years. 90-95% of the cases appear to be random, while the other 5-10% are inherited, which makes genetic testing much more difficult. One third of inherited cases share a common genetic defect in C9orf72, but the full function of the gene is unknown. More than 12,000 people in the United States alone had a positive diagnosis for the disease in 2013 costing $256-$488 million.

The first symptoms that appear are related to dexterity difficulties, such as turning a key or buttoning a shirt (Amyotrophic Lateral Sclerosis, 2013). Muscle atrophy and weakness begins to occur, in addition to muscle cramps. Diagnosis is complete only when symptoms and signs of damage are observed in both upper and lower motor neurons. ALS is very similar in symptoms to Human Immunodeficiency Virus, human T-cell leukemia virus, polio, west nile virus, and Lyme; making it harder to diagnose. Blood and urine tests eliminate the possibilities of the other diseases as well as muscle biopsies to eliminate MS or MD. Certain electromyogram tests can measure electrical energy and act as an early warning for the onset of the disease if abnormal results are present, as degenerated motor neurons generate abnormal electrical signals.

Similarly to MD and MS, ALS does not have a cure and all forms of medication address symptomatic ailments to improve quality of life (Amyotrophic Lateral Sclerosis, 2013). The main focus of one drug treatment, Riluzole, is thought to decrease the damage to motor neurons by inhibiting the release of glutamate. However, the result of Riluzole treatment is only prolonging life for a few months. A major side effect of Riluzole is liver damage, so its use must be closely monitored. Physical therapy helps maintain muscle control and muscle mass, but also increases risk of injury and degradation.

Diseases like MD, MS, and ALS would greatly benefit from a muscle model. A technology platform that allows for high content testing of drugs used to treat and cure these diseases could serve as a better model for adult human muscle tissue, as current models are insufficient in generating clinically-useful representative tissue for drug screening and diagnostic testing.

2.3 Injuries:

Injuries to skeletal muscle occur daily that cause the need for extensive natural recovery. The most common causes of injury are sports related due to increased activity and overuse of certain muscle groups that sometimes do not regenerate as fast as they are injured (Smith et al, 2008). The main break/tear usually occurs from trauma such as a collision, shear strain (force in directions perpendicular to muscle alignment), over bearing loads, and overuse. Phagocytosis is the process of cellular debris removal, however, when the removal process is faster than regrowth there is a net weakening effect.

Muscle tissue has the ability to repair minor wounds, but more serious damage to skeletal muscle is beyond the scope of repair (Burks et al, 2011). The problem with the process of natural recovery is that it is inefficient, especially when the muscles are not able to get the nutrients or materials needed to repair tissue damage and large wounds where innate response cannot effectively take place. In other cases, over inflammation leads to buildup of cytokines and growth factors which lead to swelling and provokes an autoimmune response. Prolonged exposure to inflammation causes

formation of myofibroblasts instead of myocytes; the result is fibrotic tissue where myofibers should be as seen in Figure 7 (Burks et al, 2011). More common clinical solutions include autografts to replace damaged section with some of the patient's own tissue, but the drawback is that autografts cause further damage by creating a second surgical site to perform a tissue graft.
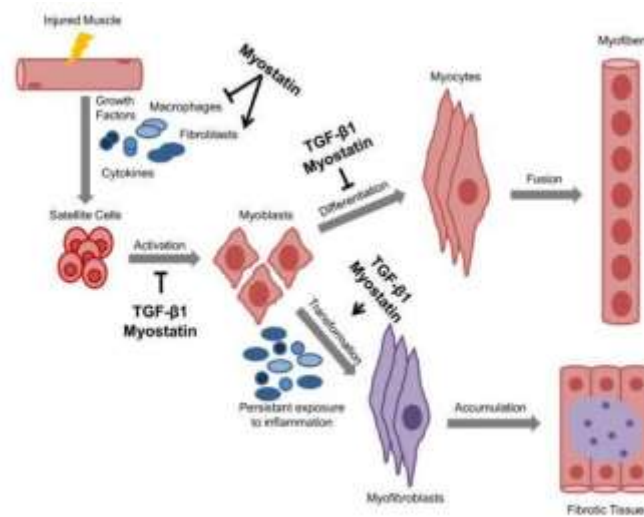
Figure 7: Innate regeneration of damaged muscle tissue top, absence of repair and fibrotic scar bottom (Burks et al, 2011)

Natural recovery occurs in two main phases: systemic awareness of the damage and the cellular process of cleanup/reconstruction and regeneration (Smith et al, 2008). The first part of recovery is the body's inflammatory response to damage that draws more blood and neutrophils to the area. Once the inflammatory response happens, phagocytosis occurs as the macrophages clear the cellular debris in preparation for new cell growth. At this point, the phenotype of muscle switches from pro-inflammatory to anti-inflammatory so muscle can be regenerated, while preventing apoptosis. Satellite cells activate and migrate to the wound sites and aid in new muscle formation. Then, precursor growth/cell activation factors (TGF-β1) are produced to promote regeneration. Cytokines are also secreted to facilitate vascularization and muscle fiber repairs.

2.4 Tissue Regeneration and Reconstruction

The goal of tissue engineering is to regenerate and reconstruct biological cell culture to improve the human condition. This is done through the manipulation and regulation of factors -- chemical, physical, and electrical -- to replace or remove naturally occurring biological functions (Bach et al, 2004). Tissue engineering encompasses a wide range of areas from drug delivery and experimentation with pharmaceuticals to the reconstruction of extracellular matrix (ECM) scaffolds. Moreover, the creation of biomimetic tissues enables researchers to accurately study the development and reactions of tissues, as well as observing the tissue behavior in response to drug exposure.

Currently, when testing preclinical pharmaceuticals, live animal models are used to determine the effects and toxicity. Alternative methods are necessary because of the rising ethical concerns that surround animal testing. In addition, genetic diseases, including Duchenne Muscular Dystrophy and Facioscapulohumeral Muscular Dystrophy (FSH), are not present in the genetic DNA of animals, making results clinically irrelevant. Since it is unethical and unsafe to test directly on humans, there is a need to be able to accurately test pharmaceuticals on in vitro models of human tissue because there is a gap with current FDA regulations (MacArthur, 2005). The use of dmd mice has been the current practice, even though it is not a perfect genetic model.

2.5 Need for an Enabling tool to test In Vitro Muscular Tissue

There is a need for a technology platform that is able to bridge the gap between incurable degenerative muscle diseases and pharmaceutical efforts to test the effects of their drugs. Such a tool would ideally generate in vitro human muscle tissue that accurately depicts in vivo human muscle tissue. This biomimetic model would circumnavigate the physiological differences and ethical concerns with animal models and increase efficiency in the drug testing process generating a more predictive in vitro bench top model.

The challenge in modeling skeletal muscle tissue is the ability to mature the tissue. If not matured correctly, the tissue will not be representative of adult muscle tissue. Other challenges and limitations inhibit accurate representation of in vivo conditions and recapitulation of such an environment via these tissues on the benchtop. The overall goal of this project is to create accurate representations of human skeletal muscle tissue.

2.6 Muscle and Myoblast Physiology

The architecture of muscle in the body is composed of three main types of muscle: cardiac, skeletal, and smooth, which control blood flow, locomotion, and digestion respectively. The team can further organize the three groups into voluntary and involuntary muscle. The main functional unit of skeletal muscle is the sarcomere; an arrangement of thin and thick myofilaments. Sarcomeres are building blocks, forming a hierarchical structure of contractile myofilaments in order to form myofibers in parallel alignment. This parallel alignment improves the speed and magnitude of lateral force transmission (Guilak et al, 2003). This project would compare the engineered tissue to the mechanical and chemical properties of in vivo tissue formation.

2.6.1 Cellular Organization and Development

Myocytes are cells that are multinucleated but are controlled by a motor neuron at one end (Shier, 2009). Skeletal muscle is organized in a hierarchical structure, as shown in Figure 4. The exterior of myocytes are encased in a sheath called the sarcoplasmic reticulum. This sheath translates the neuro-electrical signals from motor neurons into acetylcholine, which creates a chemical gradient, signaling contraction. Myofibrils (see Figure 4) are the contractile units of muscle comprised of bundles of myofibers. Sarcomeres are the contractile units that contain overlapping filaments, which contract when stimulated by a gradient of calcium ions.

2.6.2 Myogenesis, Cell Fusion, and Cell Proliferation

Muscle development begins with progenitor cells, depending on the presence of c-met-tyrosine kinase receptor, which activates the hepatocyte growth factor for delamination and migration path (Buckingham et al, 2003). The progenitor cells increase production of factor Pax3 and activate the myogenic regulatory factors and become myoblasts (Grefte et al, 2007). Differentiation into myocytes is mediated through the expression of several other factors that lead to myocyte fusion into one continuous layer of muscle fibers -- the myotome. During myotome formation, cells that express both Pax3 and Pax7—two key transcription factors in myogenesis— differentiate into satellite myocyte cells of the muscle tissue. These cells return to quiescence and lay dormant until activated following injury.
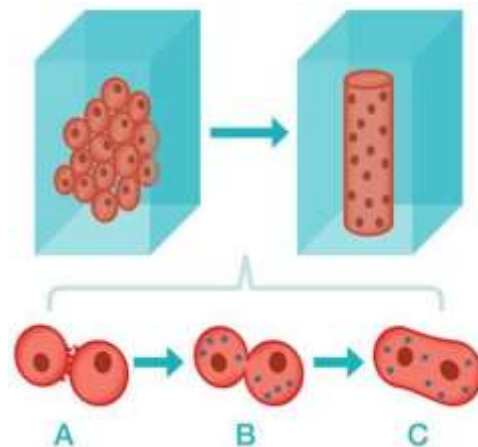
Figure 8: Cell fusion is a key characteristic of skeletal tissue. Proper cell fusion requires specific growth factors and an external load to dictate fiber alignment (Brock, 2013).

Myoblasts align and fuse, as shown in Figure 8, to form multinucleated myotubes (Gilbert, 2000). Muscle cell fusion can only occur when myoblasts exit the cell cycle and initiate terminal differentiation. Certain growth factors signal myoblasts to proliferate mitotically without differentiating. Once these growth factors are no longer present, fibronectin is secreted onto the ECM and the cell binds to it using $\alpha5\beta1$ integrin (Gilbert, 2000). This integrin to fibronectin attachment is critical in signalling myoblasts to differentiate into muscle cell. Cell membrane glycoproteins mediate myoblast alignment

through an identification coupling, while metalloproteinases, called meltrins, mediate cell fusion and

initiate differentiation (Gilbert, 2000).

2.6.3 Myocyte Structure and Function

Myocytes are multinucleated muscle cells that develop from the fusion of myoblasts during

myogenesis. Myofibrils are rod-shaped units that are segmented into sarcomeres. Sarcomeres make up

the basic contractile unit of muscle tissue and contain myosin myofilaments and actin. Each myocyte is

composed of multiple myofibrils. All of the myofibrils of the same muscle fiber structure are in parallel

as seen in Figure 9.
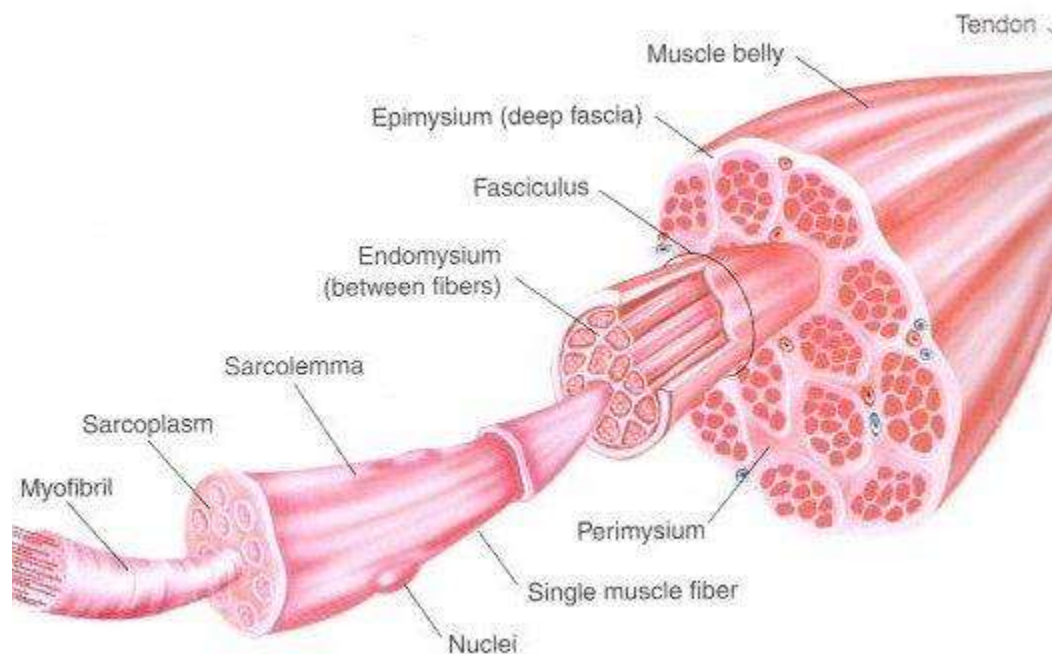
Figure 9: Muscle components and parts showing muscle hierarchy (Burns et al, 2008)

The contraction of muscle is driven by interactions between myosin and actin filaments in the
sarcomeres. Figure 5 outlines this molecular mechanism.
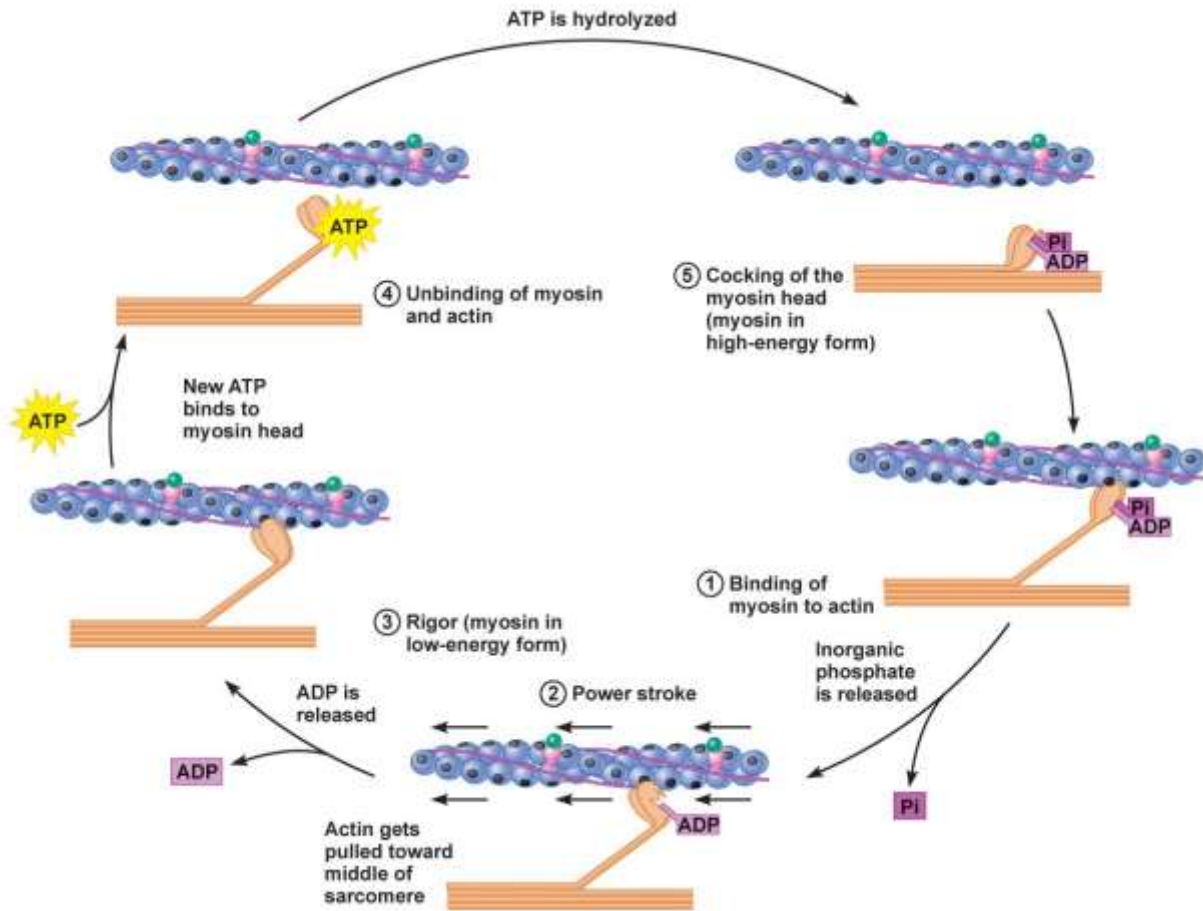
Myosin and actin move through the process of ATP binding and release as seen in Figure 5. When binding the myosin head to actin, a phosphate group is released and myosin head pulls the actin on the sarcomere, which releases ADP. After the power stroke, ATP unbinds the myosin head from the actin and ATP is hydrolyzed. This leaves myosin in its high-energy form and restarts the process.

2.6.4 Motor Neurons and the Neuromuscular Junction

Motor neurons control muscle contraction through action potentials. As shown in Figure 5, motor neuron axons attach to the end of each muscle fiber at the neuromuscular junction. The action potential signals the opening of calcium channels and the cells are flooded with calcium ions. Then, acetylcholine -- a neurotransmitter -- is released by the cell and attaches to the receptors at the motor

endplate, which directs sodium ions to enter the cell via voltage-gated channels. After sufficient influx of

sodium ions, the sodium channels close and voltage-gated potassium ion channels open to let potassium

ions diffuse out of the cell. The movement of these ions creates a depolarization action potential,

resulting in muscle contraction (Silverthorn, 2010).
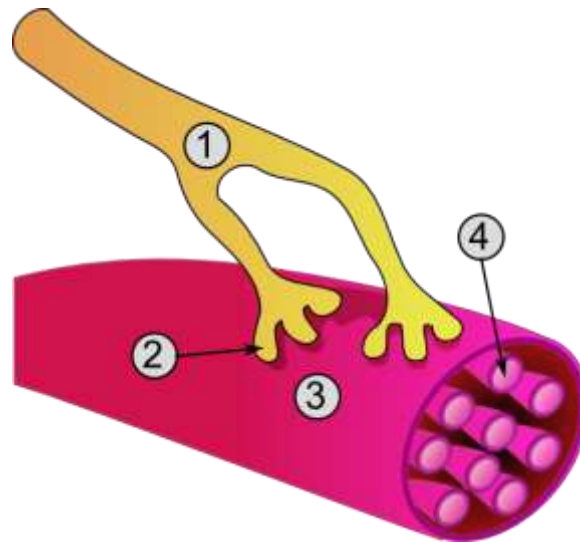
Figure 11: The structure of a myocyte and neuromuscular junction; 1) Axon, 2) Neuromuscular junction, 3) Muscle fiber (myocyte), 4) Myofibril. (Silverthorn, 2010)

2.6.5 Extracellular Matrix:

The ECM is a network of molecules that govern cell attachment, migration, proliferation, and

differentiation. ECM is a component of muscle tissue that controls cell response to injury/disease and

bears most of the passive load on muscle tissue (Gilles, 2011). Skeletal muscle ECM consists of three

distinct layers: the endomysium, the perimysium, and the epimysium (Gilles, 2011). The endomysium

encases individual myofibers and functions as a supportive load-bearing structure. The perimysium

surrounds bundles of myofibers (known as *fascicles*), and comprises longitudinally-oriented fibers that

form a dense series of bands along the fibers, as well as transverse collagen fibers that interconnect

muscle fibers at distinct points. As these connection points contain focal adhesions and intracellular

subdomains, it is hypothesized that the perimysium plays a role in cellular signaling (Gilles, 2011). The

outermost ECM layer, the epimysium, surrounds the entire muscle, and comprises large collagen

bundles that distribute load across the length of the muscle (Gilles, 2011). These divisions of skeletal ECM are illustrated in Figure 12 (Gilles, 2011).
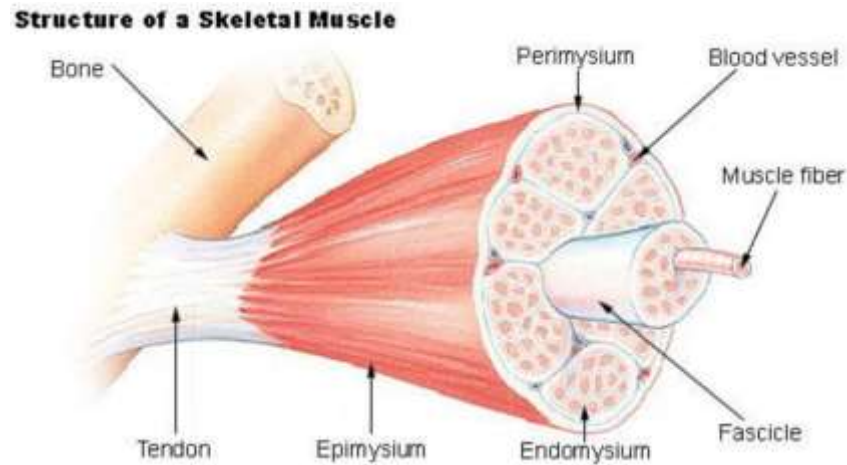
Figure 12: Skeletal Muscle Structure, including ECM divisions (Gilles, 2012)

On a molecular scale, skeletal muscle ECM is mainly made up of collagen I, collagen III, collagen IV, and collagen VI (Bach et al, 2004). Isoforms of collagen serve as structural support, while traces of elastin are also present for elastic behaviors. Within the ECM are several proteoglycan proteins that help with regulatory processes. For example, glypican promotes and stimulates differentiation, while syndecan serves to inhibit differentiation. Force transmission along the muscle is largely controlled and facilitated by integrin binding with ECM. For example, the E8 fragment of laminin in skeletal muscle ECM is known to specifically bind the integrin beta-1 on myoblast cells, providing continuity between laminin in the ECM and the cytoskeleton for contractile ability at myotendinous junctions (von der Mark et al, 1991).

Pathophysiologically, muscle dystrophy can be understood as a disorder in the bridging between cytoskeleton and ECM. Dystrophin is the largest gene found in nature at about 2.4 Mb. It is thought to be responsible for Duchenne (DMD) and Becker (BMD) Muscular Dystrophies. DMD is recessive, fatal, and x-linked. It occurs in 1 of 3,500 newborn males (Roberts, 2001). Dystrophin RNA splices differently,

which produces a range of varying transcripts and encodes for a large set of protein isoforms. More specifically, Dp427 transcripts are large, rod-like cytoskeletal proteins which are found in muscle fibers. The dystrophin-glycoprotein complex bridges the inner cytoskeleton (F-actin) and the extra-cellular matrix. The breakdown or malicious mutation of this relationship leads to degradation and weakening of the ECM and the F-actin in the cell cytoskeleton (Roberts, 2001). This degradation worsens until the patient is immobilized from the inability to use their muscles and subsequently dies (Roberts, 2001).

2.7 *In Vitro* Muscle Generation

The generation of skeletal muscle tissue *in vitro* represents an approach that seeks to mimic *in vivo* myogenesis—the natural formation of muscle during prenatal development as well as the natural maturation of muscle during later stages of development and adult regeneration of muscle following small injuries (Bach et al, 2004). Therefore, the standard metrics for *in vitro* engineered skeletal muscle arise from mimicking the morphology, functionality, and contractile force produced by native skeletal muscle tissue. Key metrics include: parallel uniaxial alignment of myofibrils (myotube bundles) with myosin and actin filaments, intracellular calcium storage, and expression of acetylcholine receptors localized to the neuromuscular junction (Bach et al, 2004). Another important metric for tissue formation is tissue anchorage similar to muscle-bone attachment, since continuous passive tension applied to skeletal muscle by growing bone during embryogenesis and neonatal development influences native levels of myofiber length and parallel myofilber alignment (Powell et al, 2002). Cell density, myotube length, and myotube diameter similar to cell composition in native skeletal muscle is also a key metric,. Notably, myofiber diameter for *in vivo* human muscle ranges from 10-100 μm and myofiber length is averaged at 23.3 μm (Vandenburgh, 1991). In the myotubes, the density of nuclei per sectioned slide of *in vivo* tissue is between 30-57 nuclei/mm^2 (Vandenburgh, 1991).In the following sections, the role of cell density in ECM structure, muscle contractility (i.e. function), and myofiber density will be discussed (Powell et al, 2002).

2.7.1 Myogenic Cell Types

Functional skeletal muscle cells have been successfully cultured *in vitro* as early as 1915 (Lewis, 1915). Numerous myogenic cell populations have been used for generating skeletal muscle tissue in vivo, including primary cultures of embryonic avian or neonatal skeletal muscle cells, or C2C12 cells (Dennis, 2000).

Primary satellite cells (myoblast precursors) for ESMT applications have been directly harvested from the muscles of neonatal rats, birds, mice, and frogs (Koning et al, 2009). Primary satellite cells have been obtained from minced explants of adult and neonatal soleus, latissimus dorsi, and tibialis anterior in rats (Dennis and Kosnik, 2000), as well as the brachioradialis in frogs (Koning et al, 2009). The current method of choice for culturing primary myogenic cells is to extract satellite cells from *ex vivo* myofibers and then derive primary myoblasts from these satellite cells. Shansky et al (1997) and Dennis and Kosnik (2000) were among the first to demonstrate in vitro generation of functional skeletal muscle tissue using primary myoblasts derived from tissue biopsy. Being derived directly from muscle tissue, primary cell cultures are able to produce tissue in a way that closely matches myogenesis (Bach et al, 2004). Yet, satellite cells from different organisms and muscles result in skeletal muscle tissue with very different properties (Koning et al, 2009). For example, skeletal muscle tissue engineered from soleus muscle satellite cells differs substantially from tissue engineered from tibialis anterior muscle satellite cells, in contractile force and frequency (Koning et al, 2009). The anatomical location of primary cells must therefore be taken into consideration in the parameters of the model tissue. Accuracy of human tissue modeling is also a concern when using xenogeneic satellite cells. There is clear evidence in studies of mouse muscle that satellite cells— both within the same muscle and even on the same fiber— differ in marker expression, function , density (i.e. satellite cells per fiber), and capacity to differentiate *in vitro*, depending on the muscle used for the satellite cell isolation (Boldrin et al, 2010). These are all observations of mouse muscle, and it is still unclear if the human satellite cell pool is heterogeneous like

the mouse satellite cell pool (Boldrin et al, 2010). Myogenic satellite cells appear to strongly imprint their muscle source (in terms of anatomy or species), producing *in vitro* tissue similar to their native tissue source (Bach et al, 2004).To obtain sufficiently large cell populations for *in vitro* skeletal muscle tissue, however, primary myoblasts need to be cultured over extended periods of time. Also, with successive passaging, differentiation becomes increasingly difficult to induce in primary cell cultures, often due to contamination from fibroblasts (Koning et al, 2009) (Li et al, 2011). Immortalized cell lines do not reach senescence and can split nearly indefinitely given the space and resources; whereas, senescence cells age and lose their potential to complete mitosis. Another difficulty in obtaining primary cell cultures *in vitro* is that the process of isolating primary cells will often activate SC's and direct them down a terminal differentiation pathway substantially reducing the differentiation potential of the cells and, making expansion of a myogenic population *in vitro* to a clinically-relevant cell number very difficult (Sabourin et al, 1999).

Recently, studies have developed engineered tissue from the well-established mouse myoblast C2C12 cell line (Okano and Matsuda, 1998; Van Wachem et al, 1996). The C2C12 cell line is a cell line of myoblasts that was originally derived from mouse sarcolemma skeletal muscle (Bach et al, 2004). C2C12 cultures do not recapitulate *in vivo* myogenesis as closely as cultures of primary myogenic cells (Bach et al, 2004); however, the use of C2C12 cells allows for a means of standardization between researchers. Leading not only to easier sourcing of myogenic cells, but most importantly to increased consistency of the properties of engineered tissue useful for validation work. In addition, C2C12's grow faster, can use relatively inexpensive media (needing fewer specialized growth factors) to grow in, which saves time and money. Generally C2C12 cells are used to pilot test systems, and create clinical relevance.

2.7.2 Culture Media

Cell culture media are rich mixtures of sugars to sustain cellular metabolism, salts for pH buffering/ osmotic balance, and amino acids for protein synthesis (ATCC, 2014). Media mixtures, such as Dulbecco's Modified Eagle's Medium (DMEM), provide amino acids and vitamins as well as trace minerals and glucose (ATCC, 2014). As a safeguard, antibiotics may also be added to myogenic cell cultures—commonly penicillin, streptomycin, or gentamycin is used (Dennis and Kosnik, 2000; Carosio et al, 2013). Serum, isolated from blood, also provides many of these proteins, along with several growth factors (ATCC, 2014). The percent composition and type of serum influences the cell cycle because the amount of overall nutrients influences it, inducing cells to proliferate or differentiate. Fetal serum (such as fetal bovine serum used by this project) is richer in proteins and growth factors, promoting cell proliferation compared to adult serum (such as adult horse serum, as used in this project), and cells favor proliferation in high-serum environments, and differentiation in low-serum environments (ATCC, 2014; Carosio et al, 2013). Cells typically exit the cell cycle, transitioning into terminal differentiation, upon detecting mitogen-reduced environments (Carosio et al, 2013). For skeletal muscle cells, high concentrations of fetal bovine serum (FBS) are typically used for cell proliferation, and low concentrations of adult horse serum are typically used for cell differentiation (Carosio et al 2013; ATCC, 2014; Bach et al, 2004). Some examples of common formulations for proliferation and differentiation media are presented below. The key takeaway is that reducing serum concentration in media induces cells to exit the proliferative cell cycle and enter differentiation. Dennis and Kosnik (2000) and Carosio et al (2013) both used primary adult rat myogenic precursor cells:

(1) Differentiation Medium (Dennis and Kosnik, 2000): 7% adult horse serum in DMEM, 100 units/ml penicillin.

(2) Differentiation Medium (Carosio et al, 2013): 5% adult horse serum in DMEM, 25 mM HEPES buffer (for pH buffering), 4 mM L-glutamine, 0.1% penicillin/streptomycin

(3) Proliferation Medium (Carosio et al, 2013): 20% fetal bovine serum in DMEM, 25 mM

HEPES buffer, 4 mM L-glutamine, 0.1% penicillin/streptomycin

2.7.3 3D Culture

The presence and composition of ECM greatly influences the differentiation of myogenic cells (Bach et al, 2004). In vivo, ECM provides myogenic cells the framework for cell adhesion and tissue organization, which includes cell migration and differentiation (Koning et al, 2009). As 3D cultures of C2C12 cells alone are unable to synthesize endogenously the ECM necessary for tissue formation, ECM-based scaffolds have been utilized for cell culture (Bach et al, 2004).

Vandenburgh et al (1988) was the first to demonstrate a three-dimensional scaffold culture for *in vitro* skeletal muscle tissue. Until then, studies of engineering muscle tissue had typically been conducted with cultured cells in 2D. After myoblasts fuse to form myotubes, they begin to passively contract. This impedes 2D culture of skeletal muscle tissue, as these contractions can detach the cell layer from its substrate. Once in a detached and free-floating layer, cells are no longer under mechanical tension—this causes the tissue to contract inward and form a 3D ball, diminishing its structural maturity and making it difficult to analyze (Vandenburgh et al, 1988).

Cell culture in 3D scaffolds remains widespread in the field of developing *in vitro* skeletal muscle tissue. Common substrates include: Matrigel (Shansky et al, 1997) (Vandenburgh et al, 1996), and type I collagen (Vandenburgh et al, 1988). These substrates are derived from ECM components and attempt to recapitulate the cues for differentiation provided by a native ECM. Synthetic scaffolds, including scaffolds composed of polylactic-co-glycolic acid (PGA), have also been studied (Koning et al, 2009). Aligned topography on both natural and synthetic scaffolds —via microgrooves and nanofibers— has been found to promote controlled myoblast differentiation and direct the parallel assembly of myofibers and cytoskeletal proteins (Koning et al, 2009).

However, cultures in scaffolds restrict the ability to measure and characterize the contractile

properties of the tissue in comparison to other culturing methods (Carosio et al, 2013). Tissues grown in

scaffolds also exhibit viable tissue formation only at the peripheries of the scaffold, with large regions of

cell and tissue death towards the center. Under *in vitro* conditions, the availability of nutrients to cells

within the scaffold is limited by diffusion of media to within 5 μm into the scaffold substrate, due to lack

of innervation and vascularization within the scaffold (Levenberg et al, 2005). Tissue decreases in

viability towards the scaffold center, following the diminishing diffusion gradient of nutrients into the

scaffold interior. One strategy to circumvent this problem is to introduce angiogenic factors into the

scaffold material, in order to stimulate vascularization (Levenberg et al, 2005).Non-contractile

substrates—as characteristic of the scaffolds listed above—also inhibit the formation of myotubes, as

well as the contractile force of the generated tissue, and therefore tissue function (Carosio et al, 2013).

2.7.4 Self-Assembly and Co-culture

Strohman et al (1990) demonstrated for the first time that primary skeletal muscle cells are able

to self-organize into a 3D tissue construct, in the absence of a scaffold. Dennis and Kosnik (2000)

developed a unique method of engineering functional units of muscle tissues, termed "myooids", which

self-organize from a monolayer into a rolled-up cylindrical tube from primary adult rat satellite cells. 2D

cultures of myogenic cell monolayers, when provided points for anchorage and allowed to differentiate,

can self-assemble into tissues as they passively contract. These anchors act as an initial mechanical

structure for a cell layer, to align into a 3D cylindrical tissue construct, via the passive contractions that

myogenic cells increasingly produce as they advance through differentiation. Carosio et al (2013) used a

pair of stainless steel pins for tissue anchorage for their self-assembly from a cell monolayer, whereas

Dennis (2000) used silk sutures tied to pins to mimic myotendonous junctions. More viable, in-vivo-like

tissue was formed through simultaneous growth with endogenous ECM, as fibroblasts secreted ECM

that directed myoblast cell growth (Dennis ,2000). Tissues from scaffolds were not as strong, due to the

ingrowth of cells into pre-existing, exogenous ECM. *As* discussed previously, another way to set up this initial mechanical structure is by providing the cells with a provisional ECM. A more recent approach attempts to do this via endogenous ECM, as through a co-culture of myoblasts with ECM-secreting fibroblasts.

Rather than a homogeneous culture of myoblasts, a heterogeneous co-culture of both myoblasts and fibroblasts self-organizes into the tissue structure more typical of native skeletal muscle (Dennis and Kosnik, 2000; Carosio et al, 2013). Carosio et al (2013) reported that pure cultures of myoblasts failed to generate mature muscle tissue via self-assembly. Co-cultures with both cell types results in tissue formation more closely resembling the symbiotic effect between native myoblasts and fibroblasts during human in vivo myogenesis (Carosio et al, 2013)(Marzaro et al, 2002). The co-culture of fibroblasts with myoblasts improves the self-organization and alignment of skeletal muscle architecture—requiring only anchorage points and exogenous ECM to direct 3D tissue formation. In vitro, NIH/3T3 fibroblasts can secrete the extracellular matrix that provides support for the adhesion, proliferation and differentiation of myoblasts (Carosio et al, 2013). 101T1/2 fibroblasts may also be used for this purpose (Dennis, 2000). As the fibroblasts within the culture secrete the ECM necessary for in vitro muscle tissue, and if sufficient anchorage and shape of 3D mold is provided for developing self-assembled tissue, there is no need to provide ECM externally, rendering the use of a scaffold unnecessary.

Dennis and Kosnik (2000) pioneered the *myooid* approach, where fibroblasts and myoblasts are cultured together to form scaffoldless 3Dmuscle tissue while also producing ECM exogenously. The co-culture method is a more accurate representation of in vivo myogenesis than scaffold methods, as the ECM is produced intrinsically by the cells, resulting in better recapitulation of native cell densities in neonatal myogenesis (Dennis, 2000). In the myooids, processes such as the fusion of myoblasts into

myotubes, the creation of the extracellular matrix, and the formation of myofibrils with successive

recruitment of fibroblasts and myoblasts all occur more similarly to denovo synthesis of muscle tissue —

in terms of muscle morphology, as well as composition and localization of cell types (Dennis, 2000).

However, the myooids of Dennis and Kosnik (2000) were only able to generate 2-8% of the force (per

unit cross-sectional area) generated by skeletal muscles of adult mice. Myotubes within in vitro tissue

are commonly arrested in an immature state, failing to develop to a more adult-like phenotype. One

reason is that in natural myogenesis, the maturation of newly-formed myotubes to adult myotubes is

dependent on electrochemical activity, in the form of tetanic nerve impulses (Huang et al, 2005). Such

stimulation has been difficult to replicate in vitro. Additionally, several key growth factors are present in

vivo. For example, insulin-like growth factor I (IGF-I) is known to play a critical role in muscle maturation

by increasing DNA synthesis, kinase activity, amino acid uptake, and the expression of important

functional proteins (Huang et al, 2005). A twofold increase in muscle size was observed in mice

engineered with muscle-specific overexpression of IGF-I (Coleman et al, 1995).

Dennis and Kosnik (2000) cultured a monolayer of co-culture on a type-I-collagen-coated plastic

dish. After 2 days incubation in differentiation medium, the confluent monolayer was delaminated from

the substrate and affixed onto a silicone-coated dish between two steel pins. Over 2-3 days, the tissue

self-organized into a rolled-up 3D cylindrical structure, containing dense, aligned myotubes that are

contractile. Figure 7 demonstrates the cross-sectional structure of a "myooid" culture—a self-

assembling co-culture of fibroblasts and myoblasts showing large amounts of collagen from the plate

(Dennis, 2000).
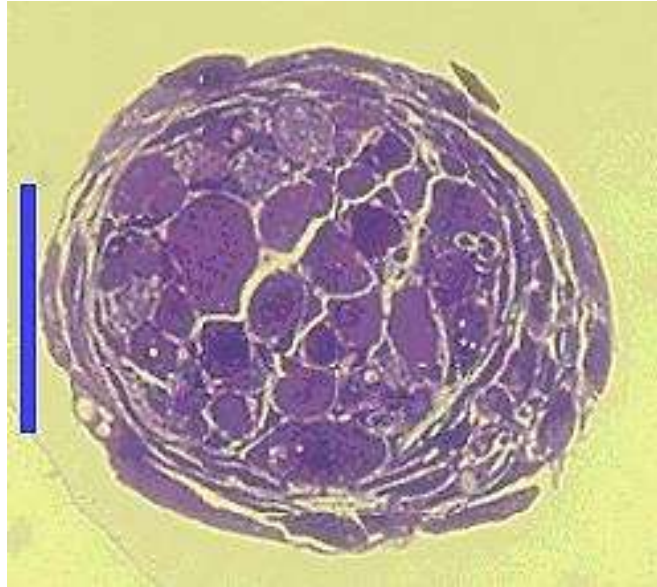
Figure 13: Cross-Section of Dennis and Kosnik's "Myooid" (Dennis, 2000). Scale bar represents 100um

A layer of flattened fibroblasts is visible on the periphery of the myooid cross-section, surrounding several thick, round myofibers (formed by fused myoblasts). In this arrangement, the peripheral fibroblasts exert a constant stress of 5kPa on the tissue, acting both longitudinally along the length of the tissue, as well as radially inwards (Dennis, 2000). The stress exerted results in an internal pressure of ~ 1 kPa within the core of the myooid (Dennis, 2000). This structure, with a periphery of flattened fibroblasts surrounding a core of myotubes, is characteristic of the cellular organization of *in vivo* skeletal muscle tissue. The final tissue constructs were each 12 mm in length and 0.1-1mm in diameter. A similar procedure was employed by Carosio et al (2013), who reported tissue construct dimensions of 197 ± 12 μm (diameter) and 9 ± 2 mm (length). While Dennis and Kosnik's (2000) source of fibroblasts is unspecified, Carosio et al (2013) used a co-culture of C2C12 myoblasts with NIH/3T3 fibroblasts.

2.8 In vitro Mechanical Stimulation and Electrical Stimulation

The formation of skeletal muscle cells, and subsequent maturation into functional adult muscle tissue, is dictated by a variety of factors as stated in section 2.6.2 Myogenesis, Cell Fusion, and Cell Proliferation. Bone elongation during neonatal development is known to direct the initial phases of

muscle organogenesis via the continuous passive tension applied to skeletal muscle by the developing

bone (Powell et al, 2002). During later *in vivo* development of muscle—following neonatal myogenesis—

mechanical strain (i.e. active stretching and loading) is responsible for many key aspects of mature

muscle functionality, including increased number, diameter, length, and parallel alignment of muscle

fibers, as well as regulation of cellular protein synthesis, protein localization, and insulin sensitivity

(Powell et al, 2002). Both active and passive tension stimulate the increase of myofiber thickness,

length, and parallel alignment (Powell et al, 2002).

The generation of mature, *in vitro* skeletal muscle seeks to mimic the mechanical stimuli found

in vivo to direct native-like myogenesis, cell metabolism, fiber orientation, and muscle morphology by

benchtop mechanical stimulation (Vandenburgh, 1991). As outlined further in Section 2.8.1, several

studies have been performed via cultures of primary cells and immortalized cell lines, showing that

varied mechanical stimulation regimes induce various alterations for in vitro skeletal muscle. Higher

rates of muscle stimulation without tissue rupture lead to more growth in these cultured tissues

(Vandenburgh 1991).

Electrical stimulation seeks to mimic chemical (tetanic) stimuli that occur via neurosignaling of

muscle tissue during development *in vivo*. In the body, the calcium gradient dictates contraction and

relaxation of muscle fibers. Electrical stimulation regimes *in vitro* attempt to mimic the effects of the

gradient in *in vitro* tissue. Electrical stimulation induces the myotubes to contract on the anchor points,

causing cells to align between anchor points. Active stimulation occurs when the cells supply the force

instead of an external source. Therefore, electrical stimulation provides a way to mediate contraction

and control frequency. The contractile force generated by the engineered tissue can later be measured

by another device. Electrical Stimulation also helps cells align and mature differently than mechanical

stimulation.

2.8.1 In vitro Mechanical Stimulation

Currently, there are methods developed for the mechanical stimulation of skeletal muscle

tissue. The Vandenburgh group (1991) developed a computerized mechanical cell stimulator for the

purpose of stimulating skeletal muscle constructs. Two different approaches were used to passively

stimulate the C2C12 cells while in culture. Figure 8 shows 2D tissue stretching radially, and Figure 9

shows 3D tissue being stretched uniaxially. The method in Figure 9 is more similar to the uniaxial passive

tension applied by bone attachment in vivo
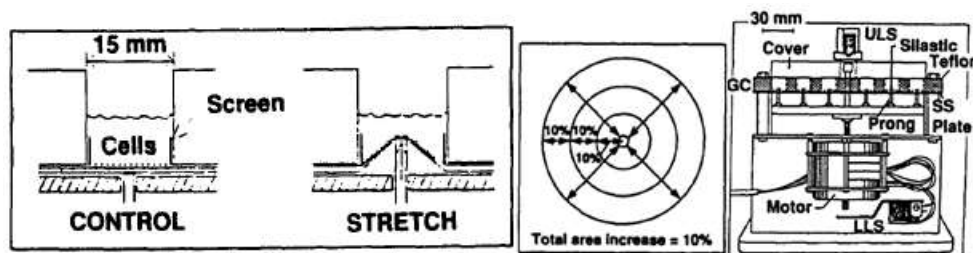
Figure 14: Circular wells and stretches in a radial (2D) direction. A pin pushes the center of the 2D tissue upwards and radially stretches it. The constructs of method 1 were adapted from methods to stretch cardiac tissue which stretches in 2D (Vandenburgh 1991).
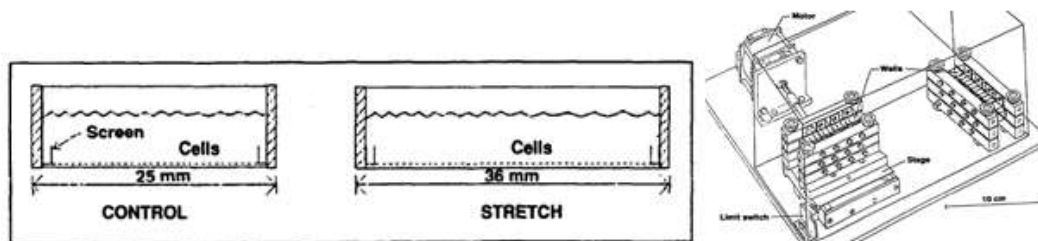
Figure 15: Rectangular wells and stretches uniaxially. (Vandenburgh 1991).

Given sufficient nutrition, the 2D Method (Fig. 8) was able to stimulate and provide viable

myofibers for 30 days without detachment or degradation. The uniaxial method led to a higher degree

of myofiber alignment than the 2D Method (Vandenburgh, 1991). Fiber alignment is a key characteristic

of skeletal tissue, as discussed in Section 2.7. Higher degrees of parallel myofiber orientation are

associated with a greater ability to sustain loads and produce greater contractile force (Vandenburgh,

1991). Myofiber diameter for *in vivo* human muscle ranges from 10-100 μm and their initial length is

averaged at 23.3 µm. In the myotubes, the density of nuclei per sectioned slide of 3D *in vivo* tissue is between 30-57 nuclei/mm^2.

With these methods, the cultures were put through various regimens. Initially, the samples were stretched passively for one cycle, with positive 10% strain for 30 minutes. This was done to activate the sarcolemma, which induces sodium pumps to increase activity for growth factors (Vandenburgh 1991). In method 1, the tissue was strained to 20% of the initial length, and within 3 to 4 hours glucose uptake increased 38%. Glucose uptake increased to 158-204% in 24 hours (Vandenburgh 1991). The uptake of glucose can be used as a metric to model maturation rates of myoblasts, as they transition from neonatal to adult muscle phenotype (Vandenburgh 1991). In this way, measuring glucose uptake provides a quantitative means to assess the maturity of the myoblast cultures. Figure 16 from Vandenburgh's study shows the exercise regimen and the glucose uptake:
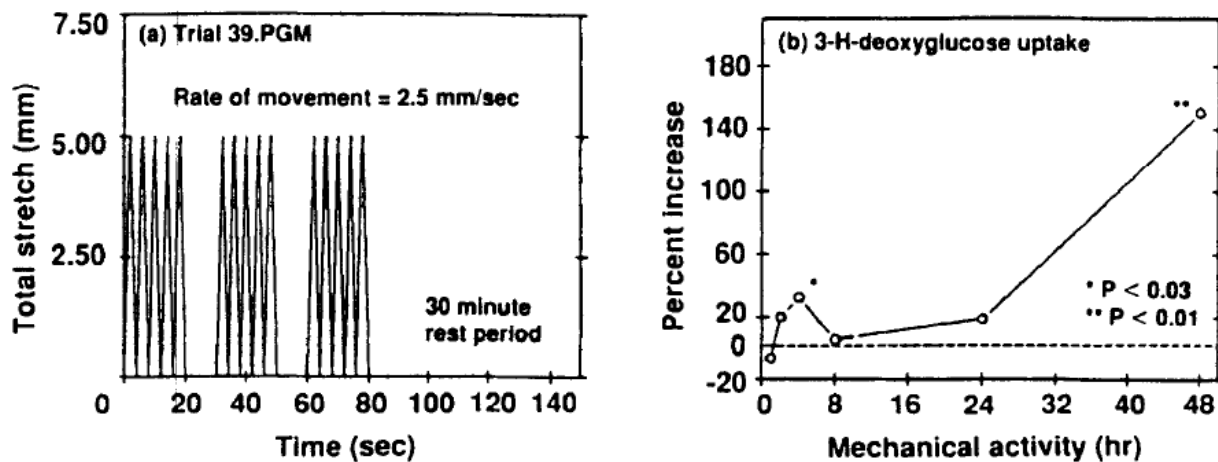
Figure 16: The exercise regimen from Vandenburgh's study (Vandenburgh, 1991). The left graph shows these cultures were stimulated with respect to total stretch. The right graph shows mechanical activity (number of cycles of stretch) led to the increased uptake of glucose in these cells for development *(Vandenburgh 1991).*

Andersen et al (2014) also studied mechanical stimulation, though in the context of determining optimal strain rates for cell fusion in stem cell/skeletal myoblast co-cultures. Vanderburgh (1991) demonstrated that mechanical stimuli is necessary for skeletal muscle hypertrophy. Andersen et al

(2014) placed 2D tissue cultures (density of 5000 cells/cm^2) through pulses of 15% strain at 0.5 Hz (Andersen, 2014). After conducting variations of this regime, of 3D tissues was found to be optimal for the stem cell /myoblast for alignment and stimulation purposes with the least rupture (Andersen, 2014). This regime also appeared to accelerate the differentiation process in C2C12 cells, which formed a greater number of myotubes compared to their control. Andersen et al (2014) came to this conclusion by comparing the rate of the development of myotubes and myogenic markers, myogenin and myosin, to the control over 48 hours.

Both Andersen (2014) and Vandenburgh (1991) conducted mechanical stimulation tests with similar parameters. Vandenburgh (1991) strained from 10% to 20% and Andersen strained at 15% strain. Vandenburgh strained at a slower pace than Andersen's pulsing technique. No test in prior works has exceeded 20% strain, possibly due to rupture with greater strains. The regimes were computerized and programmable in terms of strain rate, amplitude, and duration. In the end, both methods concluded that mechanically stimulating skeletal muscular tissue lead to the following:

1. "Mechanical stimulation increases myoblast fusion rates" (Andersen, 2014)

2. "Mechanical stimulation increases longitudinal myofiber growth rates" (Andersen, 2014)

3. "Mechanical stimulation induces organogenesis of artificial muscles capable of generating active tension in the longitudinal axis" (Vandenburgh 1991)

The team determine that it would be ideal to use Andersen's optimized 15% strain, in combination with Vandenburgh's slower strain rates as parameters for the team's experiments. Slower strain rates help protect against tissue rupture.

2.8.2 Anchorage of *In Vitro* Muscle Tissue
Anchorage is a key defining aspect of skeletal tissue. In vivo, myoblasts grow and anchor to bone, causing passive tension *in vivo* that promotes cell differentiation. Currently in vitro, there are two

main approaches to provide anchorage and uniaxial alignment using mechanical stimulation to mimic in vivo conditions called: 1) Ring Method and 2) Dog-bone Method. There are other methods used to mechanically stimulate skeletal muscle but they have been adapted from engineered cardiac tissue and are in 2D.

The first method is growing tissue in a circular band around two posts, and then moving the posts back and forth uniaxially to apply positive and negative strain (Laterreur, 2014), as illustrated in Figure 11. This method originated from a different experiment for testing the mechanical properties of blood vessels. The method is popular due to the relative ease in growing tissue in this geometry. In this method, the cells are not physically anchored to the post, but just contracted circumferentially. They are anchored to the adjacent cells in a continuous loop. Though testing can still be done, it is not the best model for in skeletal muscle tissue since there are no physical anchorage points.

The second method is growing tissue in a dog-bone shape around two posts, and then similarly applying positive and negative strain, as shown in Figure 11. Both methods function the same way, by changing the distance between the posts. The dog-bone shape more accurately simulates muscle attachment to bone, but is also useful for stress analysis testing (Laterreur, 2014). There is more tissue at the anchor points to reduce rupture and to shield from stress concentrations. The middle of the tissue forms axial (parallel) fibers with tension. This dog-bone methods is more representative of the muscle to bone attachment. Therefore dog-bone shaped 3D tissue is a better representative of in vivo muscular tissue than ring shaped.
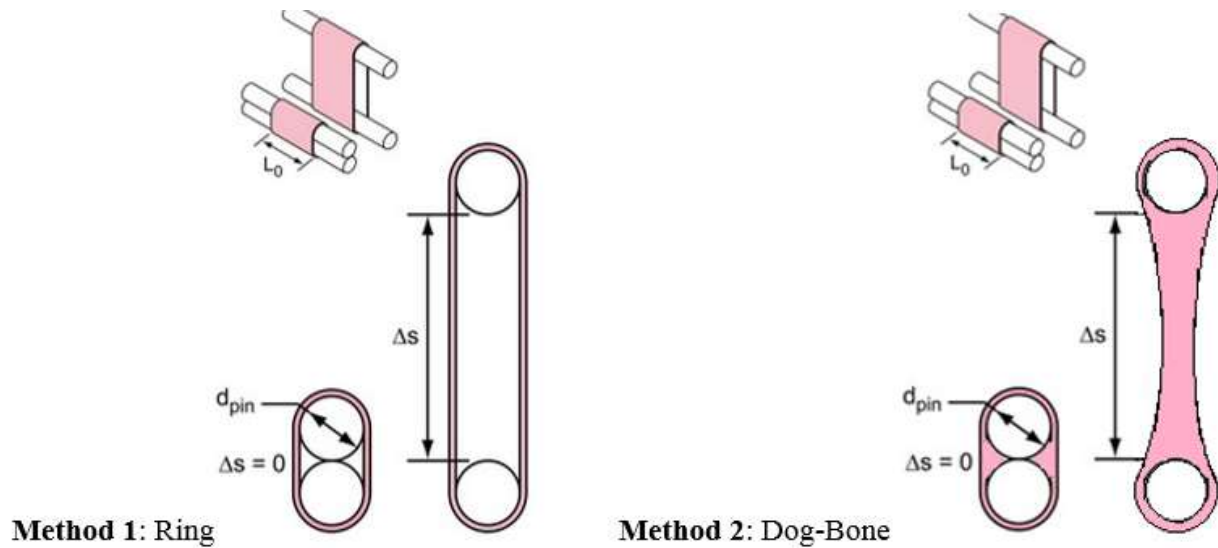
Figure 17: Two primary methods of anchoring tissue to molds for mechanical stimulation. Left: Ring-anchored technique where (Δs) represents strain of the sample (Laterreur, 2014). Right: Dog bone technique where the tissue is anchored to the physical post, simulating muscle-bone attachment (Laterreur, 2014).

2.8.3 Electrical Stimulation

In vivo, myofiber contractions are triggered by a chemical process of neurotransmitters and motor neurons. The fibers contract inward to rotate the attached bone. Applying a voltage to 3D tissue in vitro has become a substitute for natural chemical-signaled contraction in vivo (Powell et al, 2002). Studies show in vitro electrical stimulation cause myofibers to assemble and mature more rapidly and stimulate tissue contraction (Hirokazu et al, 2010)(Zhao et al, 2009).

2.8.4 Electrical Stimulation by Electrodes

Current methods electrically stimulate constructs via the insertion of a pair of electrodes into the culture well (Zhao et al, 2009). Temporary cell depolarization occurs due to the movement of calcium ions across a concentration gradient in the media when electrical current is applied.

In one study (Hirokazu et. al., 2010), a revised design of a cell culture device was created, as shown in Figure 18. The porous alumina membrane was covered underneath with a thin layer of polydimethylsiloxane (PDMS), which was stenciled with a hole. On the top of the membrane, an atelocollagen membrane was fixed. Bioinert carbon electrodes were placed on opposite sides of the

membrane. A 2D monolayer of differentiated myofibers was cultured on this membrane. The necessary

depolarization was mediated via the electrodes, as the current was able to flow through the cells

perpendicularly. The cells were able to condense at the hole within the PDMS slice.
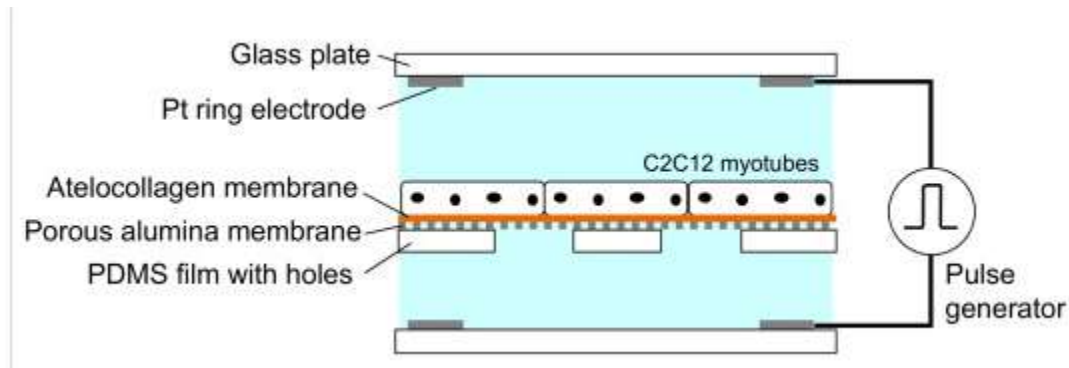
Figure 18: Schematic illustration (cross section) of the porous membrane-based electrical stimulation device (Hirokazu et. al., 2010)

An amplitude of 4 mA for a duration of 20 ms and frequency of 1 Hz comprised the current

pulses that were induced between the ring electrodes. An isolator unit or DC source was always

coupled with the electronic stimulator. Before stimulation occurred, the device was filled with the

following solutions: DMEM containing calf serum, MEM amino acids solution, MEM non-essential amino

acid solution, penicillin, and streptomycin. This solution composition sought to mimic the electrolytic

composition of the tissue culture media and be conductive.

Results indicated that myotubes began to contract as the electrical stimulation was applied.

Both the magnitude of contraction and quantity of stimuli-responding cells increased as well in

comparison to the control. Increased contraction and number of responding cells increased due to the

close resemblance of atelocollagen to actual muscle tissue stiffness. Passing the electrical stimulation

through the PDMS increased the number of myotubes that contracted in comparison to the control

(Hirokazu et. al., 2010). Increasing the number of myotubes improves contractibility and tissue strength.

2.8.5 Contactless Electrical Stimulation

As discussed in the previous section, using probes in the media stimulates the tissue and improves cell fusion. However, such methods still suffer from numerous drawbacks: pH changes in media, corrosion byproducts from reaction at the electrodes, and fluctuation in temperature (Zhao et al, 2009). An article by Zhao et al (2009) investigates the effects of electrical fields on skeletal myogenesis, using C2C12 cells. In Figure 19, the constructs used by Zhao can be seen, as well as the setup for contactless electrical stimulation.
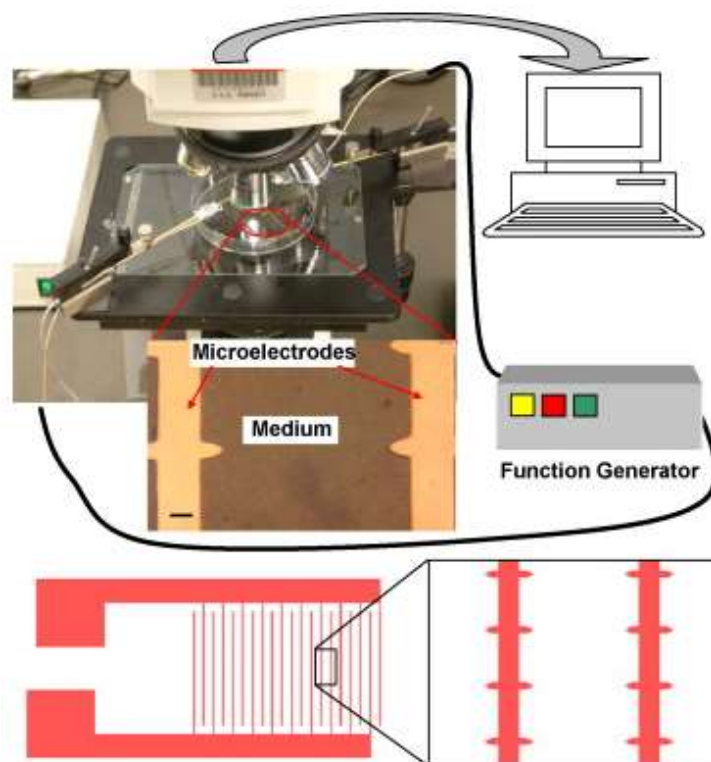
Figure 19: "*The experimental setup for electrical stimulation of skeletal myoblasts. The microchip containing the microelectrode array was placed on the stage of a high-power optical microscope. The electrical stimulations generated from a function generator were applied to the microelectrode array using two probe manipulators. The cell response to the electrical stimulation was obtained by a computer for analysis. The subfigure shows an optical micrograph of the microelectrode array. The space bar indicates 100 µm.*" (Zhao 2009)

Zhao placed an array of mirco-electrodes underneath his cultures. Zhao's group used an AC signal power source at 500mV. "High frequency AC stimulation was applied, with the frequency ranging from 100 to 5000 kHz. The data was acquired at the frequencies of 100, 500, 1000, and 3000 kHz."

(Zhao, 2009). Zhao electrically stimulated C2C12 culture for 30 minutes followed by 24 hours of incubation (Zhao, 2009).

The results of his experiment show cell proliferation and differentiation varies with the electrical stimulation, specifically with the frequency of the electric field. 1000 kHz provided the optimal electric field strength for stimulating the tissue. The results of alignment can be seen in Figure 20 (Zhao, 2009) from Zhao's paper. In Zhao's experiment, the control was probe-based stimulation and the experimental groups were performed with electric field stimulation at different frequencies. Electrical field stimulation is less effective than probe-based electrical stimulation at increasing viability and differentiation of cells based off visual comparison of Zhao's data. Thus, cell fusion rates decreased, but so did cell damage in comparison to the tradition probe methods.
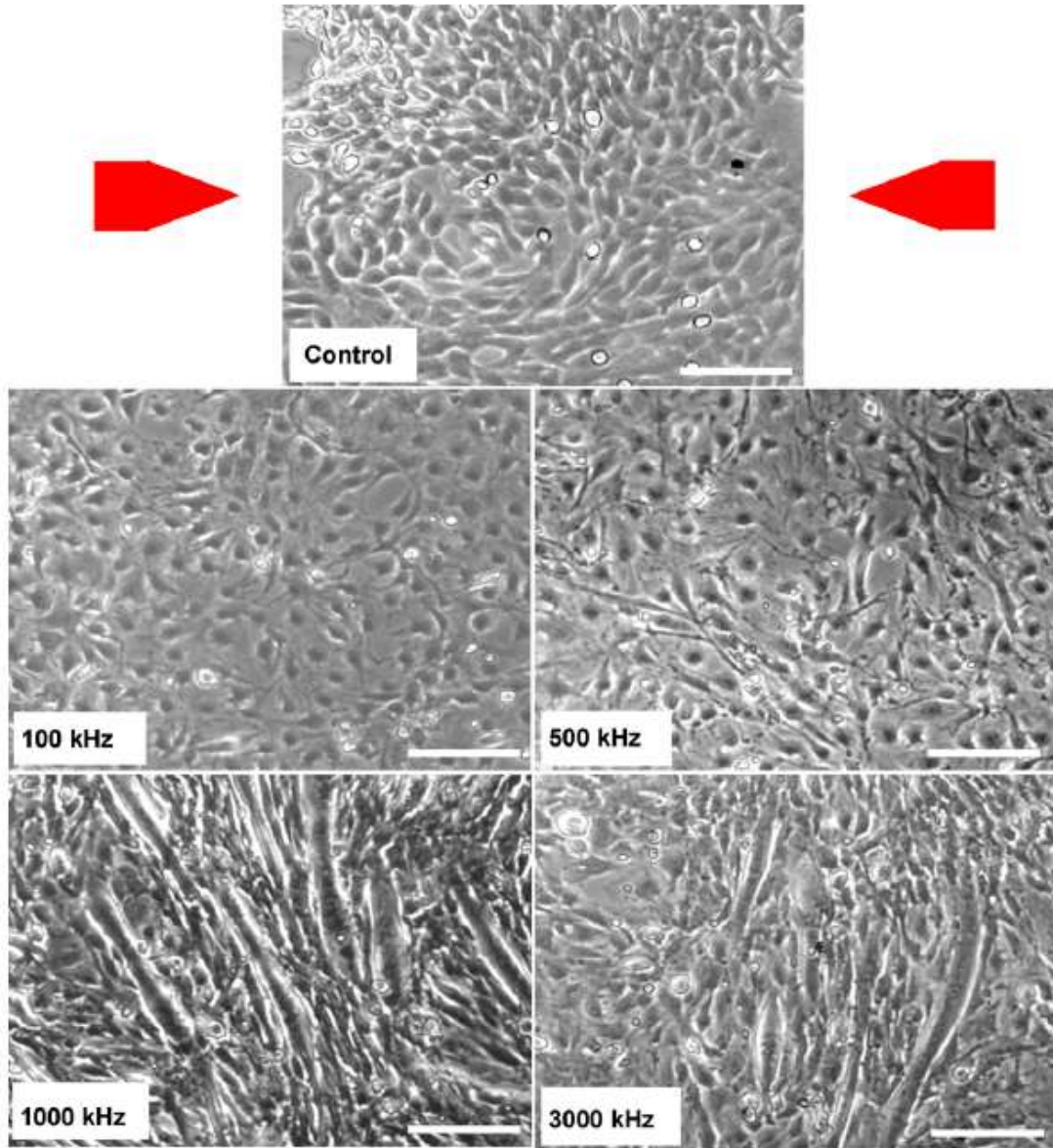
Figure 20: *"After 4 days electrical stimulation, the frequency-dependent cell differentiation was observed. The cells with low-frequency electrical stimulation (100 and 500 kHz) exhibited a fairly low level of differentiation. The cells with 1000 kHz electrical stimulation exhibited extensive cell fusion, with a large number of long and thick myotubes formed. With 3000 kHz electrical stimulation, many myoblasts remained undifferentiated even with close contacts. The images are between the opposing electrodes which were positioned on the right and left of the images, as shown in the control group. The spacebars denote 100 μm".* 1000kHz provided the best results for muscle proliferation (Zhao 2009).

Both mechanical and electrical stimulation lead to increased fiber alignment, higher fiber

density, and more accurate representations of *in vivo* tissue in comparison to non-stimulated tissue.

2.9 Validation Tests for Myocyte Viability and Intracellular Organization

To determine cell viability in seeding cultures, a variety of tests can be performed on myocytes. Such assays using trypan blue, water-soluble tetrazolium or AM calcein. The necessary changes in cell structure necessary for myotube formation and differentiation must also be validated –such as via a fusion index of cells inside and outside myotubes.

2.9.1 Assays Methods for Cell Viability and Differentiation

A common method for determining cell viability uses trypan blue to detect the cell membrane morphology and durability. Live cells exclude trypan blue via their cell membrane, but dead cells' membranes are porous and allow the dye to pass through (Strober, 2001). Water-soluble tetrazolium and AM calcein staining can also be used to determine cell viability. These two methods of staining can detect whether or not the mitochondria (via tetrazolium) and cytoplasm (AM calcein) of the cells are functioning properly. Water-soluble tetrazolium uses a UVM plate reader to examine absorbance of 690 and 450 nm wavelengths to determine mitochondrial performance, while trypan blue uses a light microscope, making it possible to count the viable cells in the sample.

Percent of viable cells can be calculated using a live/dead assay. During this process, the cells are rinsed with phosphate saline and fluorochromes before being incubated. The cells then get examined under fluorescence microscopes, and the dead cells become illuminated as the fluorochromes enter the severed cell membrane (Martin-Piedra et al., 2013). Within the scope of the project, and with cost and equipment constraints, only a trypan blue live/dead assay will be used.

To validate the differentiation of myoblasts into myotubes, myosin and actin may be visualized via immunohistochemical staining and fluorescent imaging. Antibodies for myosin conjugated to isotype-specific fluorescent secondary antibodies may also be used for fluorescent visualization (Herman et al, 1981).

2.10 Existing Patents for Tissue Mechanical/Electrical Stimulation Devices

There are several existing patents on devices used to grow and stimulate muscle tissue. Listed below are some examples of the variety of devices currently being used in laboratory settings for use of conditioning tissue engineered muscle.

2.10.1 Herman Vandenburgh: Tissue Stretch via Substrate Expansion

Herman Vandenburgh has one of the earliest patented devices, established in 1992, used for growth of tissue specimens. His patent protects apparati designed for growing tissue specimens *in vitro* including the following: an expandable membrane/scaffold to embed cells within for growth into tissue, a device designed to expand a scaffold with embedded tissue specimen, and a controller to regulate the expanding device. The expanding device allows for stimulation of the cells to mimic *in vivo* conditions, consisting of positive and negative strains applicable (Vandenburgh, 1992).
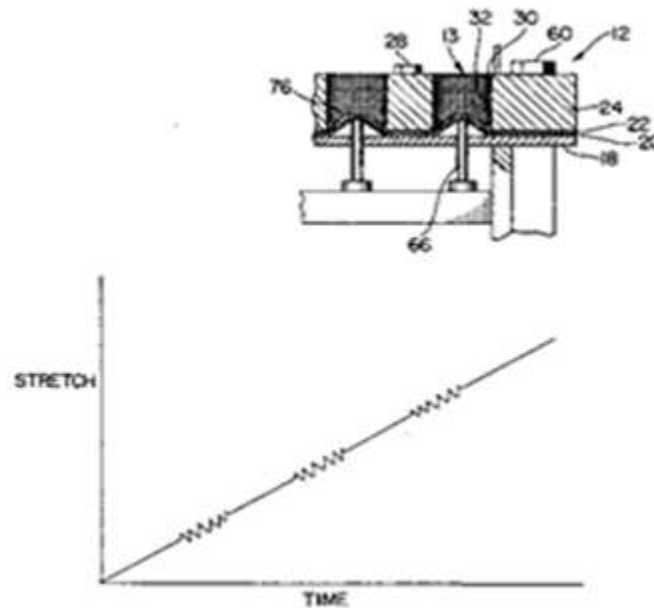
Figure 21: Top figure is a sectional view of well assembly containing tissue specimens. Bottom figure is a graph of common pattern applied by device.

Figure 21 displays an illustration of the well assembly of Vandenburgh's device containing tissue specimens, as well as the typical pattern of stimulation onto the tissue specimen. Tissue specimens (76)

37

within the well structures (12) are stimulated via blunt pins (66) that extend upwardly from the main plate through the holes (18) into the well membrane (20) and gasket (22). The upper plate (24) provides support for the wells (13) and is held in place by nuts (60). Biocompatible rings (30) are placed on the inner support surfaces (32) that allow for cell attachment (Vandenburgh, 1992). The mechanisms and results of this device are discussed more thoroughly in section 2.8.1.

2.10.2 Milica Radisic: Perfusion Electric Stimulation

Milica Radisic, in association with MIT, was issued a patent for a biomimetic electrical stimulation upon tissue during cultivation *in vitro* to improve its morphology, as well as improve integration with the host tissue after implantation of the construct (Radisic et al, 2005). A 3D construct was patented that consisted of forming a cell-seeded construct from a cell-gel suspension containing mammalian cells, a cell-seeded construct exposed to an alternating flow perfusion, providing the construct with nutrients, cultivating the construct under direct medium perfusion through which nutrients flow through the construct to generate a uniform cell density from 100 microns to 5mm, and stimulating the construct to an electrical stimulation to create a 3D cell structure similar to cells in vivo. Muscle cells that exhibit electrical excitation and are exposed to electrical stimulation in vivo may use this method for regenerating tissue. An example of the electrical stimulation setup is shown in Figure 22. Advantages of this system include its ability to provide tissue with a uniform cell density, making it easier to distribute nutrients evenly to all cells; the ability of the system to sustain electrical stimulation mimicking tetanic contractions *in vivo*; and its shown improvement of integration with host tissue following implantation in the body. The suitability of this electrical stimulation setup to cell-in-gel tissue culture is notable. Disadvantages include the system's ability to only use electrical stimulation and not mechanical stimulation and its specifications geared more to generating cardiac muscle than skeletal muscle tissue (Radisic et al., 2005).

2.10.3 George Christ: Cyclic Mechanical Stretching Regimens

George Christ of Wake Forest University Health Sciences patented methods used in culturing 3D

skeletal muscle tissue via precursor muscle cells through means of cyclic relaxing and stretching. This

conditioning takes place in vitro on a scaffold system. The tissue is then reseeded with separate

precursor muscle cells onto the scaffold to increase cell density and repeat conditioning methods once

again. The re-seeding process can occur in a static environment, or in contact with a solution containing

precursor muscle cells for a range of time between 10 minutes when in direct contact with cells and two

days when in a scaffold to allow for diffusion. Methods of cyclic stretching included the following:

extending scaffold 5-15% in length than resting position for three cycles within the first time period of 2

to 10 minutes and again for 50-58 minutes. This is continued for five days to three weeks in a scaffold

created with a porous hydrogel substance containing collagen, and scaffold dimensions of 20-1000 μm

thick. Pros of this system include the multiple variations of cyclic stretching that the device can provide

and the ability to generate nearly three times the original nuclei density in the myotubes of the formed

tissue, with 800+ nuclei between protein markers of multinucleated cells (Christ et al., 2013). The

specific strain regimen used may provide a baseline for initial stimulation regimens in this project.

2.10.4 Robert Dennis: In Vivo Emulation System

Robert Dennis of the University of Michigan patented both a method and a device to emulate

the in vivo environment for stimulate muscle tissue seen in Figure 23. Stimulation can be applied via an

electrical or mechanical stimulator. The muscle tissue response to the signal generates another

stimulation signal, and represses force production of the tissue. The stimulator is able to change initial

input signals based on response signals from the muscles, allowing the testing of a wide range of

programmable regimes. The system can be used with both mechanical and electrical stimulation

occurring concurrently. Mechanical stimulation is provided by means of a force transducer, while the

electrical stimulation is provided via servomotor and electrical stimulator (Dennis et al., 2001).
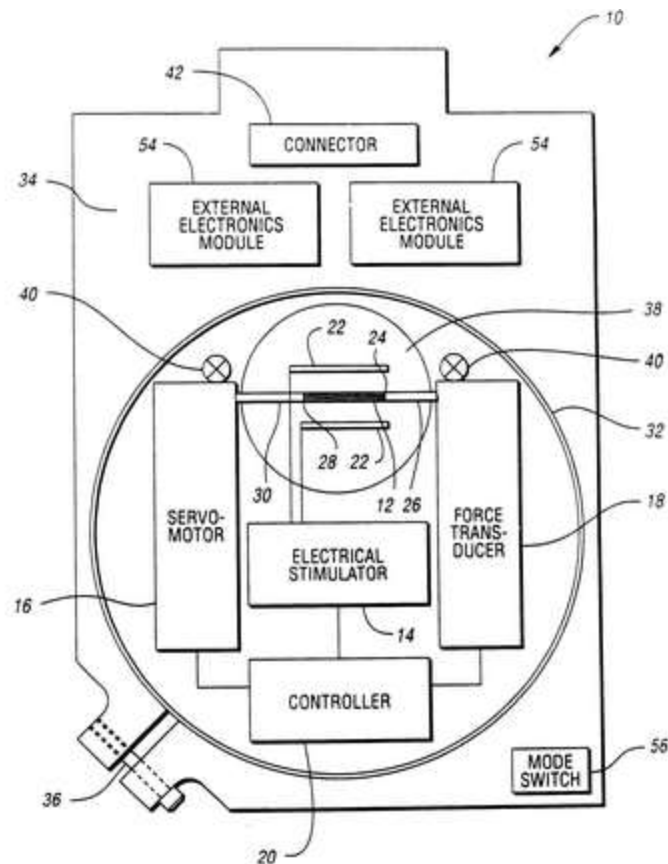
Figure 23: Schematic of emulator system for mechanical stimulation from top view (Dennis et al., 2001)

Figure 23 above displays an emulator system (10) that can deliver two or more stimuli to the skeletal muscle tissue (12); electrical (14) and mechanical (16) stimuli that can be applied concurrently or separately. Within the emulator system, a sensor (12) is able to read the muscle tissue response to the initial stimulation and create an appropriate response signal. The sensor is controlled (20), and the response signal is received through the force transducer (18). The controller has the ability to control the following factors: amplitude, train duration, pulse width, % duty cycle, pulse frequency, as well as mechanical aspects of strain rate, amplitude, and frequency. This is important for tissue development because the amplitude and pulse frequency are increased with maturation of the tissues. With 2-5 mm diameter rings, there was a success of 5% for myoid formation, which improved to 50% when 70 V, 4-ms pulse regiments were applied. Success was determined from eliciting a "twitch force" or voltage to

induce muscle contraction. Dennis et al (2001) determined the maximum isometric tetanic force

through stimulating myooids at 40 V and 40 Hz with 1.20-ms pulses for duration of 2 seconds. This is

stimulation applied to determine force, which falls outside the scope of this project. Electrodes (22),

made of platinum wire or plates, are situated in parallel to muscle tissue in order to make a transverse

electric field. The force transducer has the ability to resolve 1-3000µN of force with a bandwidth of 100

Hz that is not greater than 1% of muscle tissue length; 50 mW of power dissipation is also preferred with

resistance to high humidity environments to enable use inside incubators (Dennis et al., 2001). The

relevance of these parameters to the project will be discussed in Section 4.6.
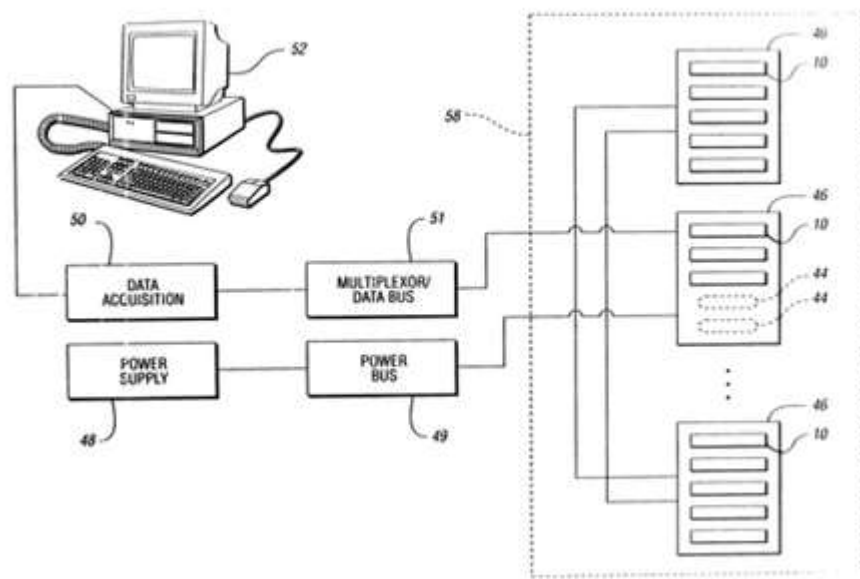
Figure 24: Interface configuration of multiple emulator systems (Dennis et al., 2001)

Figure 24 shows the interface configuration of multiple emulator systems (10) being used

concurrently. Towers (46), containing mating systems, (44) house the emulator systems within an

incubator (58), making the system high throughput while mimicking the natural body temperature.

Pros of this device include its ability to change control signals based on the response signals of the tissue, allowing the system to create a more *in vivo* like environment. In addition, the system is high throughput through due to its multiple emulator systems. Possible cons of this design include possible necrosis of the fibroblasts as a results of slow negative strain that the controller may provide in response to signals, as well as causing rupture of the fibers due to high loadings from the controller (Dennis et al., 2001).

2.11 CAD Mechanical and Electrical Design

Mechanical and electrical stimulation devices are typically created in computer aided design (CAD) software. This software allows for modeling of prototypes and creating drawings to be used for manufacturing of the product, with the added benefit of precise and accurate dimensions. Manufacturing of tissue construct molds for tissue formation in incubators can be done via computer aided manufacturing, or by using current molds available in the Page Laboratory.

2.11.1 Computer Aided Manufacturing

Rapid prototyping is a common way to manufacture special items quickly for a small cost of compared to outsourcing. Complex parts modeled in a CAD file can be created with ABS plastic. High, low, and solid densities can be chosen for the part density depending on the function of the part and system requirements. These densities are created by the amount of space set between the layers of the plastic as the printer moves from bottom to top of the part. All parts must be smaller than 13 x 13 x 6 inches in size, while their individual features may not be smaller than 0.38 mm thick. The typical accuracy of the machine is 0.02 – 0.08 mm (WPI ARC, 2013).

Use of rapid prototyping for mold creation has advantages over machining methods. More precise geometry can be obtained, at a smaller scale.

2.11.2 Current Designs

Current designs for tissue construct molds exist in the Page and Rolle laboratories in Gateway

Park. The Rolle lab creates ring shaped tissue constructs for use in creating blood vessels, shown in

Figure 25. The molds used to generate these constructs can be found in Figure 26 below, and the end

result is shown in Figure 27 (Gwyther et al., 2011). Similar molds are currently being used in the Page

laboratory to generate skeletal muscle tissue in a ring shape.
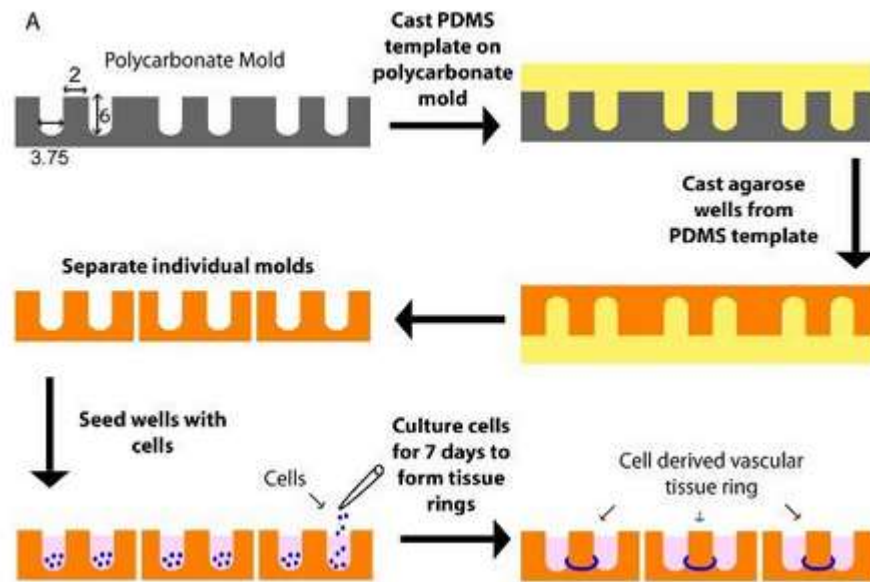
Figure 25: Process of tissue ring generation (Gwyther et al, 2011)

Figure 26: Polycarbonate mold with 2 mm post diameters used to generate ring tissue constructs. Scale bar = 6 mm (Gwyther et al., 2011)
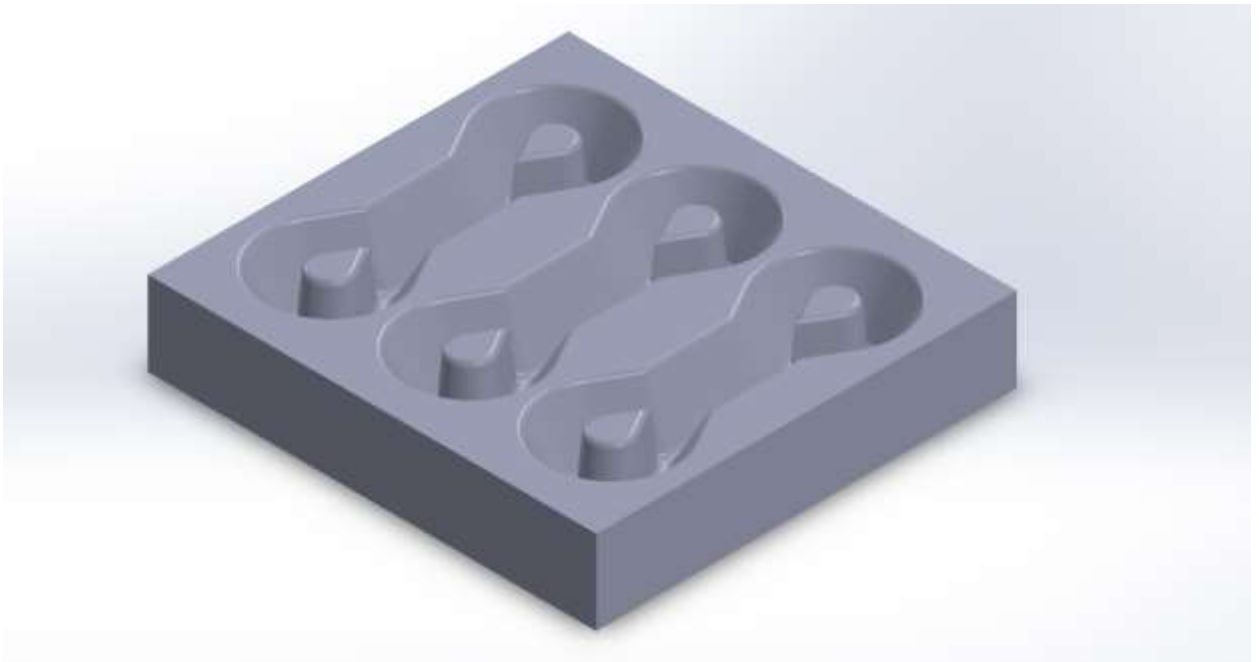
Figure 28: Example of dogbone shaped tissue mold (Forte, personal communication, 2014)

The Page Lab generates tissue in dogbone shaped formations in addition to the ring shape formation used in the Rolle lab. A picture of the dogbone shape mold is shown in Figure 28. The advantage to using dogbone shaped constructs is that they more accurately represent *in vivo* skeletal muscle. The posts on both ends of the dogbone shape serve as anchoring points, mimicking myotendonous junctions in the body. The ring structure is based on Rolle Laboratory cardiac vessel physiology, but its shape makes it much easier to create, requiring fewer cells to create a higher yield, and is used in experiments testing the effect of changing media components and supplements. The

dogbone constructs are used in mechanical testing, but are more fragile and more likely to self-rupture from stress transitioning from the post to the uniaxial section.

2.12 Project Issues/Limitations

There are many issues regarding the current processes, stated in the *in vitro* Mechanical Stimulation and Electrical Stimulation section above, that do not promote optimal skeletal muscle tissue formation similar to that of *in vivo* tissue. These limitations include small fiber diameter, low cell density, and low vascularization of tissue, and will be discussed later in this section. All of these limitations inhibit the tissue's ability to mature and generate native levels of force/unit area to be considered an accurate model adult skeletal muscle tissue.

2.12.1 Fiber Diameter

Lack of native-sized fiber diameters is one limitation to current methods of stimulation. The literature shows the *in vivo* myofiber diameter ranges between 10-100 μm and the ideal fiber length is 4-6 mm (Bian et al., 2008). The mechanical characteristics of these size constructs are: 10-15% natural strain without rupture ($\sim$3.5 μm at an initial 23.3 μm), and passive, static stress of 15.6 $\pm$ 5.4 KPa (Powell et al., 2002). Many current methods also require that tissue constructs be removed from their incubators for conditioning. This temperature change may limit the cell growth due to drastic changes in its environment from body temperature to room temperature (Powell et al., 2002). The smaller diameter of the models uses less cells in the construct seeding process thereby reducing the amount necessary for seeding and increasing the output.

2.12.2 Cell Density

Another limitation to current methods includes tissues that are too thick and do not have vascularization/innervation. Similar issues arise with cells/unit area in attempts to layer skeletal muscle myoblasts within collagen matrices; however, the common result is necrotic tissue formation in the

middle of the constructs. This is due to the inability to incorporate vascularization/innervation to deliver

oxygen and nutrients the cells need to form contractile muscle tissue found in normal adults (Bian et al.,

2008). In order to avoid this lack of nutrition, there have been attempts to vascularize the 3D construct

to deliver the needed materials (Powell et al., 2002).

2.12.3 Vascularization of Constructs
Currently, there are limited means of embedding a vascular network within an in vitro 3D

skeletal muscle tissue construct. A few methods have been able to achieve creation of endothelial

networks within a C2C12 culture, which provided a means of blood perfusion and rapid vascularization

within the tissue after implantation. For larger in vitro tissue constructs, and tissues more

representative of in vivo tissue, tissues need to be cultured with a system that develops a blood vessel

network in a final tissue. The addition of endothelial cells and vascular endothelial growth factor, for

instance, would be a further direction to this particular project—which only focuses on a seeding culture

comprised of myoblasts and possible fibroblasts. Vascularization techniques would result in denser *in

vitro* tissues for testing and a better model of *in vivo* tissue (Bian et al., 2008).

This section presented a background examining clinical significance, muscle and myoblast

physiology, current methods for creating stimulation, and limitations of these methods. These findings

will drive the design process, as plans to address and improve upon the limitations of current simulation

systems to incorporate what has been learned from researching the physiology behind myoblasts and

the creation of tissue constructs.

Chapter 3: Methodology

3.1 Initial Client Statement
At the beginning of the project, the team was presented with the following client statement:

"Currently, the laboratory uses extruded fibrin microthreads with human skeletal muscle derived cells seeded onto the surface and transplanted into SCID mouse skeletal muscle injury models to study the effect of various cell derivation and culture methods on functional tissue regeneration. The use of animals is time consuming and costly which severely limits the number of parameters that can be evaluated. Currently, the microthreads are produced first and then cells with myogenic potential are seeded onto the microthreads using a rotational cell seeding system. The limitations of this system include the ability to only achieve a cell density limited to the surface area of the microthreads and the system is not compatible with long term culture to evaluate the differentiation potential of the cells in vitro. For cylindrical tissue such as skeletal muscle fibers to form, the cells must degrade the microthread material and proliferate and migrate into the core. The proliferation phase of the cell cycle is not compatible with the quiescent phase required for cell fusion and matrix synthesis needed for skeletal muscle tissue formation. This could to lead to premature breakdown of the tissue structure before the seeded cells can synthesize new matrix. An optimal situation would involve a system where cells could be seeded at the density required for cell fusion and tissue formation. However, the current microthread production process involves a stretching and drying step to produce axially aligned fibers, which is not compatible with seeding the cells within the microthreads at the time of formation.

A tissue engineered skeletal muscle system would enable the study of skeletal muscle tissue formation, maturation and the potentiality of cells entirely in vitro that could be used to approximate the utility of their use for the replacement of lost or damaged skeletal muscle tissue. The goal of this project is to design and produce a system that recapitulates skeletal muscle fiber structure into which myogenic cells can be seeded such that skeletal muscle tissue is formed. The system must be either produced aseptically or must be sterilizable and fit into

an incubator in order to permit study of live cultures over time. The engineered system should

further be amenable to the study of effect of mechanical strain and electrical stimulation on

muscle fiber maturation and contractile function."

This statement guided the team's initial efforts to understand the design problem, including initial research into the field of skeletal muscle tissue engineering. The first paragraph is interpreted as background on the project and the second paragraph as more of the need statement; from which the team later derived the objects and the client's needs. Objectives and constraints have been developed for design space from this statement, review of current literature, and interviews with client and user.

3.2 Objectives and Constraints

This section describes the main objectives of the project and analyzes the constraints upon which a design will be formulated. This was achieved through client feedback and literature review.

3.2.1 Objectives

After extensive literature review and client interviews, eight main objectives for the device were formed. These included the following: Provide electrical stimulation to muscle, provide mechanical stimulation to muscle, capacity of samples, user friendliness, efficiency, low cost, reliability, and compatibility with other plate sizes.

A Pairwise Comparison Chart (PCC) was completed by the user, Jason Forte, who is a graduate student in Professor Page's lab. He ranked the objectives in the following order from most to least important: reliability and consistency, mechanical advancements, electrical advancements, capacity of samples, user friendliness, and low cost. A copy of the chart can be seen in

Table 1: Objectives Pairwise Comparison Chart

Table 1.

	Reliability	Electrical	Mechanical	Capacity of Samples	User Friendly/ difficulty of use	Efficiency/ Accuracy	Low Cost	Compatibility with other plate sizes	Total
Reliability	X	1	1	1	1	1	1	1	7
Electrical	0	X	0.5	0.5	1	1	1	1	5
Mechanical	1	0.5	X	0.5	1	1	1	1	6
Capacity of Samples	0	0.5	0.5	X	1	1	1	1	4
User Friendly/ difficulty of use	0	0	0	0	X	1	0.5	1	2.5
Efficiently/ accuracy	0	0	0	0	0	X	0	0	0
Low Cost	0	0	0	0	0.5	1	X	0	1.5
Compatibility with other plate sizes	0	0	0	0	0	1	1	X	2

Upon further analysis, it was determined that the eight initial objectives could be compressed into four main objectives. The revised objectives included reliability, stimulation of muscular tissue, efficiency, and user friendliness. These objectives have been ranked in order of importance, and are

shown below in Table 2. In the revised version several objectives were combined into single groups such as "stimulation methods" which encompasses both electrical and mechanical design aspects. The category of "efficiency" includes capacity of samples and efficiency/accuracy to save time and money. The new category of "user friendly" combined user friendly and compatibility with other plate sizes. User friendliness will allow for the device to be intuitive and compatible with laboratory equipment.

Table 2: Revised Pairwise Comparison Chart

	Reliability	Stimulation Advancements	Efficiency	User Friendly	Total
Reliability	X	1	1	1	3
Stimulation	0	X	1	1	2
Efficiency	0	0	X	1	1
User Friendly	0	0	0	X	0

From the PCC, user friendliness was valued the least because efficiency is combined with accuracy and the other objectives were of higher value. User friendliness is still an objective and a goal for this project because every user values the ease of use and a device that is too complicated cannot be widely used without a steep learning curve. An objective tree, shown in Figure 29, was formed to provide further description of each objective, termed secondary objectives. Both the primary and secondary objectives are ranked from most to least importance. The primary objectives are presented in the rectangles, while the secondary objectives are presented in the circles.
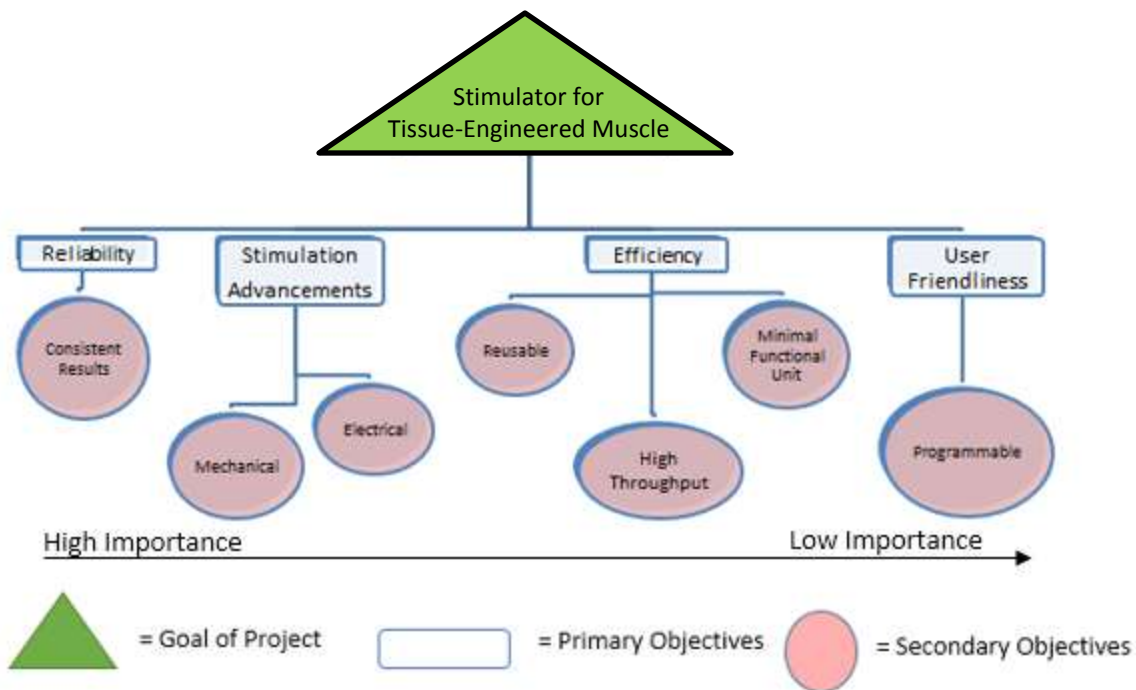
Figure 29: Objective tree for skeletal muscle stimulator showing breakdown of objectives. The objectives and secondary objectives are ranked from left to right, the left-most objectives having more importance.

Reliability was the highest-ranked primary objective. The user (Jason Forte) values accurate, repeatable results from the device over all other objectives. The secondary objective of reliability is reproducibility. To be reliable the device must produce consistent results and be durable.

Stimulation advancements were ranked as the next highest primary objective. The device must provide accurate methods of conditioning and stimulating the skeletal muscle tissue in a way that improves upon the current practice to mimic in vivo environments. This objective is comprised of two secondary objectives, mechanical and electrical. Mechanical stimulation advancements can be applied to either the dog-bone shaped tissue constructs or the ring-shaped tissue constructs. Electrical stimulation advancements may take the form of traditional probe (contact) stimulation, or the newer technique of electric field (contactless) stimulation. Mechanical stimulation is the main focus of this project, as determined by the client and user.

52

Efficiency is the third highest-ranked primary objective. The device should be reusable, capable of high output, and require a minimum number of cells for testing (by minimizing construct size). Minimizing the number of cells needed to create the tissue would reduce cost, minimize reagents, and space used. Minimizing the number of cells reduces the amount of time for tissue growth prior to stimulation. Reusability is ranked as the first secondary objective, since it would not be an efficient use of money to buy multiple devices for the stimulation purposes. Next, generating a minimal functional unit was ranked higher than high-throughput. Increasing the throughput for the larger scale replication of the stimulation is less important than using a minimal number of cells to create better engineered tissue that can function more precisely like adult skeletal muscle. To the user, it was more important to require fewer cells per tissue construct than to have a high throughput unit.

User friendliness is ranked last among all of the objectives. It should encompass an automated aspect of the device. If the device could condition itself, the user would not have to tend to the tissue as often. Therefore, the secondary objective for user friendliness is programmability. This system would ideally be programmable to run overnight and possibly over weekends to accommodate the user's schedule.

3.2.2 Constraints
A constraint is defined as a limitation of a factor contributing to the solution of the given problem. Constraints serve to narrow the realm of possibilities to find an optimal solution in given ranges, conditions, or materials. Based upon the initial client statement and research, the constraints are as follows:

- Design and materials must be sterilizable and/or assembled in a sterile environment; avoiding leaching/side effects of sterilization that affect cell culture.
- Design must withstand cell culture conditions (37 $^{\circ}$C, 99% humidity, and 5% CO_2)

- Budget consists of $156 per teammate which is $624 - $100 = $524 (for lab materials)

- Time limitation (25 weeks)

- Cell line available is the C2C12 cell line until there is proof of concept

- Cells are viable and functional only within a certain range of pH, temperature, and cell density

    ○ Cells can be frozen and thawed, but metabolic proteins denature around 32°C. Cells therefore must be kept above this temperature during functional tests.

    ○ Optimal pH is 7.4

    ○ At 75-80% confluence, cells lose myogenic potential

The above constraints must be taken into consideration when creating the design for the tissue constructs. Since the device needs to handle developing tissues, it must be sterile as to not contaminate the cells or induce foreign body response. Thus, the device is constrained to be sterilizable. Since cells need to be viable for testing and maturation experiments, they need to be kept at incubator conditions. The design must withstand the temperature, atmosphere, and humidity requirements inside the incubator. The budget restricts the expenditure and keeps the design within reasonable cost. To provide proof of concept for the design, the project is restricted to using C2C12 cells because they grow quickly, are readily accessible, and more easily cultured compared to human cells. However, these cells still need to be kept under specific conditions so that their proteins do not denature. Since skeletal muscle is anchored tissue, the constructs must be anchored to mimic bone attachment.

With these constraints in mind, a prototype will be constructed that satisfies the objectives within the capability of the constraints.

3.3 Revised Client Statement

From the client interviews and user feedback, the team gained better understanding of why this device is needed. Information regarding specifically what the client is trying to obtain from the device and key objectives, drive the design process. The client statement must revolve around client objectives and goals for the project. From the initial client statement, research, and interviews with users and client, the team developed a final client statement. This statement brings more focus to the client's needs and states project's relevance.

The revised statement was centered on the main objectives that the client wanted to address. For example, the client emphasized that the project should use in vivo metrics as a benchmark for the project success and that the interaction and manipulation of tissue culture should be justified by natural in vivo processes. The revised client statement focused on four main sections: 1) mimic the tissue interactions of the extracellular matrix by anchoring tissue to posts representative of myotendinous junctions; 2) allow for positive and negative strain of anchor points by mechanical stimulation; 3) electrically stimulate tissues to emulate motor neuron stimulated contractions; 4) determine the minimal functional unit necessary to accurately depict in vivo skeletal muscle tissue.

The client statement must capture client objectives and goals for the project. From the client interviews and user feedback, the team gained a more complete understanding of the need for this device. With this knowledge, key objectives, constraints, and functions were resolved from the initial client statement. From the initial client statement, research, and interviews with users and client, a final client statement was developed. This statement brings more focus to the client's needs and states project relevance.

Final Client Statement:

Researchers need a method to rapidly produce functional skeletal muscle models in vitro, enabling drug therapeutic screening and diagnostic testing for injury and disease. Currently, the methods used to generate skeletal muscle models are costly, inefficient, and fail to accurately replicate salient attributes of native skeletal muscle. The goal of this project is to develop a high-content in vitro system which conditions skeletal muscle tissue mechanically and/or electrically, more precisely simulating in vivo myogenesis and maturation, compared to current in vitro methods. The produced tissue should be a suitable/compatible model for future injury and disease modeling drug testing. There are several key characteristics of in vivo skeletal muscle that the system must address, along with parameters to facilitate high throughput testing:

1. *Tissue anchorage representative of muscle-myotendinous junction attachment.*
2. *Mechanical stimulation representative of muscle-myotendinous growth relationship, active muscle contraction, and passive muscle contraction.*
3. *Electrical stimulation representative of tetanic (biochemically-induced) contractions and myofiber alignment, in vivo.*
4. *Generation of minimal functional units of engineering muscle, to minimize seeded cell quantity, while still accurately representing in vivo skeletal tissue.*

The system must encompass a device in which the skeletal muscle tissue will mature and be stimulated in a way that mimics in vivo conditions. The device will include controllable, accurate stimulation through mechanical and electrical means. While working with a minimal functional unit of tissue, the device will maximize efficiency for a number of wells tested at a given time. The device must withstand in vivo conditions to better represent the environment in which native tissue matures. The four key points within the final client statement firmly establish the direction and

areas of focus of the project. The revised client statement was the basis for a project strategy—a

means to accomplish the tasks comprising this project.

3.4 Project Approach

This section outlines project approach and timeline.

3.4.1 Management Approach

For completion of the project in a timely manner, it is necessary to create a project timeline with

due dates. Division of tasks between team members also needs to occur in order to accomplish multiple

tasks concurrently. The project timeline and division of tasks is monitored through a Gantt Chart.

MQP Gantt Chart

ACTIVITY	START	DURATIO	START	DURATION	COMPLETE
Research Project	1	7	1	7	100%
Client Interviews	1	2	1	2	100%
Client Lab Shadow	3	2	3	2	100%
Brainstorming	1	7	1	7	100%
Chapters 1-3 Report	1	6	1	6	100%
Experiment with Agarose	9	2	9	2	100%
CAD Drawings	9	2	9	2	100%
Order Materials	9	3	9	3	100%
Build Prototypes	11	3	11	3	100%
Prototype Testing	12	3	12	3	100%
Improve Prototype	14	2	14	2	100%
Finalize Prototype	14	2	14	2	100%
Chapters 4-8 Report	5	20	5	20	70%
Tissue Analysis	20	3	20	3	50%
Device Implement	21	3	21	3	10%
Device Testing	21	3	21	3	10%
Finalize Report	25	3	25	3	0%
Presentation	28	1	28	1	0%

Figure 30: Gantt chart for MQP . Weeks 1-7 occurred in A Term, weeks 9-15 in B Term, weeks 16-22 in C Term, and weeks 23-28 in D Term.

The general task schedule can be seen above in Figure 30. As the project progresses, this schedule will be further broken down to allow each individual team member to have specified parts of each task to make the process even more efficient. A work breakdown structure can be seen below in Figure 31.

For further division of labor, the team has decided to split up into two sub-teams: one with emphasis on the biological aspects and the other with the emphasis on the mechanical and electrical aspects of the project. Team members are evenly split between specializations in tissue engineering and biomechanics, and therefore it will be beneficial for the members to work within their area of expertise. Spencer and Shreyas will be completing the biological tasks, while Syed and Stephanie will work on the mechanical and electrical tasks.
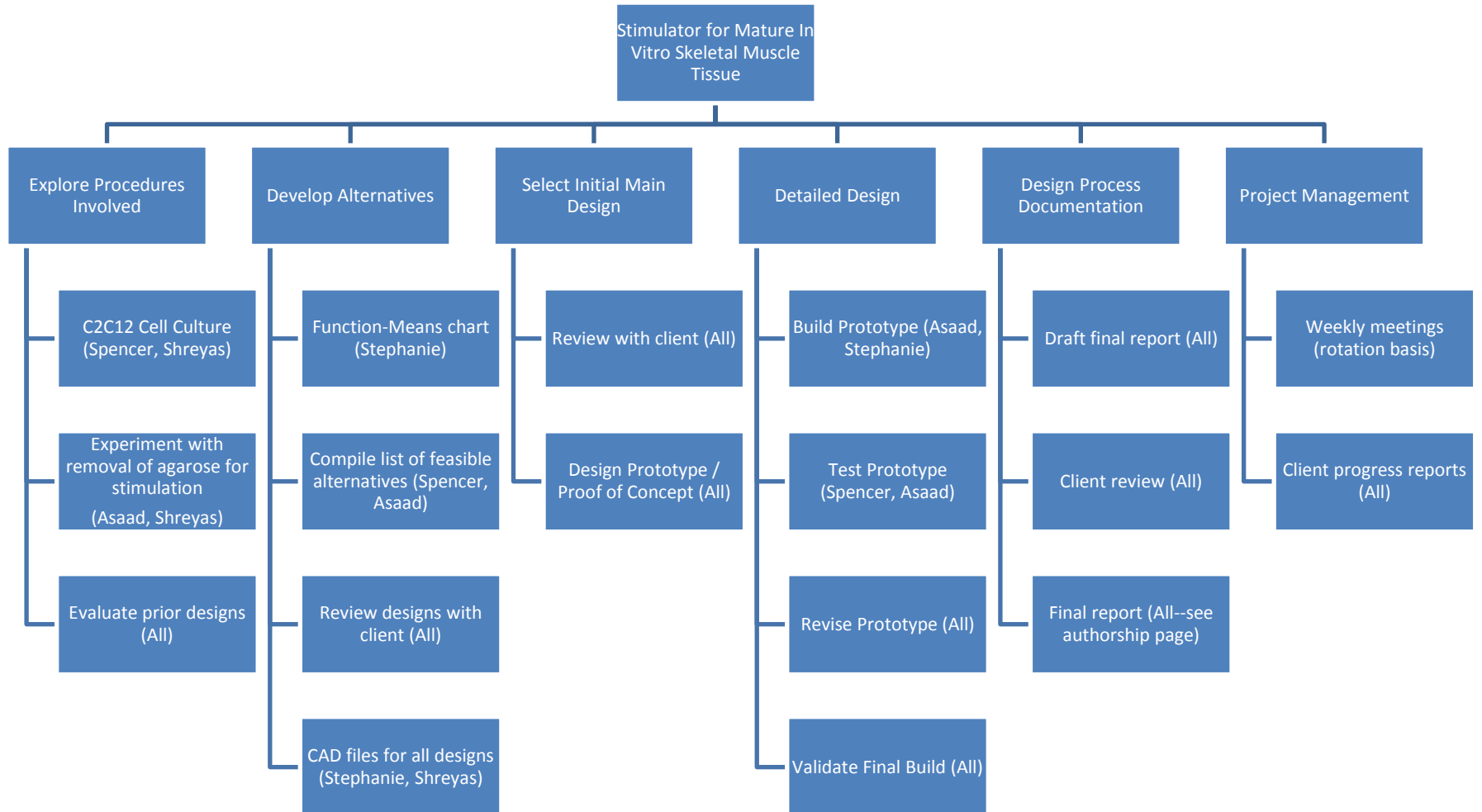
Figure 31: Work Breakdown Structure of MQP displaying tasks and subtasks for the project

Chapter 4 Alternative Designs

After iterative revisions of client statement following meetings with the users and client, the team developed clear objectives of what the device needs to accomplish. To help move towards a final design, the team laid out client "needs" versus "wants" listed below in the Needs Analysis section. As the team can see there are a multitude of design concepts to perform the desired function. Focusing on the pros and cons of each design in context to performing client needs, the team moves towards a finalized design.

4.1 Needs Analysis

From the revised client statement and discussion with the client and user, the team separated objectives into client needs (primary objectives) and client wants (secondary objectives). Constraints of time and budget were also considered when differentiating between needs and wants. The needs are the team's primary focus, and wants are desirable, but not necessary for success. The needs and wants are listed below and heavily influence the development of alternative designs.

Needs:

1. Mechanical stimulation of skeletal muscle tissue ranging from positive 50% strain to negative 50% strain (passive contraction)

2. Tissue anchorage representative of muscle-bone attachment

3. Stimulate myogenesis and tissue maturation from C2C12 cells

4. Ability to expand design concept for high-content testing

Wants:

1. Electrical stimulation of skeletal muscle tissue to test functionality of tissue. The primary focus of the design is on mechanical elements, which is why electrical stimulation will be addressed secondly.

2. Minimize the number of cells used per construct (current use is 400,000 total cells/construct, with 3 myoblasts per fibroblast) in co-culture.

Outside of needs and wants, basic requirements for a device interacting with biological materials include operating in a standard incubator space and incubator conditions (99% humidity and 37 degrees C), being able to be sterilized and last, but most important, results must be reproducible.

4.2 Functions (Specifications) and Means

There are several functions that the design must have in order to satisfy the client's wants and needs. The device must take into account for the specifications of these functions when considering feasibility of designs. Listed below are the five main functions with specifications needed for the project.

4.2.1 Mechanical Stimulation

The device needs to mechanical actuate in order to provide the tissue with positive and negative strain representative of active and passive contraction found *in vivo* during muscle myogenesis and maturation; this stimulation must be uniaxial. Uniaxial stimulation is more accurate of tissue development *in vivo,* thus the tissue must be a linear shape (dog-bone shape). The stimulation specifications should occur at least up to 20% positive strain and 5% negative strain at a rate of 0.5 Hz. These specifications are justified by the current literature as previously mentioned in section 2.8. Andersen et al 2014 performed a multitude of strain test on C2C12 cells and found optimal strains at 15% positive strain and 0.5 Hz, and to reduce the risk of tissue rupture negative 5% strain given to relax the tissue (Andersen, 2014).

The means of mechanical stimulation can include the following: machine driven means, such as a stepper motor driving a camshaft or scissor linkage system; fluid dynamic methods, such as a pneumatic or hydraulic pump; or posts made of a piezoelectric or thermos-responsive "smart" material

that can shape modulate to allow for both positive and negative strain. The methods can be done in patterns making them expandable to accommodate high throughput testing, 96 samples simultaneously.

4.2.2 Electrical Stimulation

Electrical stimulation by the device provides stimulation that is representative of tetanic contraction found naturally in the body. Specifications of electrical stimulation are dependent on the type of stimulation technique. Means of electrical stimulation can be contact or contactless, either through electrodes or electrical fields respectively. The ideal parameters for electrode stimulation occur at 4mA for 20 millisecond of stimulation at 1Hz (Hirokazu et. al., 2010). These specification for electrode stimulus not only result in a single contraction but improved magnitude of contraction and improve the number of responding cells. Greater number of responding cells shows greater functionality of the tissue as previously discussed in section 2.8. Optimal stimulation via contactless techniques are done using an AC power source consisting of 500mV at a power source frequency 1000 kHz, stimulated for 30 minutes daily with 24 hours between cycles, producing the best results for proliferation and differentiation (Zhao et al. 2009).

4.2.3 Tissue Anchorage

Tissue anchorage is a vital aspect of the project. The 3D self-assembly of myogenic cells into skeletal muscle tissue requires anchorage attachment points to direct the axial alignment of myofibers. For accurate modeling of native muscle, the anchorage method should simulate *de novo* bone attachment*,* creating uniaxial tension. Means of providing anchorage include: dog-bone, circumferential tension (ring shaped tissue), and uniaxial (self-assembly of monolayer into cylindrical tube) .

4.2.4 Using the Minimal Functional Unit

Cell culture experiments will determine the optimal efficiency of cells seeded per construct. This minimal functional unit will maximize efficiency of construct generation and allow for high-throughput

processing. The Vanderburgh group uses a gel thrombin/fibrinogen seeding method with a primary

human myoblast seeding density of 200,000 per construct. Current practice in the Page Lab uses

400,000 C2C12 myoblasts per construct. Minimizing the seeding density reduces materials and

resources needed and improves efficiency; however, past a point reducing seeding density would result

in undesirable loss in tissue functionality. Consequently, optimization testing will be conducted to

determine the least C2C12 cell seeding density required for the formation of contiguous tissue that

contracts into a dogbone shape, via active tension generated by differentiating myoblasts. C2C12

myoblasts do not differentiate as well as primary myoblasts into myotubes, and have reduced

expression of certain key components of myogenesis—notably lower expression of mRNAs that mediate

cell-cell adhesion (Grabowska et al, 2011). Compared to the Vandenburgh group's seeding density

(using cells in gel), the optimal seeding density for the minimal functional unit would likely be higher.

Due to limited budget, time, and resources, the chosen method is using C2C12 myoblasts in an

exogenous fibrin matrix that provides an extracellular matrix for the cells.

4.2.5 Differentiation

The differentiation of C2C12 cells into functional myofibers is one of the most important

functions of this project. Media is a key design component to the design, as it influences both the

growth and differentiation of the 2D cells into 3D tissues. Serum supplements are added to basal media

to set cells to either proliferate and differentiate—typically, high serum concentrations in media

maintain cells in proliferation mode, while low serum concentration induces cells to exit the cell cycle

and enter terminal differentiation.

4.3 Conceptual Designs

After clearly defining function and specifications, conceptual designs were developed. The conceptual designs are based off the group's brainstormed means. These brainstormed means are specified in

Table 3. The following conceptual designs separate each function and use various means to accomplish each individually.

Function	Means							
Mechanical stimulation expandable for high throughput testing	stepper motor	screw driven plate	vibration motor	scissor/ linkage system	pneumatic or hydraulic pump	piezoelectric material	conductive polymer	Thermos-responsive material
Electrical stimulation	electrodes	electric field						
Tissue Anchorage (tissue culture shape)	ring formation	dog-bone formation	monolayer (self-assemble dog-bone)					
Minimal Function unit	using C2C12 at 400,000 cells	using C2C12 less than 400,000 cells	using C2C12 more than 400,000 cells					
Differentiation (media types)	fetal bovine serum (fbs)	adult horse serum (ahs)						

4.3.1 Electrical Stimulation Means

For electrical stimulation it is necessary for certain components to conduct electricity. There are two leading methods on how to use conducting elements for electrical stimulation of tissue cultures. One method is directly inserting electrodes into the media and applying a voltage. The media will conduct a current to the tissue and this current causes depolarization within the tissue, resulting in a muscle contraction. The second method is electrical field stimulation. By running wires within 1mm of developing tissue, the tissue will be within an electrical field (Zhao et al, 2009). Placing the developing cells in an electric field also creates depolarization within the tissue, causing contraction. Conceptually, designs based on these means shall provide the system with the ability to electrically stimulate the tissues and mediate a contraction.

4.3.2 Mechanical Stimulation Means

There are a multitude of means to produce linear mechanical motion. To produce -5% to 15% strain in small tissues specimen, the design could incorporate motor and linkage systems, fluid dynamic systems, or specialized materials.

Motor systems are the most widely used mechanical systems to generate motion. They range from large/industrial motors to micro-scale motors, programmable for controlled use. Motor system can be very versatile. By manipulating the torque from motors the team can provide linear motion to links. These links can exist as sliding plates, threaded shafts, rollers and levers, and standards linkages and joints. These links can be specialized and directly provide precise mechanical stimulation to tissue cultures. Vibration motors can be used for small scale motion.

Fluid dynamic systems are another way to approach mechanical stimulation. The tissue cultures have to be submersed in a media fluid to survive. By manipulating media, the device could use material directly in contact with the tissue cultures to stimulate them. Fluid dynamic systems can also mediate mechanical stimulation, via hydraulic or pneumatic actuators.

Biomaterials comprise a large field in biomedical engineering. Typically, materials are not used to provide motion, but used more for their biocompatibility and as a scaffold. However, certain materials have the ability to expand and contract at changes in temperature or changes in voltage. The amount of force needed to strain these tissue cultures is very low, as mentioned in section 2.6. These thin myofibers provide little to no resistance to the expanding or contracting of these materials, which easily provide stimulation. Also, some biomaterials are bioinert and can be in direct contact with skeletal muscle cells to provide stimulation. By culturing tissue within constructs made of these materials, strain can be controlled through external stimuli.

4.4 Electro-Mechanical Preliminary/Alternative Designs

Using the conceptual designs and ideas of the previous section, alternative designs were created to fulfill the functions specified. In this section, the potential designs will be compared based on their functions, capabilities, and limits. From this comparison of alternate designs, it becomes clear which design is best to pursue and further build models, prototype, and testing.

4.4.1 Electrical Stimulation: Electrodes

Using electrodes is the traditional method to electrically stimulate tissue cultures. In this design, non-corrosive carbon-based probes are inserted into culture media. Other probes may be used based on resources and budget, such as titanium or gold electrodes. This completes an electrical circuit and a current can be generated across the tissue for active contraction. As Figure 32 shows, the electrodes would attach to a lid apparatus that would also actuate mechanically (via motor) up and down. When the lid is lowered, the circuit is completed and stimulation can occur. In this design there would be a power source outside the incubator with wires leading into the incubator to deliver the current. A preferred method is to have a power source outside the incubator due to the 100% humidity in the incubator. The power sources would be on DC current with adjustable voltage and current settings. In an experiment by Hirokazu et. al. (2010) 4mA (current) was used to stimulate C2C12 cells to contract, therefore this would be the primary setting for this device. This design uses proven methods and technologies for electrical stimulation. However, this design is complex, requires many parts, is difficult to expand for higher throughput, and would be more expensive than electric field stimulation.
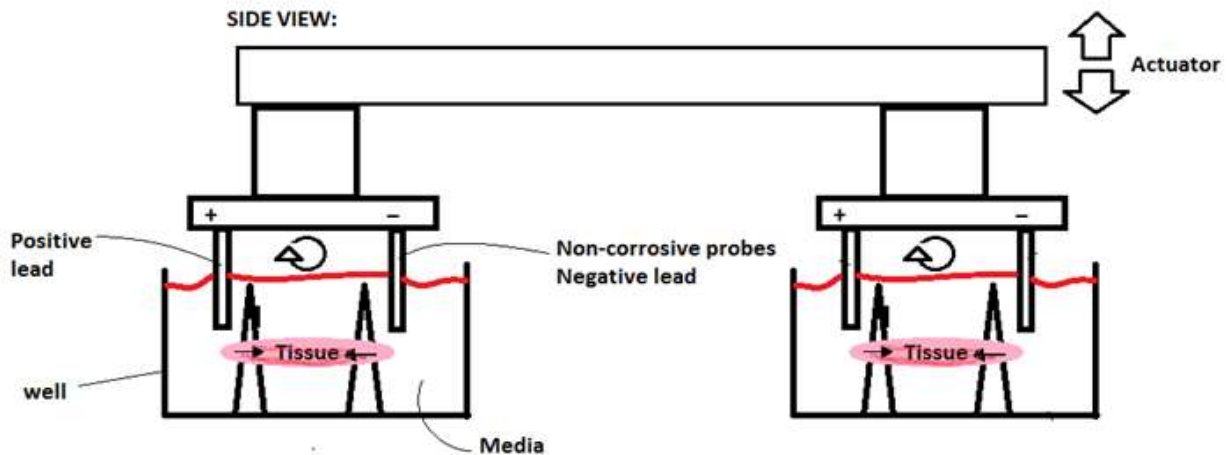
SIDE VIEW:

Figure 32: Electrode Design: This figure shows the side view of the electrode design, where probes are lowered into culture media, completing an electrical loop, and providing a current to pass through the tissue to mediate contraction.

4.4.2 Electrical Stimulation: Contactless Electrical Field

Another method for electrical stimulation is electrical field stimulation. Conductive wire or a

conducting metal plate is placed below the tissue culture (not in contact). As an alternating voltage is

applied, oscillating current passes through and generated a radial electrical field. The field stimulates the

tissue to actively contract. Figure 33 and Figure 34 shows a conceptual image of the theory behind

electric field stimulation. Figure 35 shows the wire mesh or conducting plate options.
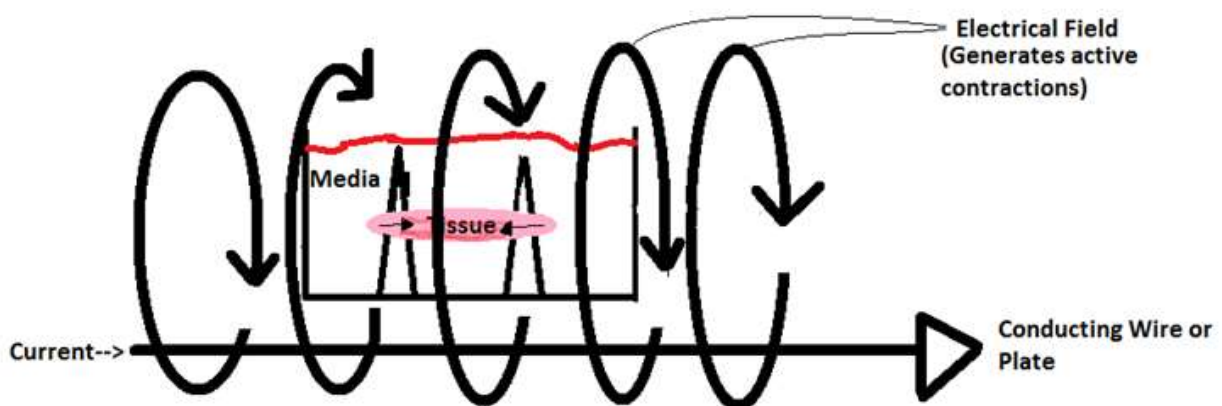

Figure 33: Concept of Electrical field Stimulation: As a current runs through the wire, an electrical field is generated radially, which then stimulates the tissue to contract.
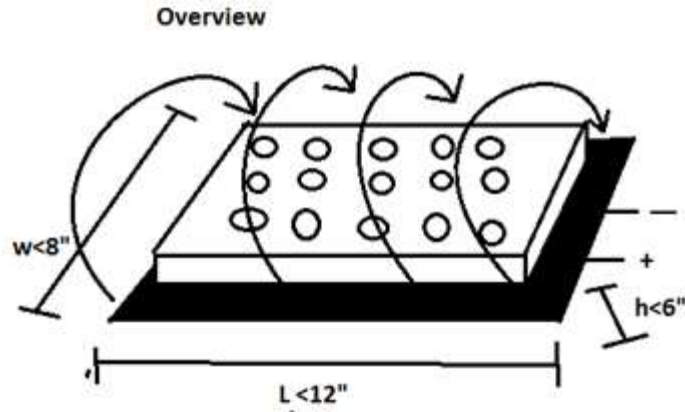
Overview

Figure 34: Overall design layout for electric stimulation: This figure shows the overall design using a solid metal plate. Wire patterns are dependent on the size and well density of the plate.
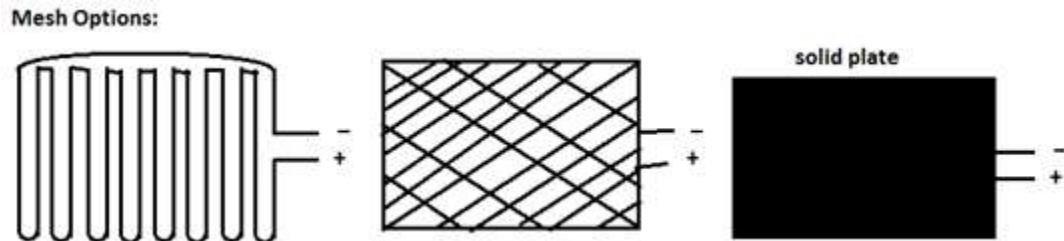
Mesh Options:

Figure 35: Options for wiring layout: This figure shows potential designs of laying down wire to generate an electrical field. The first option is the simplest for there is only one input and output for the current, thus it is easier to predict the electric field.

4.4.3 Mechanical Stimulation: Stepper and Cam

Cam and motors are one of the easiest and simplest ways to transfer torque to linear motion. Cams provide great control over amount strained and the strain rate. The following stepper motor and cam design allows for controlled strain of skeletal tissue, yet can be compact enough to fit inside an incubator. The amount of power needed to operate the cam to strain these tissue cultures is minimal. A 5 volts electric motor surpasses the design needed. The posts are initially 3.5mm apart, and to reach 20% strain, they move further apart by 0.7 mm. With such small distances to move, the design is not much larger than a common 96 well plate. The design is depicted in Figure 36.

Figure 36: Stepper CAM design: This figure shows the side view of the stepper cam design. It shows the working mechanisms of the design and how the mechanical stimulation would occur.
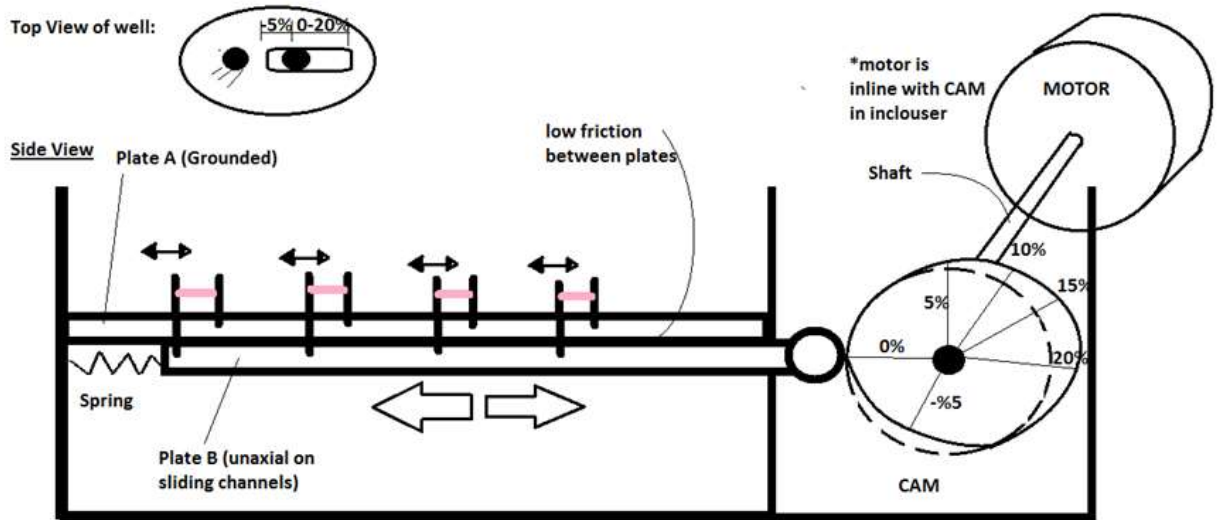
1. Well: This device requires a specialized well with one fixed post and one movable post. The movable post is able to strain the tissue from -5% to 20% strain from the fixed post. Each set of posts is attached to separate plates A or B.

2. Plates (A and B shown in Figure 36): Plate A is fixed to the housing of the device. The fixed post is anchored to Plate A. Below plate A is plate B attached to the "movable" post. Plate B is fixed on sliding channels, only allowing uniaxial motion. The sliding channels will also help to minimize friction. The materials chosen shall be bio-inert plastics with low coefficients of friction.

3. Cam: The cam controls the motion of plate B. The radii is directly proportional to -5% to 20% strain between the posts. Plate B remains in contact with the CAM via compressed springs (common cam and follower design).

4. Motor: The motor spins the CAM to push the follower (plate B). The motor is programmable for positive and negative linear motion. By making the motor programmable the user has control over amount strain and strain rate. The motor comes with a microcontroller and computer software for the user to be able to set exercise regimes. The motor is in the enclosure aligned

with the CAM to be compact, but is drawn offset to show the premise of the design. The

enclosure is airtight to prevent leakage and contamination.

One of the major problems with this design is leakage from the tissue reservoir to the lower

chamber. As seen in the top view of the well from Figure 36, media can leak through slits between

plates A and B. However, media is easily made. To counter the leakage, the design allows for

flooding. The outside walls are much taller than the post, thus the entire device can be flooded to a

point above the post, submerging the tissue completely.

4.4.4 Mechanical Stimulation: Screw Driven

The screw-driven design is similar to the CAM and stepper design, but the driver mechanism is

different. In this case, the design uses a long threaded rod or "screw", which converts torque from the

motor to the linear motion of plate B. The threads on the screw can push or pull plate B to specified

strains, thus moving the post to specific strains. The thread density is controllable and machining

techniques allow for high accuracy and precision. The leakage problem exists in this design as well, but

can be handled in the same way as the stepper and cam. Figure 37 gives a visual of the driving
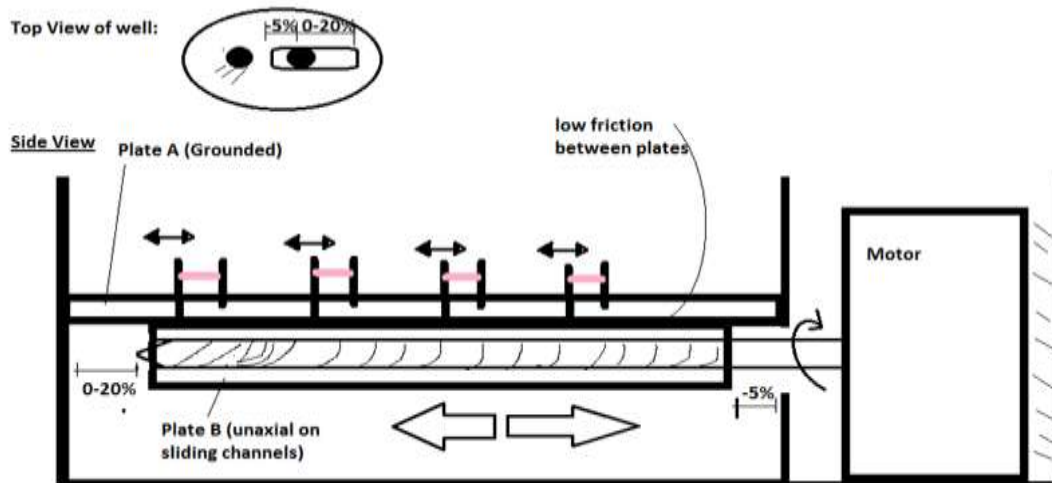
mechanism.

Figure 37: Screw Driven Design: shows the side view of the screw driven design. It shows the working mechanisms and how the mechanical stimulation would occur.

4.4.5 Mechanical Stimulation: Scissor Linkage

The scissor linkage design originated from observations of similar linkage systems in scissor lift platforms used by the construction industry, and in vehicular lift tables used by the transportation industry. It was clear that the distances between joints through expansion and contraction were reliably some function of force applied in the parallel direction to one end of the linkage system. This idea for mechanical stimulation would focus on strain rates varying from -5% to +20%. Similar to the screw driven method, this design is controlled by the movement of the structure. The compression and expansion is controlled through an external pneumatic or hydraulic pump. The pump fills a fluid sac within the base instigating compression and expansion. The sac may be substituted for a fluid base actuator to improve the controllability of the compression and expansion. The device itself would be comprised of a combination of polycarbonate and high-density polyethylene (HDPE) for its flexibility and sterility. A rough schematic of this design can be seen in Figure 38, where red lines are representative of the tissue constructs.
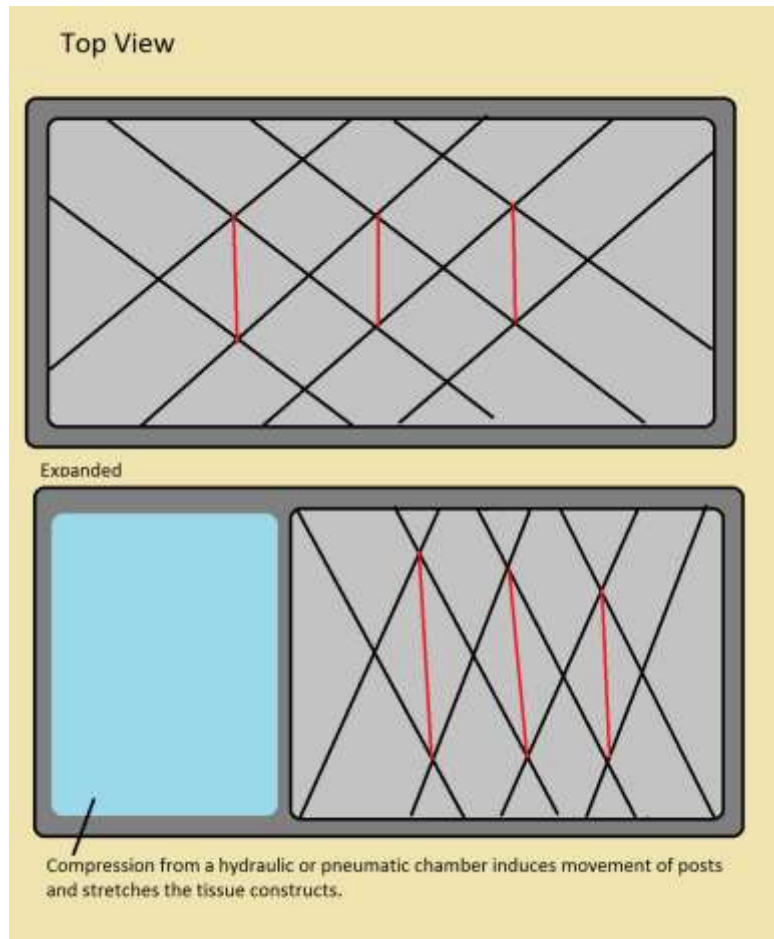
Figure 38: *Visualization of the Scissor Linkage Design: This figure shows the working mechanism under which this design operates.*

Problems with this design are the ability to manufacture/machine all the tiny links, ability to expand for high-throughput, toughness of device (fragile parts), and consistency of strain rate for all test samples. With precision, low-tolerance, manufacturing processes, this design is feasible.

4.4.6 Mechanical Stimulation: Sublevel Deformation

This design, much like the two previous, is controlled through a movable base component. In this case a roller is moved along the bottom of the posts thereby inducing compression and extension on the tissue constructs. This method is not as viable for many reasons. Firstly, a constant strain rate is more difficult to achieve. Secondly, there are several moving parts that would need to be carefully coordinated. Thirdly, the method to move the posts proves to be problematic. For example, if the roller

bar was moved via gravity forces (i.e. via tilting the plate), it would then require physical rotation and the tissues could fall off of their posts; there would also be no way to control the strain rate accurately. If the roller bar was on a string or wire, it could be controlled by an external motor which could enable more controllable mechanical stimulation. Figure 39 details this design:
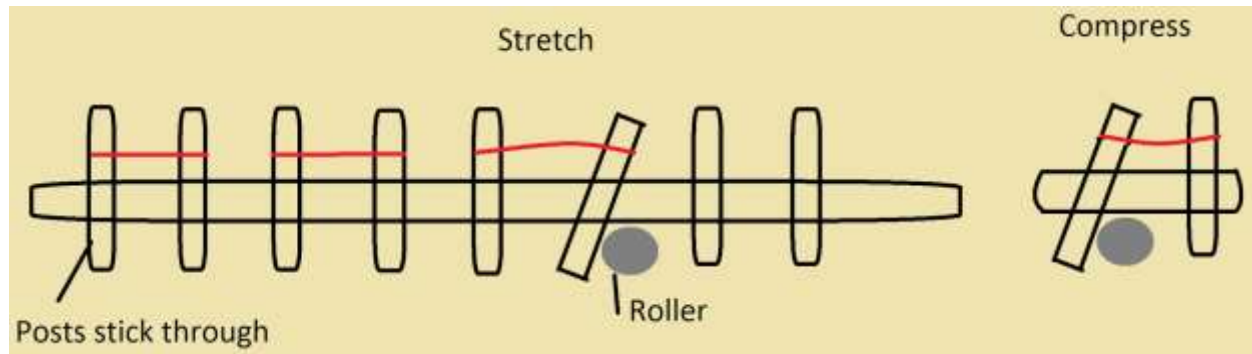
Figure 39: Visualization of the Sublevel Deformation Design: This design uses a roller and lever arm to mechanically stimulate the tissue. The roller pushes a post (back or forth) pivoting around a fulcrum, stretching or relaxing the tissue.

4.4.7 Mechanical Stimulation: Pulsatile Method

The pulsatile method would mediate increases in force production and parallel fiber orientation through uniaxial vibration. Vibration has been shown to increase in tissue construct stiffness and improve myofiber alignment (Milano, 2014). The ideal vibration device, seen in Figure 40, would be capable of varying its frequency from 0.5 Hz - 2.5 Hz, which would induce a stretch length of 3.5 µm in the positive and negative directions and pulse duration from 0.5-250 ms. This method does not compare directly to *in vivo* because the body does not have micromotions in the same manner; the closest equivalent would be stretching before exercising.
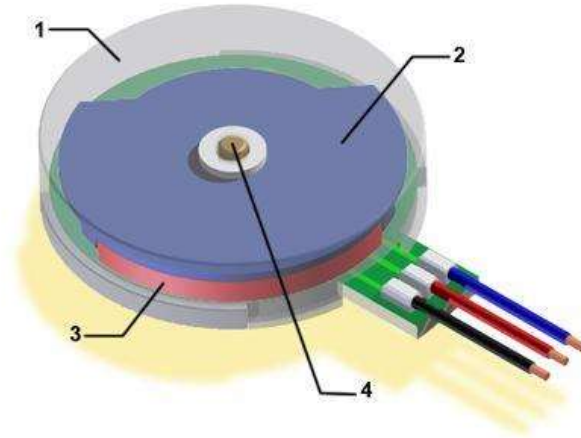
Figure 40: Coin-type vibration motor. A relatively flat eccentric weight spins in a protective enclosure. (1) enclosure, (2) rotor base, (3) weight, and (4) shaft (Milano, Shaun. (2014). Allegro MicroSystems, LLC.)

In Figure 41, the overall design can be seen. The tissue is either placed or molded to two posts, and forms anchored uniaxial tissue constructs. The posts are attached to a base, and this base is attached to the vibration motor. The vibration is transferred to the post which will positively and negatively strain the tissue. The issues with this design is that the strain reached by the design is not able to reach the specification. However, this could be supplemented with another design or could be used as a pre-exercise regime for the tissue.

Flexible posts for contractile forces and motion

Vibration motor inducing positive and negative strain

Vibrating base causes the posts to move

The entire unit would be self contained, and need only a start and stop for vibration. The downside would be limited variety other than change in vibration intesity/frequency.

Figure 41: Visualization of the pulsatile design with high-throughput modeling.

4.4.8 Mechanical Stimulation: Fluid Dynamic Designs

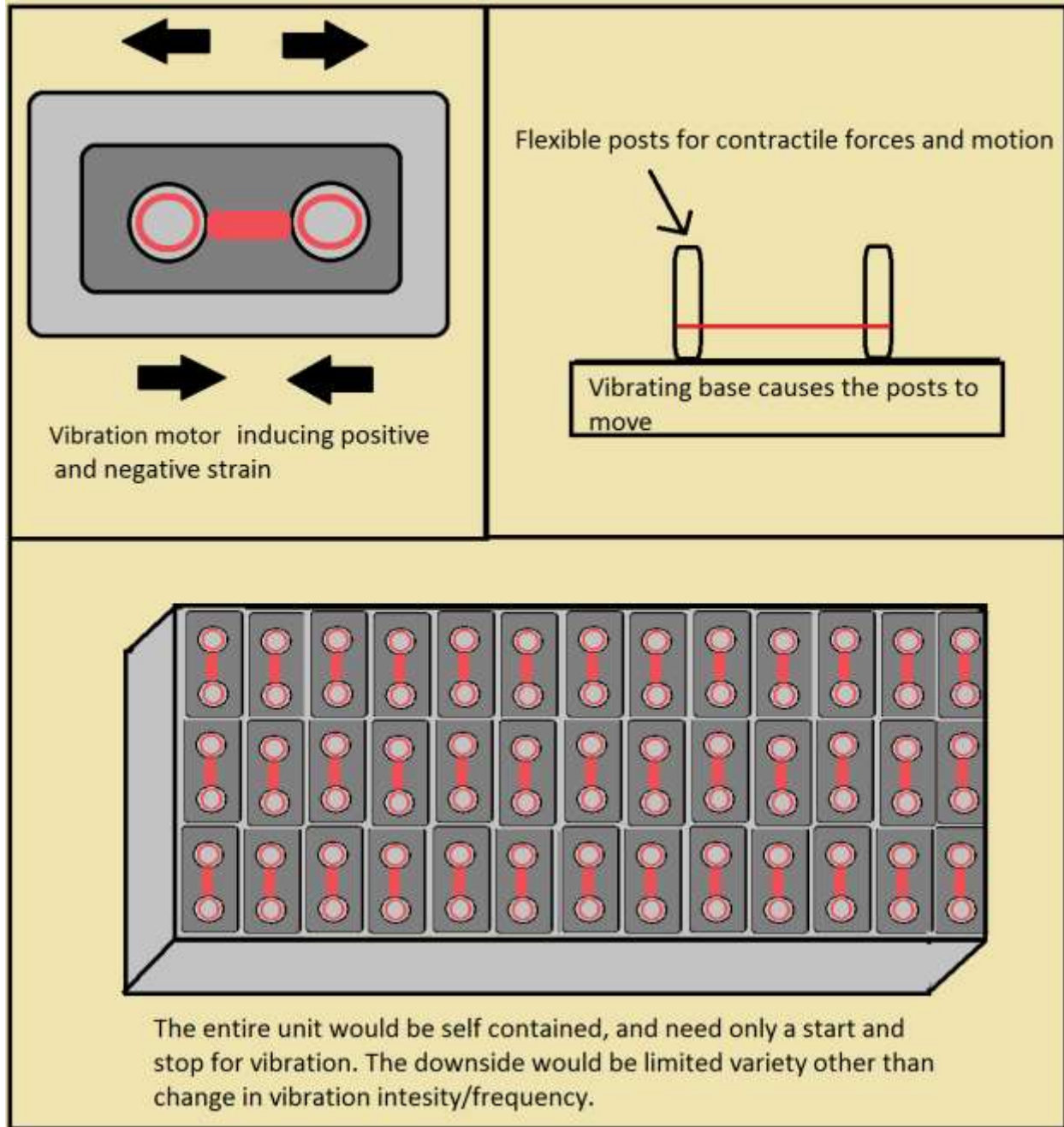Using hydraulic forces is another way to mechanically stimulate the skeletal tissue. This design would use a syringe pump to expand or collapse the scaffolding. As the scaffold inflates positive strain occurs, while deflation results in negative strain. The posts rest on a flexible base, which brings tissues apart or together based on the change in pressure. An airtight model could be designed to permit strain between -5% to +20%. The force applied to the tissue constructs can be calculated based upon the angle of the posts and the pressure within the scaffold. As seen in Figure 42, a tube would lead outside of the incubator so that the driving mechanism would not be constrained to the size or atmospheric requirements of the incubator.

There are many fluids that can be used to provide force transmission in this design. It could be pneumatic or hydraulic. Using a pneumatic source is cheaper, and easier to maintain. Using an incompressible hydraulic source allows for greater accuracy and precision. Fluids such as mineral oil can keep constant volume at various temperatures –room temperature to incubator conditions because of low coefficient of thermal expansion. However, one downside of hydraulic systems is potential buildup of mold/fungus/bacteria. It may be harder to maintain a sterile system using hydraulics, due to diffusion and leakage concerns. To prevent these risks, the fluid should be changed regularly and only sterile fluid should be used. Figure 42 and Figure 43 show the pneumatic and hydraulic designs.
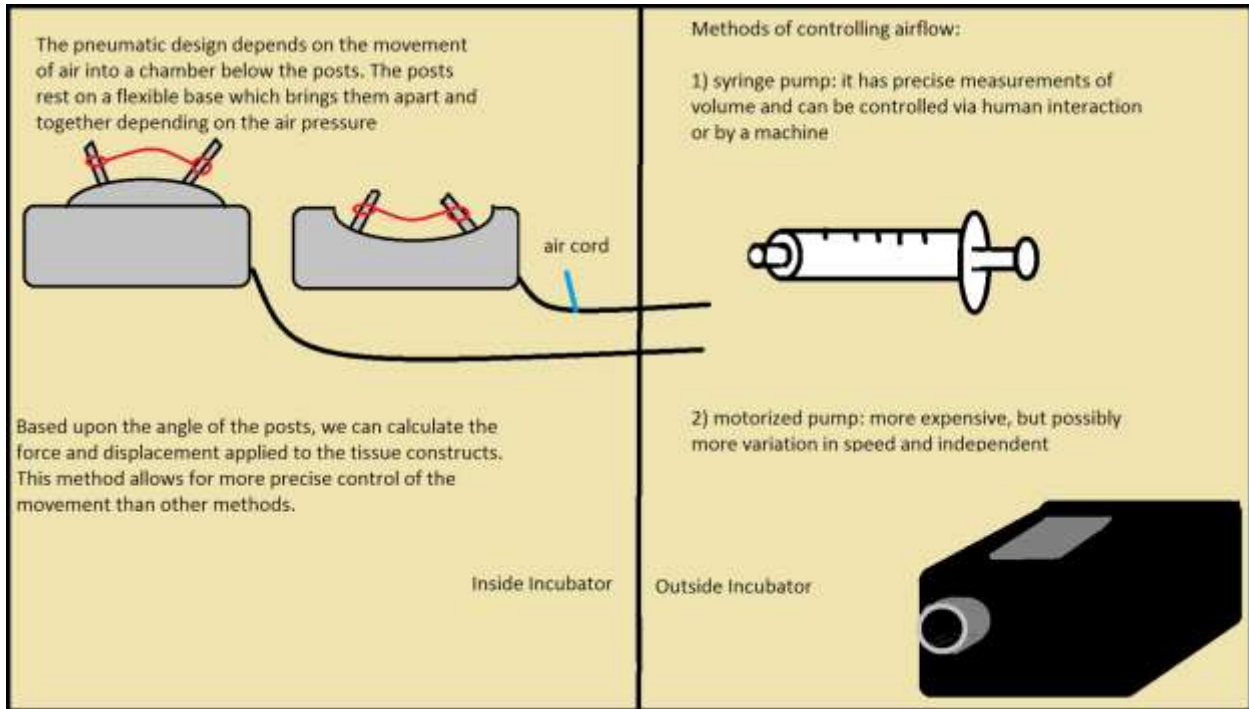
The pneumatic design depends on the movement of air into a chamber below the posts. The posts rest on a flexible base which brings them apart and together depending on the air pressure

Based upon the angle of the posts, we can calculate the force and displacement applied to the tissue constructs. This method allows for more precise control of the movement than other methods.

Inside Incubator

air cord

Methods of controlling airflow:

1) syringe pump: it has precise measurements of volume and can be controlled via human interaction or by a machine

2) motorized pump: more expensive, but possibly more variation in speed and independent

Outside Incubator

Figure 42: Visualization of the pneumatic design showing mechanism in design to cause strain

The hydraulic design depends on the flow of water into the chamber below the posts. The posts rest on a flexible base which brings them apart and together based on the water pressure.

Based upon the angle of the posts, we can calculate the force and displacement applied to the tissue constructs. This method allows for more precise control of the movement than other methods.

Inside Incubator

While air is compressible, liquids such as water are not. However, a downside to hydraulic designs are evaporation of the liquid, buildup of mold/fungus/bacteria. To prevent evaporation and contamination, the water should be changed regularly and only distilled or autoclaved water.

Methods of controlling volume of water

1) syringe pump: it has precise measurements of volume and can be controlled via human interaction or by a machine

2) motorized pump: more expensive, but possibly more variation in speed and independent
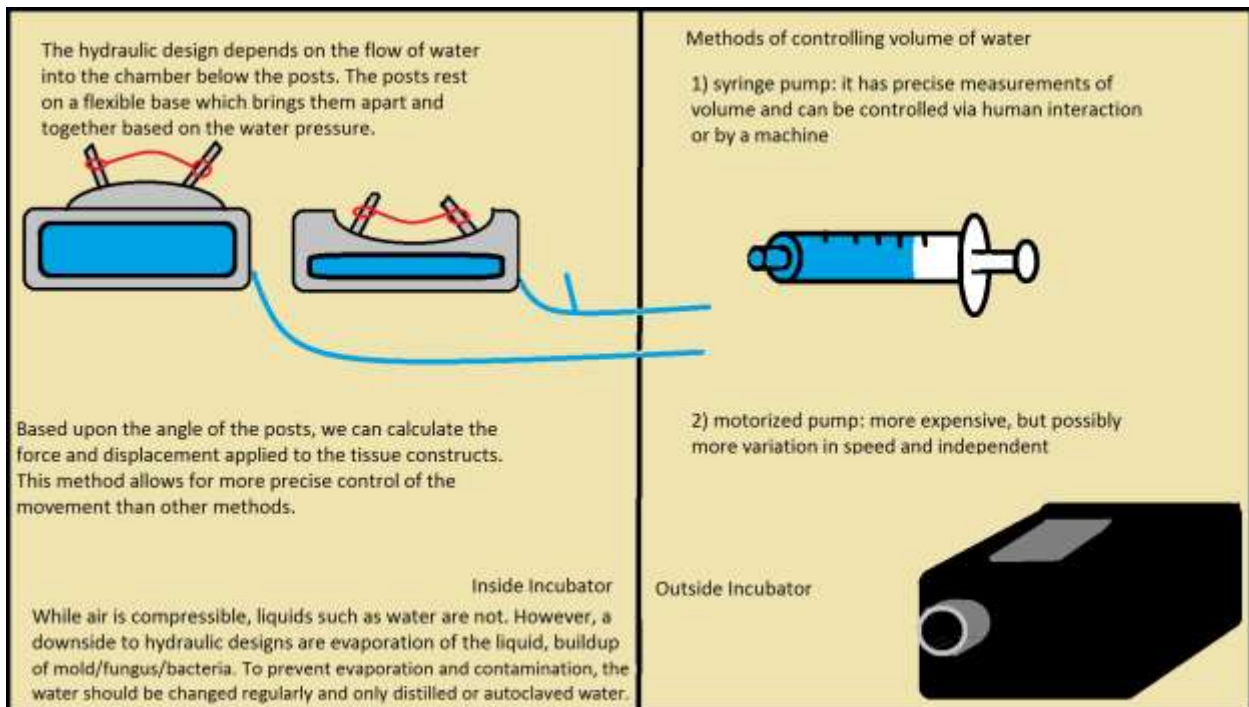
Outside Incubator

Figure 43: Visualization of the hydraulic design showing mechanism in design to strain the muscle constructs

4.4.9 Mechanical Stimulation: Biomaterials Design

Biomaterials can be used for the mechanical tissue stimulator due to their biocompatibility and conformational changes based off stimuli. The design expands to thermo-responsive materials, conducting polymers, and piezoelectric materials. Based off their specific stimuli, these material expand or contract. An example of one of these piezoelectric materials is shown in Figure 44. As a voltage is applied the post constructed of the material expands, thus stretching the tissue. The removal of stimuli causes the polymer to revert to its original size. Controlling the stimulus means controlling the circumference or the strain. Based on the control of the stimulus, directly correlates to control over strain. The rate and magnitude of stimulus change would be proportional to strain rate and amount strain. Preferably, this design uses conductive polymers or piezoelectric materials, that way only a power supply is needed (which can be kept outside the incubator). It is easier to program a power supply to control rate and magnitude for electrical stimulus than to change temperature in an incubator. Thermo-responsive materials require temperature changes in the incubator, which is impractical.
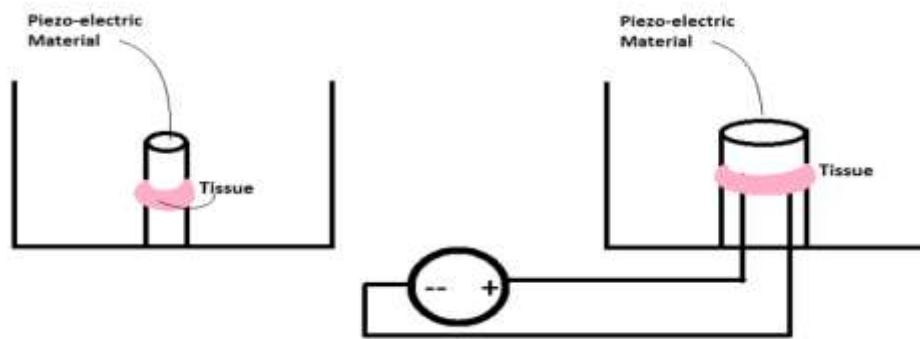

Figure 44: Material Design (Piezoelectric example) for mechanical stimulator. In this figure, the post is piezoelectric. When a current is passed through the material it expands radially, straining the tissue that is cultured around it. This concept can be applied to thermo-responsive and conducting polymers.

4.5 Tissue Formation Techniques and Alternative Methods

There were two main tissue construct formations used in this project: ring and dogbone shaped constructs. The ring tissue constructs originated from vascular tissue ring molds and were used as proof of concept because the rings were more stable and easier to create than dogbone constructs.

Throughout the experiments, C2C12 immortalized cell line was used because they grew at a reliable rate and had myogenic potential greater than 90%.

4.5.1 Ring Tissue Formation

Ring tissue constructs were created in 2% agarose molds that were cast from a reverse positive PDMS mold (attained from Page Lab). Hot liquid agarose was poured into the reverse positive PDMS mold, which formed the agarose into 5 annular wells with a post in the center (2mm diameter). The agarose was removed from the PDMS after solidifying and C2C12 cells were seeded into the wells at a density of 400k/55µL. There was limited self-assembly testing performed for ring constructs because the dog-bone structure was more mimetic of myotendonous junctions than ring constructs.

4.5.2 Dog-bone Tissue Formation

Dog-bone tissue formation is more complex than ring tissue because it requires the cells to form/fuse to make tissue around two posts, with an adjoining section between them. This complex geometry results in a less successful formation percentage. The posts are representative of cellular attachment to bone *in vivo*, but certain groups such as the Vandenburgh Group (1991) employed clamps at each end of a construct instead of forming the tissue around posts. One of the main goals is to perfect a means of "self-assembly", which is the ability for cells to form around posts themselves, without the use of ECM or other protein cues. This can be formed with gel seeding methods such as a fibrin/collagen gel; however, these methods lack native ECM and contain too much synthetic ECM. The alternative is increasing the density of cells to form a similar construct, but this ultimately results in a greater amount of necrosis in the center of the tissue.

There are several molds that aid in dogbone tissue construct formation. PDMS molds are mostly bioinert and can be used as a 3D guide to direct cells to fuse together or simply posts in self-assembly seeding. The trough method is not preferred because transfer of tissue to a device could lead to rupture

or damage. The self-assembly methods are much more complex with the need for an ECM that could pull the cells together and hold them in place (the mold/trough performed this task).

Two materials that mirror each other's thermo-responsive properties to form molds are NIPAAm and agarose. NIPAAm is solid at temperatures over 32 C and is liquid below (Lian et al, 2012), while agarose is solid at 45 C and below, and liquid at higher temperatures. Agarose holds shape at room temperature when molded, whereas NIPAAM begins to melt. If the project requires easy removal of construct, NIPAAM can be cooled, liquefied, and then removed. Agarose would need to be melted at high temperatures to achieve this same ability, which would most likely boil and kill the cells. NIPAAM was selected in this project because of its easier removal and manipulability.

4.6 Comparison of alternative designs

Design Pros, Cons, and Cost Comparison

Table 4 compares all the pros and cons of the alternative design means. These pros and cons help to eliminate means that will not lead to the optimal design. Costs were estimated by general pricing from common hardware providers, namely *McMaster Carr.* The allowed budget is $524 for supplies not include in the lab fee. Table 5 compares pros and cons of electrical stimulation methods. Table 6 compares pros and cons of mechanical stimulation methods.

Table 4: All potential design means to perform objectives, pros, cons, and cost.

Design Mean	Pros	Cons	Cost
Electrode	• Improve fusion between cells • Stimulate tissue representative of tetanic contractions	• Must be used in addition to mechanical method • Sterile is difficult to maintain • Difficult to expand for high throughput	$135

Electric Field	• Less expensive (compared to electrode method) • Improve fusion between cells • Stimulate tissue representative of tetanic contractions • Less cell damage than probe method • Easily to maintain sterility and easily implemented	• Must be used in addition to mechanical method • Weaker cell fusion rates than electrode based simulation • Not as developed in literature (not much work proving validity)	$130
Stepper Motor and Cam	• Well developed • High precision and control over strain • Uses commercial plate dimensions	• Friction • Motor in incubator • Leakage	$430
Screw Driven	• High controllability	• Friction • Motor in incubator • Leakage	$430
Vibration	• Easily manufacture-able	• Strain Specification not met	$230
Scissor Linkage	• Large range of mobility • Aesthetically pleasing	• Complex • Lack of control over distance • Difficult to prototype • Many fragile parts	$500
Hydraulic/ Pneumatic Pump	• Minimal risk for contamination to tissue • Smooth motion of moving posts • Capable of manipulation in 3D	• Complex design • Multiple parts/bulky • Higher Maintenance	$410
Piezoelectric	• Inexpensive material • Compact and stiff system • Can be used for 3D	• Require high voltage for displacement. • Difficult to shape post	$270

	manipulation		
Thermo-Responsive	• Ability to melt out material to extract cells	• Limited material selection due to restricted range of cell viability • Slower contraction rate of posts • Requires change temperature in incubator	$325
Conductive Polymer	• Provide support scaffold • Mechanical and electrical stimuli can be transferred through this single material • Bio-functional	• Possible low degrees of proliferation/cell adhesion/differentiation • Possible high surface roughness	$325

Table 5: Means comparison for electrical testing

Design Means	Cause active contraction by Tissue (Most Important)	Expandable for high throughput	Operates at least at Frequency of 1 Hz	Representative of muscle bone attachment (uniaxial) (Least Important)	Number of Functions Fulfilled
Electrode	Yes	Yes	Yes	N/A	3/3
Electric Field	Yes	Yes	Yes	N/A	3/3

Table 6: Means comparison for mechanical stimulation

Design Means	Strain -5% to 20% (with initial length of 3.5 mm)	Representative of muscle bone attachment (uniaxial)	Expandable for high throughput	Electric/power components outside incubator	Operates at least at Frequency of 1 Hz	Number of Functions Fulfilled

	(Most Important)				(Least Important)	
Stepper Motor and Cam	Yes	Yes	Yes	No	Yes	4/5
Screw Driven	Yes	Yes	Yes	No	Yes	4/5
Vibration	No	Yes	Yes	Yes	Yes	4/5
Scissor Linkage	Yes	Yes	No	Yes	Yes	4/5
Hydraulic/ Pneumatic	Yes	Yes	Yes	Yes	Yes	5/5
Piezoelectric Material	Yes	No	Yes	Yes	Yes	4/5
Thermo-responsive	Yes	No	Yes	Yes	No	3/5
Conductive Polymer	yes	No	Yes	Yes	Yes	4/5

4.6.1 Discussion of alternative designs comparison

From the preceding Table 5 and Table 6 and data, the project team was able to eliminate

aspects of designs that were not useful and focus on combining aspects from designs that fulfilled client

needs, functions, and specifications.

From the large pool of design means, the team eliminated many options due to not being able

to meet project needs or function specifications. The first ideas eliminated were all the biomaterial

based designs (piezoelectric, thermos-responsive, and conductive polymers) due to their inability to

85

model muscle-bone attachment. The materials based designs only functioned with rings of tissue, but dog-bone shape tissue constructs were preferred. Motors were the next aspects eliminated from designs, because motors have to be in the incubator for the designs to function. This was undesirable. Vibrations motors didn't reach strain specifications.

From the pool of design means, the team pulled out aspects of designs that functioned well. These aspects meet specifications and can be combined to form better designs. Using hydraulics for the driving force of the mechanical stimulation optimizes the design by fulfilling all design function, unlike other means. Pneumatic was eliminated due to the compressibility of air. Air can compress at body and room temperature and cause overshooting in strain, thus impeding on accuracy and precision. For the mechanisms directly straining the tissue constructs, both the sliding plate techniques and scissor linkage method were both viable options and filled requirements. For electrical stimulation, both electrodes and the electric field stimulation were viable options. From the viable function left, further models and experimental testing was performed to help optimize the design.

4.7 Experimental/Design Validation

This section describes the experimental and validation testing performed to further the design ideas and improve the components of the final design. The experiments are meant to determine if materials, methods of stimulation, and methodologies need improvement or are not compatible with the design.

4.7.1 Tissue Ring Validation Testing for Preliminary Experiments

Successful ring formation can be seen in Figure 45 and Figure 46. The agarose posts are 2 mm in diameter and the thickness of the cells in the table above display a thickness of less than 1 mm. This is either evident of over-seeding, loss of myogenic potential, or lack of differentiation. Notice how the rings below are much thinner, individual cells cannot be distinguished because of the cellular fusion, and the tissue has contracted around the post.
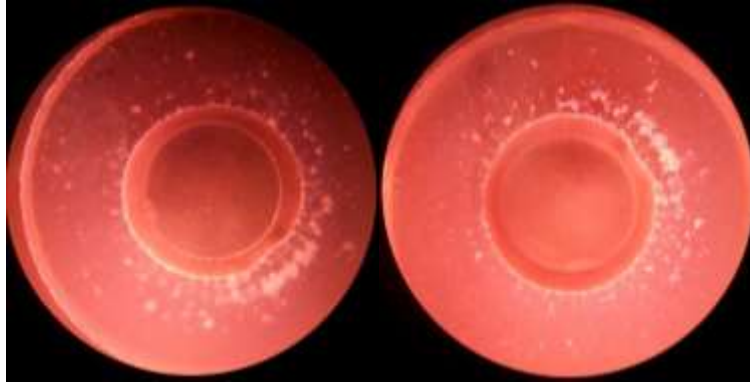
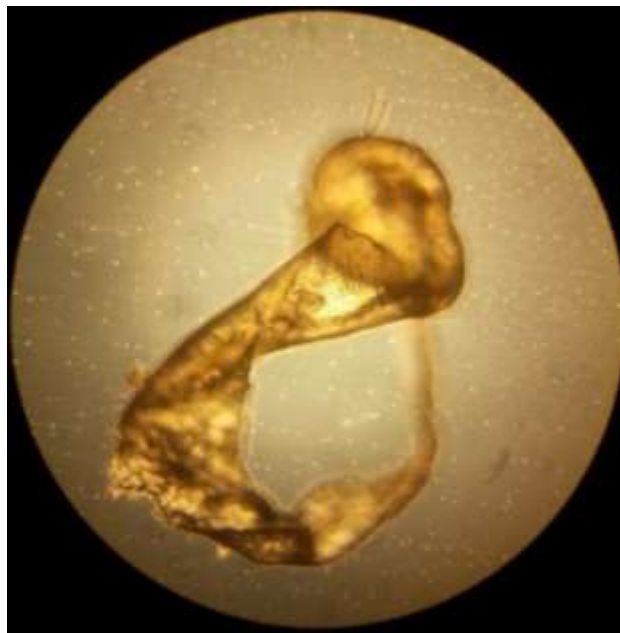Figure 45: Successful ring formation from a previous experiment.

Figure 46: From a prior experiment this ring displays tissue formation and cellular fusion as well as some internal structure.

The C2C12 cells used in the experiment had been through 21 passages. In that time they had

become very confluent during some of the passages, which potentially led to a decrease or loss in

myogenic potential and loss of contractibility. These cells have not been continued in culture.

In case inadequate ring formation observed was due to loss of myogenic potential of cells, a cell

culture will form from a fresh frozen stocked of C2C12 cells. To study cell morphology in the formed

tissue, histological staining will be conducted on horizontal slices of fixed tissue. The same stains as in

the Cell Differentiation Assay were used —Hoechst 33342 for nuclei, AlexaFluor 488-tagged anti-myosin for presence and morphology of myosin protein.

4.7.3 Staining/Cell Validation

Before the C2C12 cells are seeded into molds for tissue formation, the cells are incubated for a period in mitogen-reduced differentiation media. Incubation with a large reduction in serum within the culture media induces the cells to exit the cell cycle and enter terminal differentiation. This period is critical to maximize myogenic potential and synchronize the culture for tissue formation from cell seeding. It is important to study the rate at which cells differentiate during this incubation time in differentiation media, as this provides clues about myogenic potential at cell seeding. Additionally, as studying cell differentiation (See "Tissue Histology", below) is a prolonged and complicated process, studying differentiation rate in 2D culture also provides a general reference value for the rate of C2C12 cell differentiation.

To evaluate cell differentiation rate, the team conducted a staining assay on 2D cultures of C2C12. Different, known numbers of cells were seeded in two control wells (in proliferation media) and then in two treatment wells (in differentiation media). This variation was set up so as to observe myotube formation at different (2D) cell densities. 5,000 cells were seeded in the first control well, and 25,000 cells were seeded in the second control well. 50,000 cells were seeded in the first treatment well, and 75,000 cells were seeded in the second treatment well. The setup of each row (two control wells, two treatment wells) was carried out in quadruplicate. Wells were imaged at 0 days, 3 days, 6 days, and 8 days. After at least 8 days of incubation in differentiation media, myosin fibers and cell nuclei were assayed for. Though myosin is already present in undifferentiated myoblasts in very small quantities, myosin quantity increases dramatically over differentiation, concentrates around the nucleus, and forms filaments as the myoblasts fuse to form myotubes. Thus myosin serves as a late-stage marker for C2C12 cell differentiation. Myosin fibers were visualized via a green-fluorescent

immunocytochemical stain, with mouse anti-myosin IgG as a primary antibody (MF 20, Developmental Studies Hybridoma Bank), and isotype-specific goat anti-mouse IgG (Alexa Fluor® 488 conjugated Goat Anti-Mouse IgG (H+L)) as a secondary antibody. Cell nuclei were imaged via the blue-fluorescent Hoechst dye (Hoechst 33342, Thermo Scientific Pierce), which selectively binds to DNA, thus allowing for visualization of the nucleus. With images from fluorescence and phase-contrast microscopy, two indices were calculated. Using myotube formation as a measure of cell differentiation, the percentage of nuclei in myosin-positive cells allowed for a quantitative analysis of myotube formation. The differentiation index was calculated as the ratio of (number of nuclei inside myotubes) to 100*(number of total nuclei) after at least 8 days of myogenic differentiation. The number of nuclei was estimated by averaging the number of nuclei counted in twenty separate, randomly-chosen microscope fields. The number of myotubes was similarly determined, but a myotube was defined by the presence of at least three nuclei within a continuous cell membrane. This calculation of differentiation index follows the calculation of Goudenege et al (2009).

4.8 Modeling of Alternative Designs

From the viable means left, the team began to model two potential options for the mechanical aspect for the final design. Modeling gives the client and user more of a hands-on view of the potential design, and allows the inventors to map out how to manufacture the device. There are many types of models, but the following two are functioning models (mechanisms only). This means the mechanics of the models accurately represent how the device will function, but is not made of the ideal materials or to the correct size yet. Both models were initially developed on a 6-well plate.

4.8.1 Scissor Linkage Model

This design was selected for modeling due to the relatability of applied hydraulic force to output mechanical strain from the design. The final scissor linkage model was constructed using two rows of separate scissor links. The linkage system in each row of the plate consists of interlocking stiff segments,

which extend linearly when a parallel force is applied on one end. For ease of construction, the model's

interlocking segments were fabricated from repeated units of a cardboard pattern. Figure 47 shows thiis

pattern.

Figure 47: Repeating unit of Scissor Linkage design

This design was planned with the aim that a final model would be constructed with segments of

laser-cut metal or stiff plastic (polycarbonate or polystyrene). Short acrylic rods, extending upwards

from the linkage, were used to simulate posts for tissue anchorage. Figure 48 provides a side view

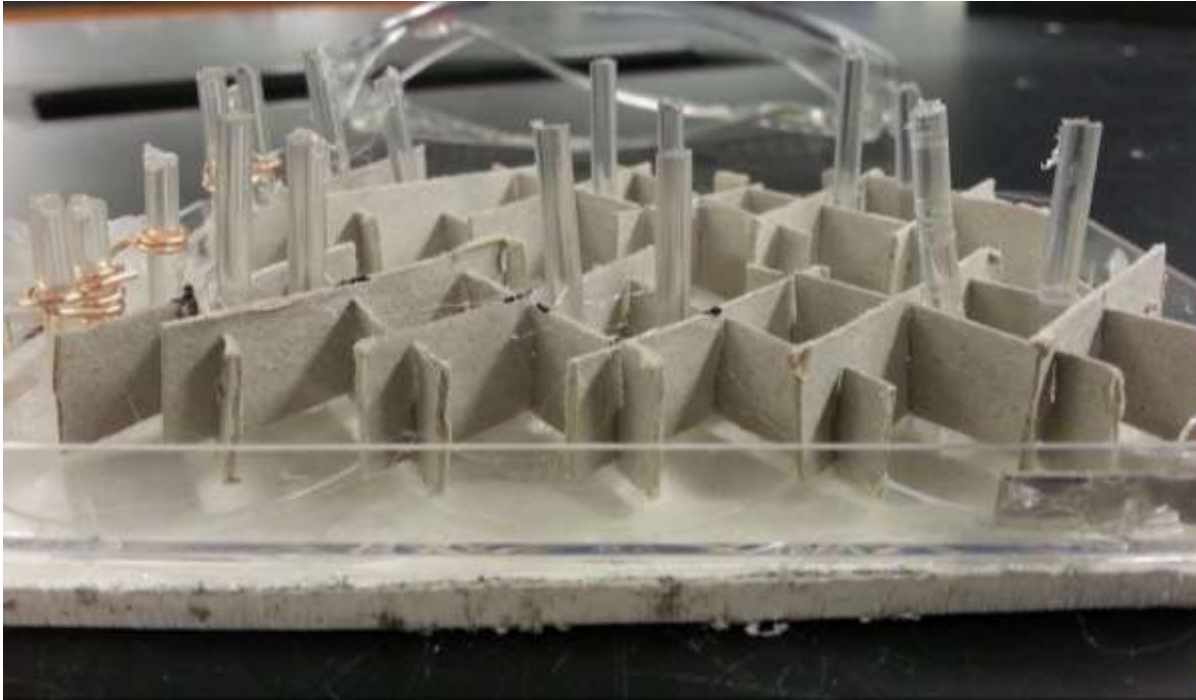detailing the post attachment to the linkage.

Figure 48: Post Attachment to Linkage. Posts were situated close to but not exactly on joints. Also visible are the interlocking joints of the repeated units.

During construction of the model, it was clear that adhering the post at the joint between links was difficult. The acrylic posts were attached to the segments, close to the joints, via hot glue. This attachment procedure allowed for the control over distance between posts via extension and contraction of the linkages.

The final model comprised two rows of scissor linkages, both attached on one end to a plate that is hydraulically actuated by a fluid-filled syringe. Figure 49 provides a top view of the completed model.
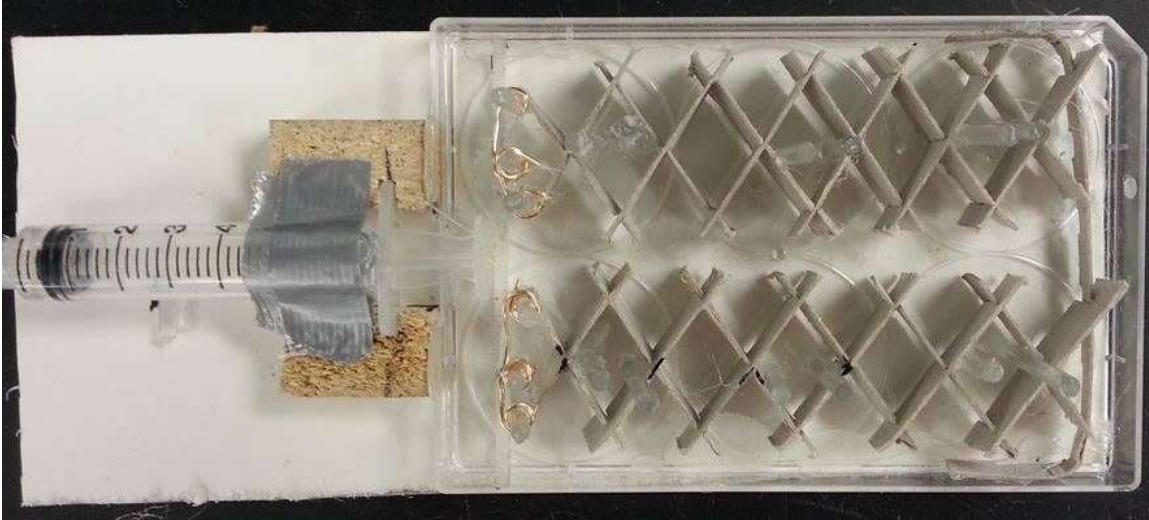
Figure 49: Top View of Scissor Linkage Model. The hydraulic actuator syringe is visible on the left, anchored in place by two wooden blocks and some tape. The end of the plunger is attached to a plate that moves the scissor linkages on each of the two rows. A thin cardboard strip at the other end (right) restricts motion to only one axis, acting as a slider.

During operation of the completed model, movement of the linkage system appeared non-uniform. By obvious visual comparison, certain pairs of posts moved by different strain amounts at different strain rates than others other posts. In particular, for a given distance moved by the actuator syringe plunger, joints closer to the actuator moved a greater distance. Additionally, likely due to friction at the joints, motion of the linkages was not continuous. This caused interrupted motion when applying positive and negative fluid force. Friction at the joints appeared to be an inherent flaw in this design, interfering with consistent and reproducible strain.

4.8.2 Sliding Plate Model

After the scissor linkage model**,** the team modeled the sliding plate mechanism using a hydraulic driving force. The alternative design appeared to work theoretically, however when it comes to manufacturing, all designs are not feasible depending on the resources available. Modeling can help optimize designs, see other ways to orient mechanisms or use other items that make it easier to prototype, and fully manufacture.

During the modelling process of the sliding plates and hydraulic driving force, many changes were made in contrast to the original design. To keep model manufacturing expense down, the model was constructed out of everyday lab equipment.

Figure 50 provides a new schematic of this model's mechanisms. General ideas are the same as the original sliding plate method, however, in this design the bottom plate is grounded, and the top plate is movable. By making the top plate move, the design requires less parts and is easier to assemble, yet still performs the same functions. One post is fixed to the bottom plate and the other post to the top plate. The top plate can be pushed back and forth, changing the distance between posts, creating strain. The strain is controlled by the liquid volume change in the syringe. By using a smaller syringe outside the incubator with the pump, there is less force and friction to slide the plate creating a mechanical advantage. The models using a 20mL syringe attached to the plate and a 5mL syringe in the pump outside the incubator. Figure 50 provides a side-view cross-section of this design.
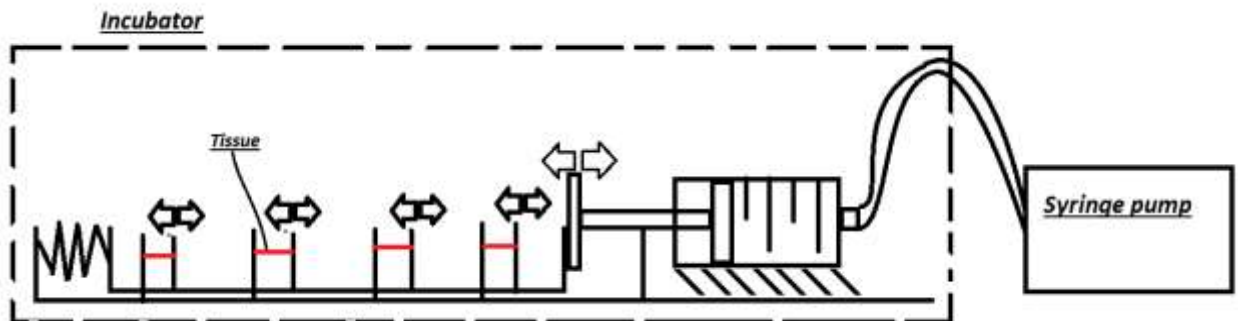

Figure 50: Schematic showing mechanisms used in plate model: two independent plates, the post, and driving mechanisms.

While constructing this model, the team had to constantly think of what material are needed to build a fully functional prototype. While this model was built with household and lab materials, as seen in Figure 51, it prompted thinking about which raw materials, adhesives, and techniques are required. The model used polystyrene and hot glue but these are not autoclavable. For future prototyping, the design uses polypropylene and silicone sealant.
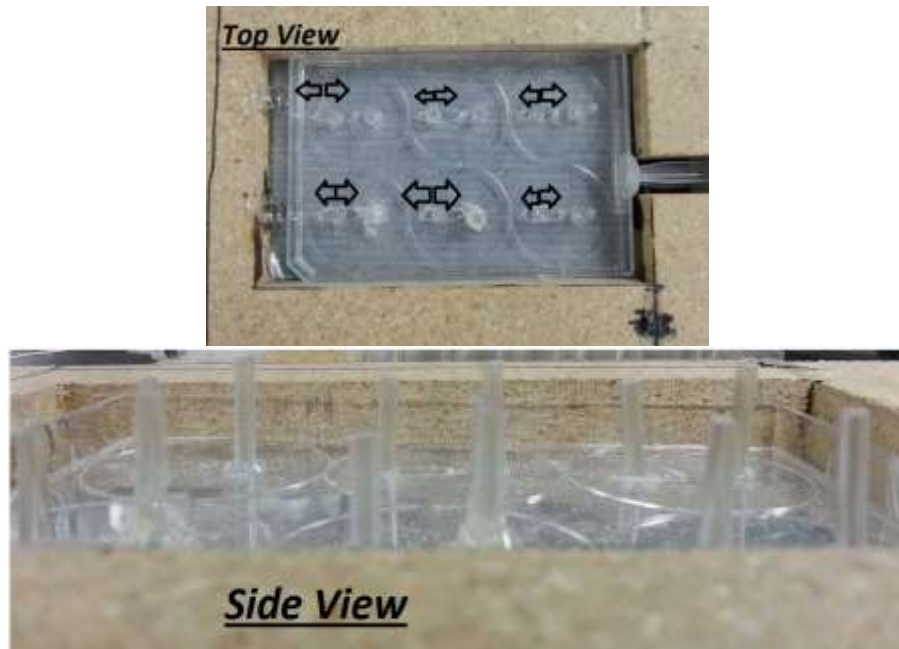
Figure 51: Views of model constructed showing general set-up of design. (a) Top view with arrows indicating direction of movement for positive and negative strain (b) Side view detailing post positioning. One post is attached to the bottom (fixed) plate and the other is attached to the top (sliding) plate.

After modelling this design, the team discussed positive and negative features of the design with the client and user. From this discussion, more ideas and possibilities were discussed on improving the design to increase user friendliness. These ideas, along with slight redesigning formed the final design.

Chapter 5: Final Design
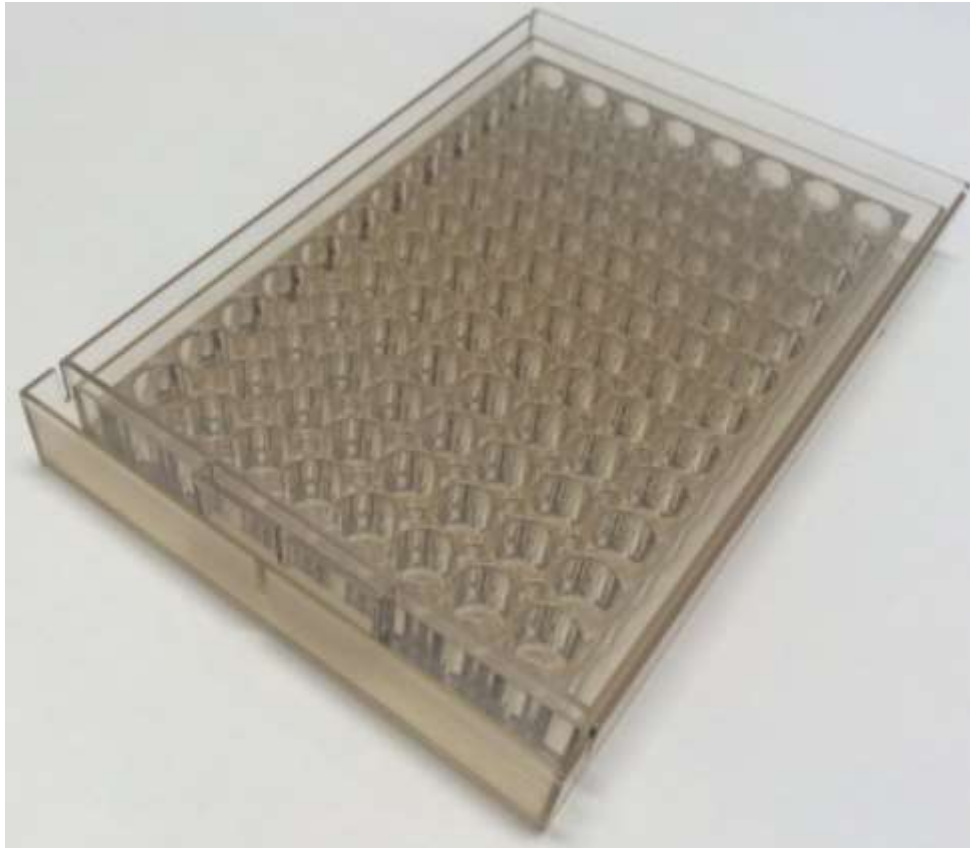
The following chapter discusses the final design, its components, and procedure for use.

5.1 Overall Design and Major Components

The final design consists of four major components including the a lid, the top and bottom plates, the posts and wells, and the syringe pump system. The assembly can be seen below in Figure 52. The lid covers the entirety of the device with a slot for the syringe. This ensures the lid can remain on the device even when the syringe is actuating, keeping the contents sterile. Within each well of the top plate, one post is fixed and a slot is present to allow the post from the bottom plate to extend upwards into the well, as shown in the CAD model in Figure 53 and the final 3D printed device in Figure 54. The device was 3D printed using Objet 260 Connex Rapid Prororype machine on WPI campus. All device features and wall thickness were accurate within 0.02032mm to 0.08382mm. The material choosen was MED610 plastic, which is biocompatible (WPI ARC, 2013).
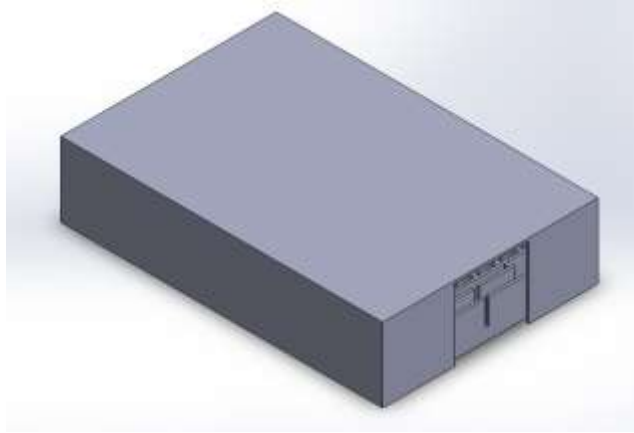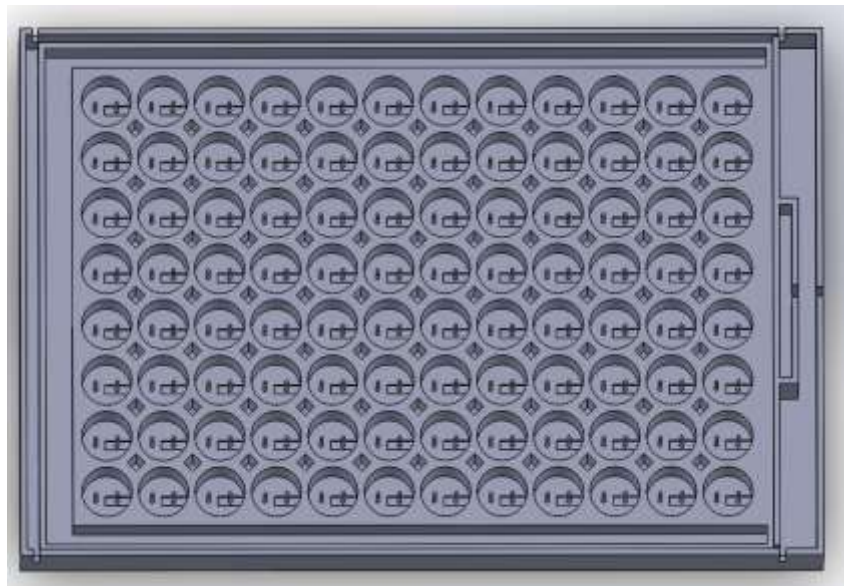
Figure 52: Final Design with Lid

Figure 53: CAD Model of Inner and Outer Plates

Figure 54: Final 3D Printed Prototype of Inner and Outer Plates

To actuate the device, a two syringe system is used. The syringes are attached with tubing and filled with mineral oil. One syringe attaches to the device, while the other is modulated by syringe pump. The syringe plunger in the pump either dispenses or withdraws the mineral oil. The mineral oil actuates the plunger of the syringe attached to the device, which actuates the top plate. When the syringe pump is infusing there is positive strain, withdrawal of mineral oil causes negative strain. In Figure 55, a close up of the syringe attachment point is shown. Figure 56 shows how the syringe plunger attaches to the device.


Figure 55: Syringe housing attached to plates for actuating tissue

Figure 56: Syringe attached to device in the syringe holder

5.2 Posts and Slits

With given general explanation of the device, greater detail about the major components can be given. A major component is the post and wells of the device. Figure 57 displays a close-up of a single well in the top plate in the CAD model and a close-up of 9 wells in the final prototype including both plates. One post is grounded to the top plate, the other post is grounded to the bottom plate. This allows the post attached to the top plate to move independently in relation to the other post. This ability to move independently is how the device directly strains the muscle tissue once formed on the posts. The posts (diameter of 0.5 mm) extend up 8 mm from the bottom of the 10 mm tall well to maximize space for setting of NIPAAM, and cell culture components. The lower 5 mm of the post is conically shaped at a slope of 1 degree to prevent the formed tissue from sliding down the post to the bottom of the plate when resting or being negatively strained. The slots in the top plate allow for 50% positive and 50% negative strain, giving the device flexibility to be used for a multitude of research and experimental purposes. The user can make their own experiments that vary within this range. Also, the design of the wells is based on the dimensions of standard 96 well plates. This makes the design intuitive for the user.
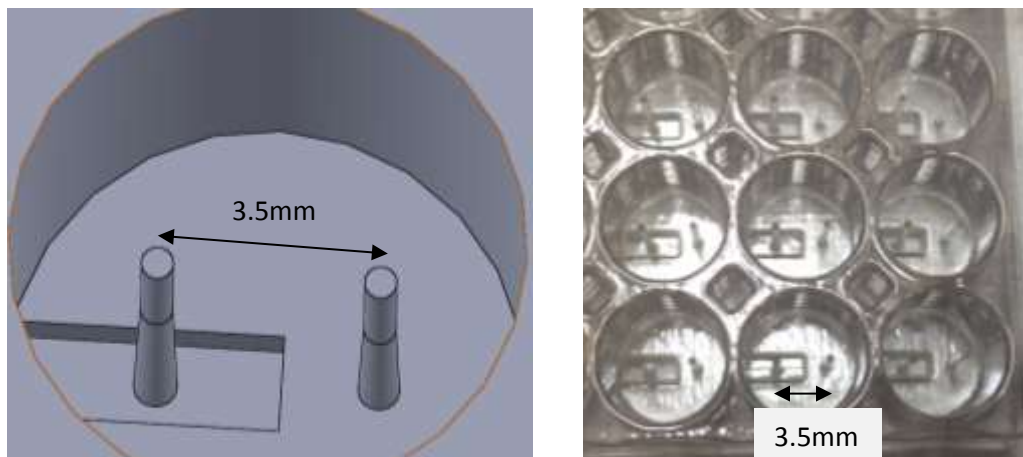
Figure 57: On the left a close-up of the inside box well in the CAD model is shown. On the right a close-up of the wells in the final prototype including both plates is shown.

The initial horizontal displacement of the posts at 0% strain is 3.5 mm apart. The slits allows for one dimensional movement of 1.75mm in either positive or negative direction (+50% strain). However, starting tissue formation at the initial length of 3.5 mm is crucial for easy and proper formation. Tissue formed at a length of 3.5 mm uses the minimal functional unit of tissue that users can easily stimulate and analyze.

5.3 Top and Bottom Sliding Plates

The top and bottom plates comprise a linkage system that converts displacement by the syringe plunger to displacement between the posts. One post within each well is grounded to the top plate and the bottom plate. The bottom plate is grounded to one stationary location, thus so is its post. The top plate and its posts are moveable by 1.75 mm in either direction. Thus by sliding the top in the positive or negative direction, the user moves the post in relationship to each other straining the tissue. This is the mechanism by which displacement from the plunger strains the tissue.

The design allows for easy way to align the two plates so that the post are 3.5 mm apart for initial tissue formation. The bottom plate has slits that correspond to the exact placement the top plate so that the posts are 3.5 mm apart. Figure 58 shows a close-up of the back slits, where a thin piece of plastic can be inserted across the device locking the front of the top plate into the initial position. The syringe is used to lock the back of the top plate into position, but another set of slits are present in the back of the device to insure correct alignment. Vertical alignment is also important, since the top plate has a slight potential of becoming buoyant due to the bottom plate being filled with fluid. To prevent this, a channel exterior of the wells on three sides was added, as well as diamond-shaped holes between each of the wells shown in Figure 59 and Figure 60. The channel and holes can be filled with a denser substance, such as water, to add weight to the box and prevent it from floating in media.

The bottom plate is the largest part, but its dimensions are barely larger than a standard 96-well plate (128mm X 86 mm X 15 mm). The top plate fits right inside with clearance to strain positive and

negative 50%. This is significantly smaller than current products. The device minimizes resources

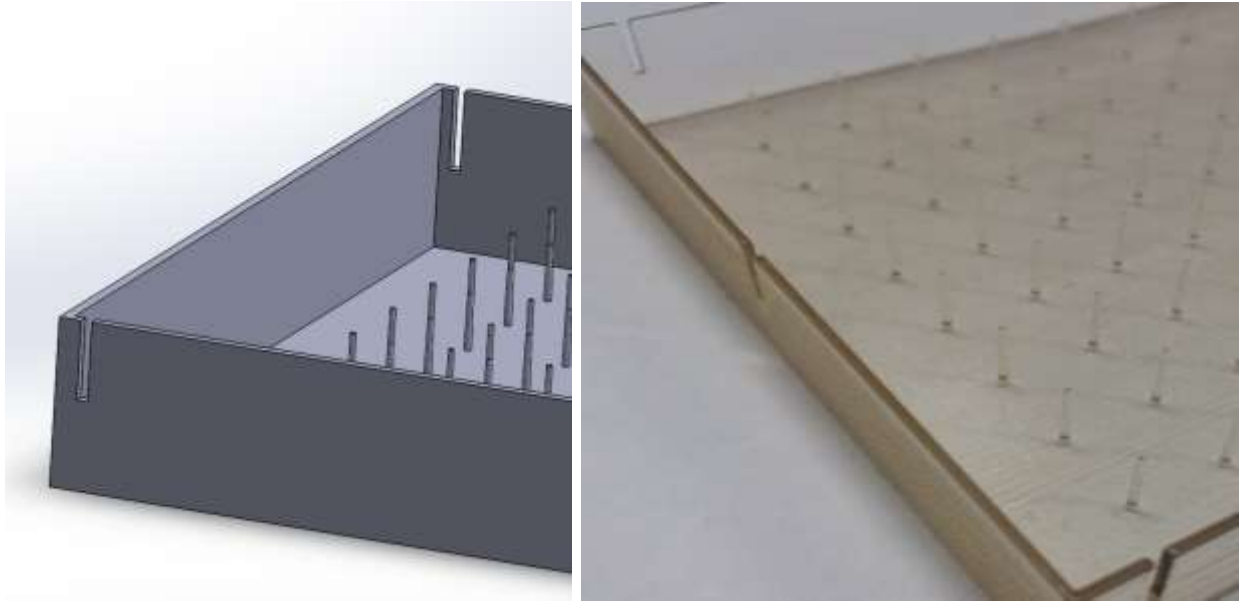(NIPAAM, cell culture components, cells), unlike competitive devices on market, due to its small size.

Figure 58: Bottom Plate Close-Up of Alignment Slits. CAD model (left). Final prototype (right).
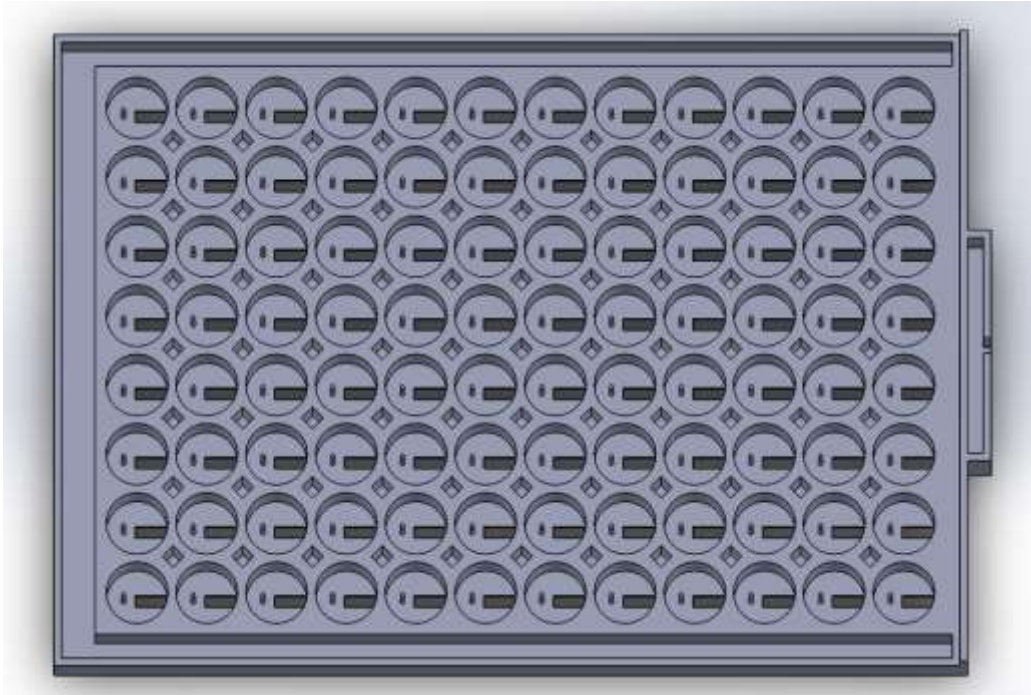
Figure 59: Top View of Top Plate showing the outer channel and diamond holes to counter act buoyancy.
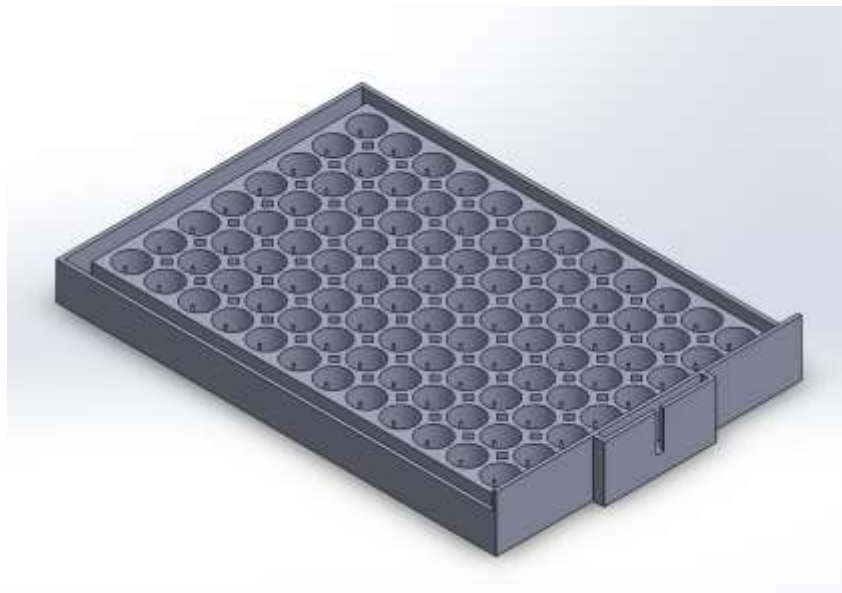

Figure 60: Isometric view of Top Plate showing the outer channel.

103

5.4 Syringe Pump System

The syringes, tubing, and the syringe pump system are the driving forces to strain the tissue. This system of actuating the top plate in the device allows the use of electrical motors outside of the incubator.

The plunger end of a 30 mL syringe (1/4th filled) attaches to the device inside the incubator. The dispensing end is attached to tubing leading outside of the incubator to a second syringe (1 mL ½ filled), which is operated by a syringe pump. The outside syringe being smaller, creates a mechanical advantage when infusing/withdrawing the fluid to control the larger syringe in the incubator. Mineral oil was chosen because it is incompressible and does not undergo thermal expansion from room temperature to 37°C (conditions in which the device will operate). The attachment point on the device can be seen in Figure 56.

This system also allows for optimal control in actuating strain of the device. It operates on one simple principle of fluid mechanics. Fluid volume in a closed system is constant; between the syringes and the tube, the enclosed system has a constant volume. Thus, as the plunger of the outside syringe is actuated by the syringe pump, the volume change in the outside syringe is the same as inside syringe. Based on the geometry of the inside syringe, the amount the plunger actuates is directly proportional to its volume change. Therefore, by controlling the volume infused or withdrawn outside, the system directly controls the amount of strain delivered by the tissue. Figure 61 demonstrates the mechanics with generic syringes. Equations 1-4, show below, the calculations with variables. Equation 4 gives the relationship between desired tissue strain and change in volume of outside syringe.
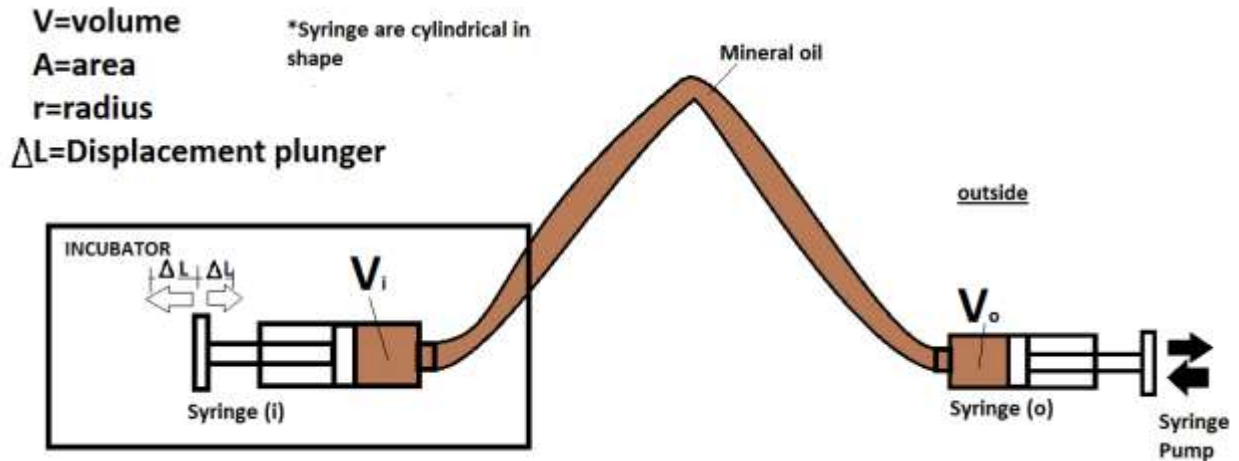
Figure 61: Diagram of syringe/mineral oil fluid dynamic system

Knowns:

Initial Length of Tissue: 3.5 mm = (L_i)

Displacement of tissue (mm) = Displacement plunger (mm) = (ΔL)

Radius of inside syringe (r) in mm: product specification/manufacture/measurable

Desired Strain: $\varepsilon = \dfrac{\Delta L}{L_i}$

Calculations:

Input: Desired strain (ε)

Output: ΔV_o required to reach desired strain

$$\Delta V_{incubator} = \Delta V_{outside} \qquad \text{Equation (1)}$$

$$\text{Volume of Cylinder: } V = \pi r^2 * \Delta L$$

$$\Delta L = \varepsilon * L_i \qquad \text{Equation (2)}$$

$$V = \pi r^2 * \varepsilon * L_i \qquad \text{Equation (3)}$$

$$\boldsymbol{\Delta V_{outside} = \pi * r_i^2 * \varepsilon * L_i} \qquad \textbf{Equation (4)}$$

$$\Delta V_{outside} \text{ is in } (mm^3) must\ convert\ to\ milliliters\ (mL)$$

$$\Delta V_{outside}(mm^3) * \frac{0.001\ mL}{1\ mm^3} = \Delta V_{outside}(mL)$$

Figure 62 shows a visual representation of the relationship between -50% to +50% strain and

the required volume change in the outside syringe. This uses a 30 mL syringe inside the incubator

attached to the device. A 1 mL syringe is used outside, this information is needed in order to program

the syringe pump the user is operating.
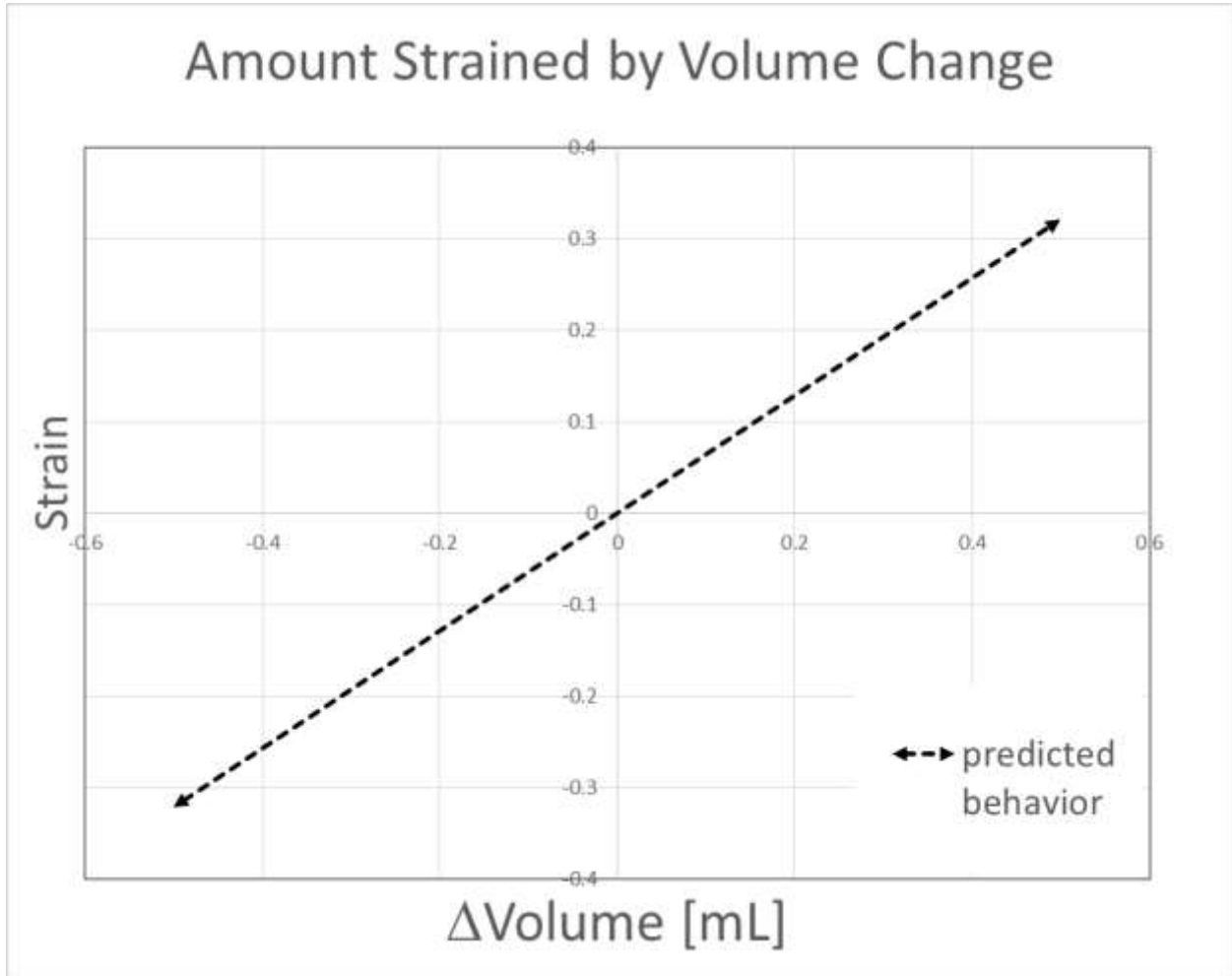
Figure 62: Desired Strain by Volume Change Compared to Actual Strain from Volume Change

5.5 Tissue Final Design

Due to the inability of the C2C12 cell cultures (as available to the team) to self-assemble into

tissues, even with seeding densities of 1 million cells per 60µL, the team utilized a fibrin matrix-assisted

system to function as a scaffold and aid in 3D generation of tissues. The fibrin scaffold provides an initial

structure for tissue organization and ECM formation, eliminating the lack of contiguous tissue formation

in the team's previous attempts at self-assembly. In literature, compared to self-assembly under similar conditions, the use of such a scaffold has proven to generate tissue more rapidly from pure myoblast cultures (Huang et al, 2005).

The finalized methodology for tissue culture within the device resembles that used by Vandenburgh et al (1988), and more recently, Huang et al (2005). Vandenburgh et al (1988) pioneered the technique of seeding a cell suspension within a gel mixture, embedding primary myoblasts in a collagen matrix via a simple gelation process. Though Vandenburgh et al (1988) used collagen gels, recent studies have generated *in vitro* tissue from myoblasts with a similar "cell-in-gel" technique using fibrin gels. Huang et al (2005) showed that seeding primary myoblasts in a fibrin gel mixture produced completely-formed tissue in 10 days. Additionally, the tissue/gel constructs formed remained intact for 6 weeks in culture.

Fibrin gels act as provisional matrices, providing an initial structure for cells to freely migrate and proliferate, while also stimulating cells to produce their own ECM and partially replace the gel (Ross and Tranquillo, 2003) (Huang et al, 2005). Fibrin is known to strongly bind to several key stimulatory factors involved in myogenesis—including FGF-2, VEGF, and IGF-binding protein 3 (Huang et al, 2005). Fibrin gel is produced via the simple combination of two components—fibrinogen and thrombin. To achieve homogenous seeding of cells within the fibrin gel, the team suspended cells within a thrombin solution, and then subsequently added fibrinogen to the suspension to induce the gelation process.

Unlike previous methods as described above, the fibrin gel in this project's procedure acts to assist self-assembly: over time, the tissue/gel constructs contract from a disc-like shape conforming to the surrounding well into a tubular dogbone shape stretched between two posts. This is a result of passive contraction of cells on one another and around the posts—which facilitate tissue organization solely around those two anchorage points. Such anchorage mimics myotendinous attachment to bone,

which is critical in myogenesis. To space the tissue construct from the bottom of the wells (and facilitate

stimulation), NIPAAm was added first to the wells. Once the tissue-gel construct forms on the solid

NIPAAm surface, the NIPAAm is easily removed by cooling the device, and aspirating the NIPAAm,

leaving the tissue construct suspended between the two posts. This suspension of the tissue construct

allows for mechanical stimulation of the suspended tissue without contact or "scraping" of tissue on the

bottom of the well. The procedure for generating tissues on the device is illustrated in section 5.6.

5.6 Device Operation (Flow diagram)

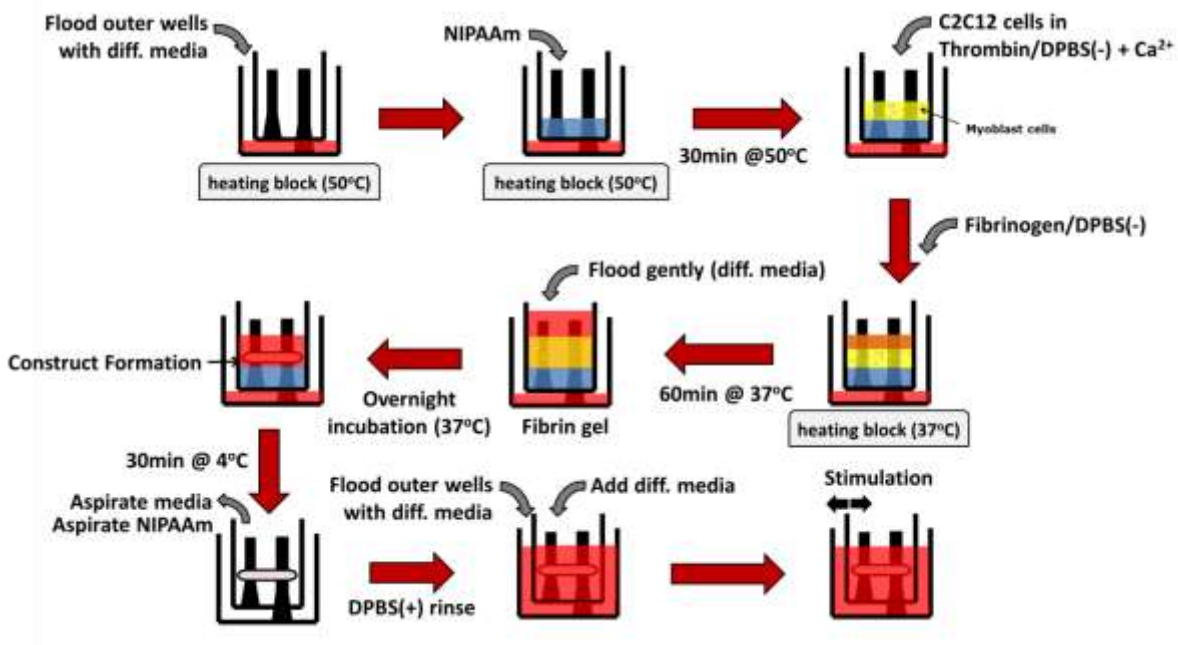Figure 63 shows the procedure for device use in context of this project.

Figure 63: Flow diagram of thrombin/fibrinogen cellular seeding method

The device is first kept on a heating block at 37°C for about 20 minutes, and then 100uL of 2%

NIPAAm (in PBS) is added to each well. The device is then transferred to the refrigerator and left to cool

for about 30 minutes to re-liquefy the NIPAAm into an even layer. The device is removed from the

refrigerator, and cells suspended in a 0.4% thrombin/PBS solution (500,000 cells per 60uL per well) are

then added. Immediately, 60uL of a 10% fibrinogen/PBS solution is added to each well, to start the

gelation process. The formation of fibrin gel is left to continue for 60 minutes at 37°C in an incubator.

The wells are each gently flooded with differentiation media to submerge the tops of the posts, and the device is incubated overnight (~16 hours) in the 37°C incubator. Overnight, the cells within the gel begin contracting, and a translucent, early construct is visible the next morning. The device is then cooled in the refrigerator at 4°C for 30 minutes to liquefy the NIPAAm, and then both NIPAAm and media are aspirated out gently, without disturbing the construct. 200uL of differentiation media is then added to each well, setting the stage for the next phase of device operation: mechanical stimulation. Media is replaced every 48 hours, to maximize stable tissue formation and minimize necrosis.

5.7 Limitations

The final design accomplished many of the objectives, set out originally for the project. However due to time constraints and allowed budget, not all objectives were covered.

Time constrained the team's ability to master the cell culture techniques to make this device more user-friendly. The device was intended to use self-assembly culture techniques, bypassing the need to grow tissue in separate molds and transferring tissues. Self-assembled culture is a proven technique, however it can be difficult to master. Therefore, the team found a provisional matrix gel technique that achieves the same effect. Also, little time was left for the team to execute electrical based tests and further detail design, than what is already shown in the alternative designs section in chapter 4. This resulted in a purely mechanical stimulation device.

The budget and available resources was another limiting factor to the final design. When dealing with biological material, the device is limited to materials that are not cytotoxic. Non-cytotoxic materials tend to be more expensive. Being restricted by the budget, outsourcing for special manufacturing processes was not possible. Restricted to on campus manufacturing resources, the Objet 3D printer was the only resource to manufacture the device. However, when using biocompatible plastics (MED610), the Objet 3D printer cannot use other plastics without compromising the biocompatibility factor of MED610. This restricted the design to one rigid material. This impeded on the ability to use flexible

PDMS posts, which would have allowed the device to measure force of tissue contraction based on post deflection. These limitations should be examined in future works to improve the final design.

Chapter 6: Device Verification Testing (DVT)

This chapter compiles the experiments for validating the device and the device function. In all these biological validation experiments (cytotoxicity and tissue-culture), growth media was used to expand C2C12 cells in 2D culture, and then differentiation media was used to stimulate cell differentiation and nourish tissues. These media formulations were prepared as follows:

- Growth Media (per 100mL)
    - 88mL Dulbecco's Modified Eagle Medium, 10mL Fetal Bovine Serum, 1mL Glutamax supplement, 1mL penicillin/streptomycin
- Cell Differentiation Media (per 100mL)
    - 95mL Dulbecco's Modified Eagle Medium, 2mL Adult Horse Serum, 1mL insulin-transferrin-selenium supplement, 1mL penicillin/streptomycin
- Tissue Culture Differentiation Media (per 100mL)
    - 89mL Dulbecco's Modified Eagle Medium, 2mL Adult Horse Serum, 1mL insulin-transferrin-selenium supplement, 1mL penicillin/streptomycin, 5mL aprotinin, 1mL tranexamic acid

6.1 Cytotoxicity test

To validate the compatibility of the device materials with cell differentiation, a cytotoxicity test for leachates was conducted. C2C12 cells were seeded (in 2D) on eight experimental wells and two control wells, at a density of 500,000 cells per well. The control group was incubated in differentiation media untouched by device materials (i.e. in contact with only tissue-culture polystyrene). Cells in the experimental group were cultured in differentiation media pre-incubated with a device material:

polypropylene pre-incubated for first four wells, 3D-printing resin (MED610) pre-incubated for the

second four wells. A sterilized piece of polypropylene and a sterilized piece of MED 610 were each

separately placed in a vial of differentiation media, and allowed to leach into the differentiation media

for several days. The pre-incubated media was then aliquoted from each vial into the experimental

wells, such that there were samples pre-incubated with each material after 1, 2, 4, and 6 days. The cells

were placed in the incubator for 7 days, at the end of which a Trypan Blue stain—which selectively

stains only dead cells—was added to visualize cell death in the wells. The wells were imaged via phase

contrast microscopy at 10x magnification, and the percent of live cells out of total cells was determined

in each image frame. This percent-viability data was then graphed for each well, as shown in Figure 64.

Viability of cells cultured in media incubated for 1, 2, 4, and 6 days in polystyrene, polypropylene, or
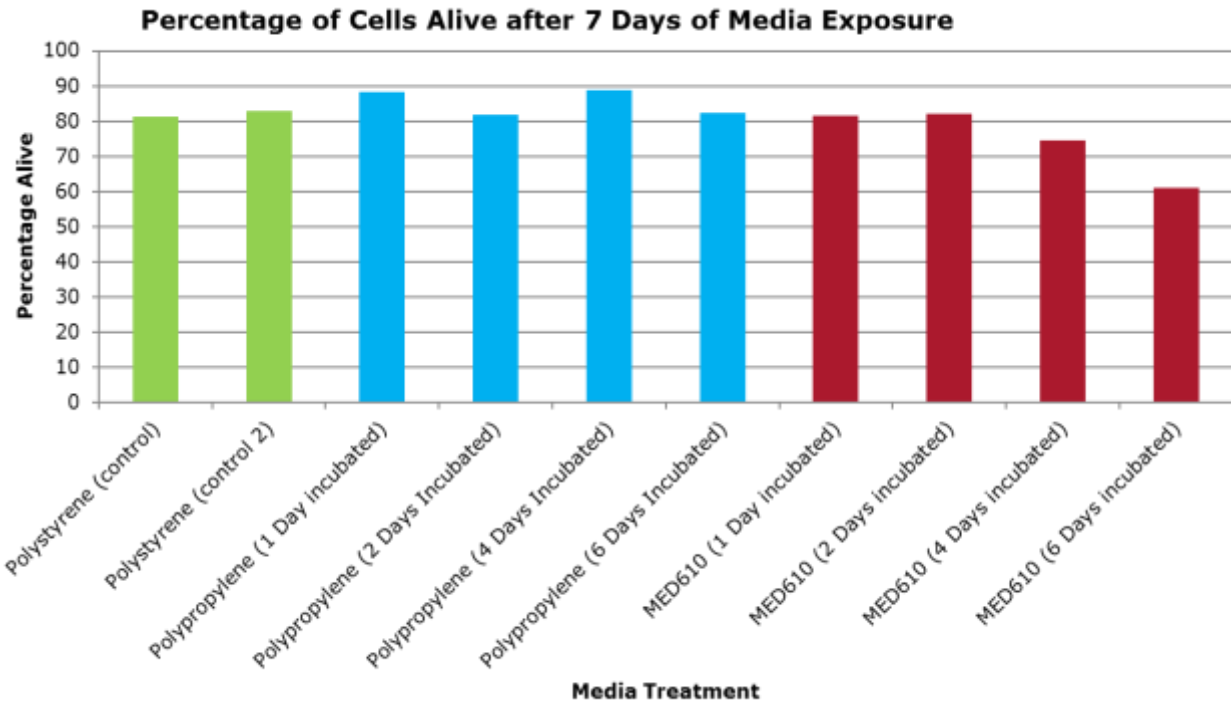
MED610.

Figure 64. Viability of cells cultured in media incubated for 1, 2, 4, and 6 days in polystyrene, polypropylene, or MED610.

Both polystyrene control wells consistently showed around 80% viability after 7 days. Percent viability in the polypropylene-treated wells also proved to be highly consistent among all durations of pre-incubation, with average percent viability slightly above 80%. The MED610-treated group demonstrated similar percent viability of around 80% for the 1- and 2-day pre-incubated wells. A decrease in viability is visible at for longer durations of pre-incubation. Cell viability falls to about 75% with 4 days' pre-incubation with MED610, and 60% with 6 days pre-incubation. The "Day 6" MED610 well shows the greatest cell death out of all wells. An ANOVA (Analysis of Variance) test was run to compare all experimental and control groups, and the p-value was determined to be 0.092.

6.2 "Cell-in-gel" Seeding of C2C12 cells in fibrin matrix

C2C12 murine myoblasts were cultured in growth medium, and passaged every 3-4 days at about 75% confluence. Prior to seeding, cells were pelleted via trypsinization and subsequent centrifugation, and then incubated in differentiation media for 24 hours.

The fibrin-gel seeding method, outlined in Section 5.5, was found to produce contiguous dogbone-shaped tissue constructs, as illustrated in Figure 60. Dogbone-shaped constructs were observed at 24 hours after seeding.

A preliminary experiment (data not shown) was conducted to determine optimal seeding density for tissue formation within the device. Following 24 hours' incubation in differentiation media, C2C12 cells were seeded in the device at densities of $2.0*10^5$, $4.0*10^5$, $6.0*10^5$, $8.0*10^5$ and 1.0×10^6 cells per well. After 24 hours' incubation, the wells were observed for contiguous dogbone-shaped tissue formation, and then observed again at 48 hours. By 48 hours after seeding, contiguous tissue formation around the posts was only observed in wells seeded at densities of $4.0*10^5$ and $6.0*10^5$. No macroscopic difference was visible between the two seeding densities. Wells seeded at $8.0*10^5$ and $1.0*10^6$ cells per well appeared to contain only disconnected, free-floating cell clumps or tissue fragments. Finally, no tissue was visible in the wells seeded at $2.0*10^5$ cells per well. The optimal density for cell seeding within the device was determined by averaging the two densities at which contiguous tissue formed: $(4.0*10^5 + 6.0*10^5)/2 = 5.0*10^5$.

This density of $5.0*10^5$ cells per well was used for all following device validation and tissue validation experiments. Figure 59 provides an example of tissues formed in-device after seeding C2C12 cells at this density.
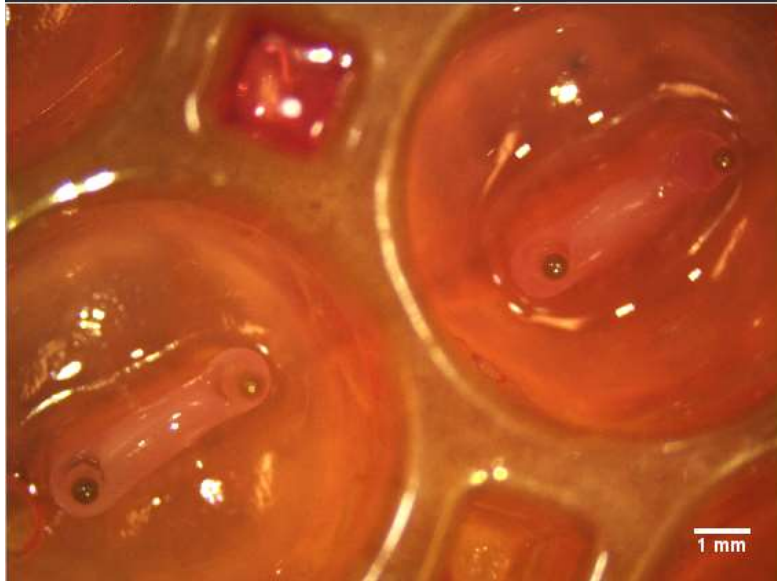
Figure 65. Top view of tissue constructs in device, 24 hours after seeding. Scale bar shown in mm.

Eight tissues were produced in the device seeding test shown in Figure 60, out of which two are shown for the sake of visual clarity. The tissues shown in Figure 60 are visibly contiguous and dogbone-shaped even at 24 hours after seeding. Each tissue is suspended between a pair of posts as anchorage points. The length of each tissue is about 3.5mm, determined by the neutral position of the posts relative to each other—i.e. without stimulation. Pre-stimulation, the diameter of each tissue is about 1.0mm at the body or "belly" of the dogbone.

6.3 Mechanical Analysis of Strain

A series of tests were conducted to ensure that device behavior—specifically the actuation of the device via the syringe hydraulic system—was reproducible and consistent.

6.3.1 Thermal Expansion of Fluid

The chosen fluid for the device was mineral oil for its incompressibility and resistance to thermally expand. The thermal expansion coefficient of mineral oil is near $6.4 \times 10^{-4}\,^{\circ}C^{-1}$ (Totten, 2011). This shows that at relatively low temperature changes (such as room temperature to body temperature) the volume of the fluid does not change. However, the team verified that the fluid would not interfere

with operational use of the device within operational conditions. The fluid would operate from 21°C to 37°C in the syringe pump system.

The team partially filled two 1mL syringes and completely filled tubing with mineral oil. A closed system was formed between all components as in the final device. One syringe was completely depressed and the other filled to 0.5mL. The completely depressed syringe was fixed so no fluid could enter. The depressed syringe and half of the tubing was submerged in a 41°C water bath, and the other syringe at room temperature. This models the environment under which the device would operate. The system was held for 20 minutes to insure the system has reached equilibrium. After 20 minutes the syringe at room temperature was still only filled to 0.5mL of mineral oil. Thus showing no thermal expansion of mineral oil under operational use, and no interference in amount strained applied to the tissues. Figure 60 shows the experimental setup.
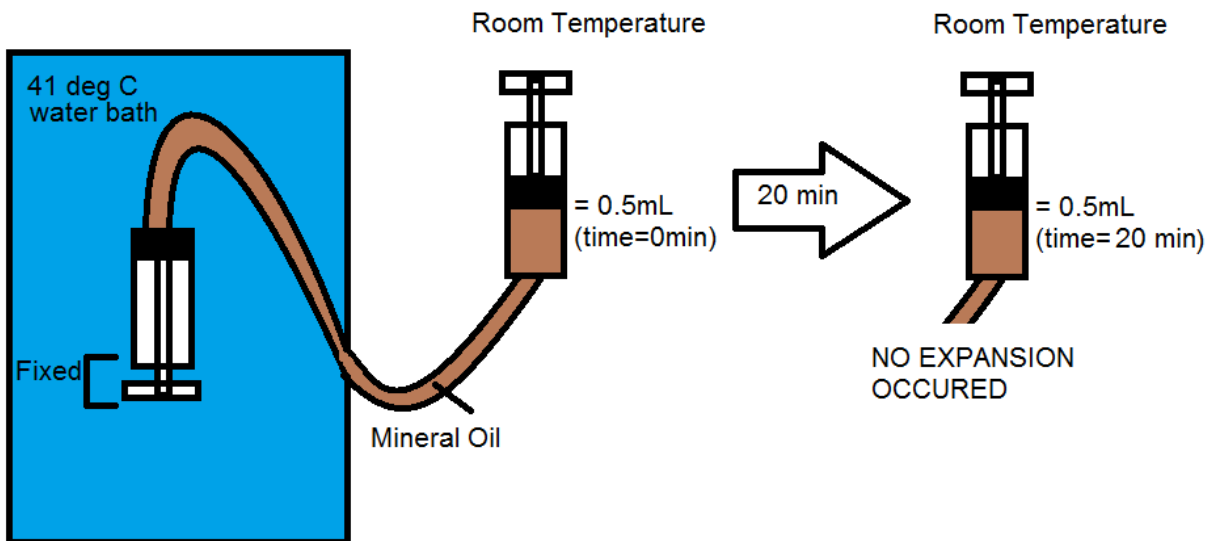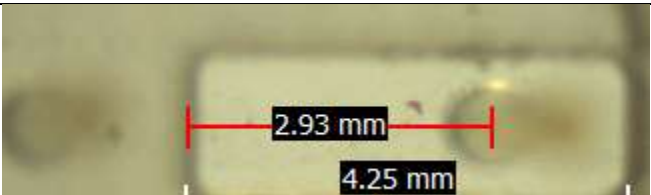

Figure 66. Thermal expansion test of mineral oil showing no expansion and no interference for operational use of device.
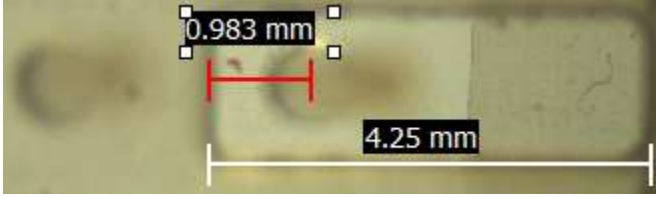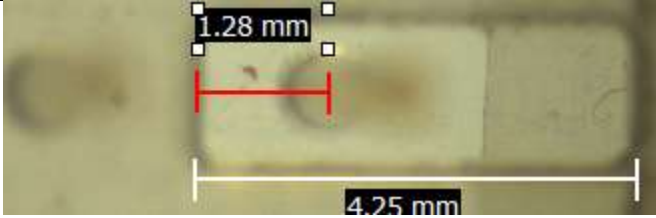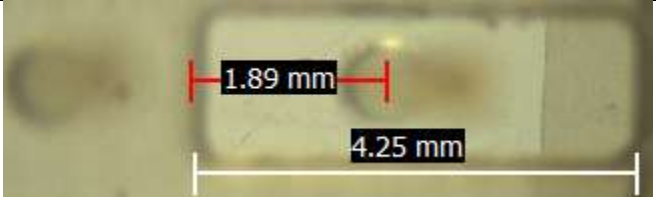
6.3.2 Verification of Amount Strain/Volume Change of Fluid

To verify the device applied the desired strain between the posts, a series of experiments were performed. First, the device was actuated in dry conditions. This narrowed down the variables. The input was volume of fluid changed in the outside syringe, and the output was distance changed between

the posts in the device (observed by an overhead microscope). The distance between the top plate post

and the begin slit is known (1.5 mm) and the length of the slit is also known (4.25 mm). The microscope

software used this information to convert pixels to distance, thus enabling the team to measure the

distance changed at each increment. In the experiment, volume was change in increments of 0.25 mL,

starting at 0% strain then cycled first to 30% positive strain, then negative 30% strain, and back to zero.

The results from the dry experiment can be seen in Table 8.

Table 7. This table shows the results of the dry device strain verification test
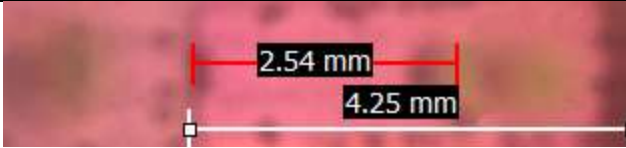
ΔV (mL)	Image	Strain (decimal) from other post
0.0	2.00 mm / 4.25 mm	0
0.25	2.41 mm / 4.25 mm	0.117142857
0.5	2.93 mm / 4.25 mm	0.265714286
0.25	2.62 mm / 4.25 mm	0.177142857
0.0	2.16 mm / 4.25 mm	0.045714286
-0.25	1.60 mm / 4.25 mm	-0.11428571

-0.5		-0.29057143
-0.25		-0.20571429
0.0		-0.03142857

The same experiment was performed, but now the device was flooded with media. This better mimicked how the device would operate under operational conditions. The results from the media test can be seen in Table 9.

Table 8. This table shows the results of the media based device strain verification test

ΔV (mL)	Image	Strain (decimal)
0.0		-1.31E-16
0.25		0.135693215

0.5		0.271386431
0.25		0.191740413
0.0		0.014749263
-0.25		-0.13864307
-0.5		-0.24483776
-0.25		-0.179941
0.0		-0.01179941

    The data generated was used to show how the device functions compared to the predicted behavior. This is shown in Figure 62. The device functions very closely to the predicted behavior, however there are some sources of variance discussed in section 7.1

Amount Strained by Volume Change
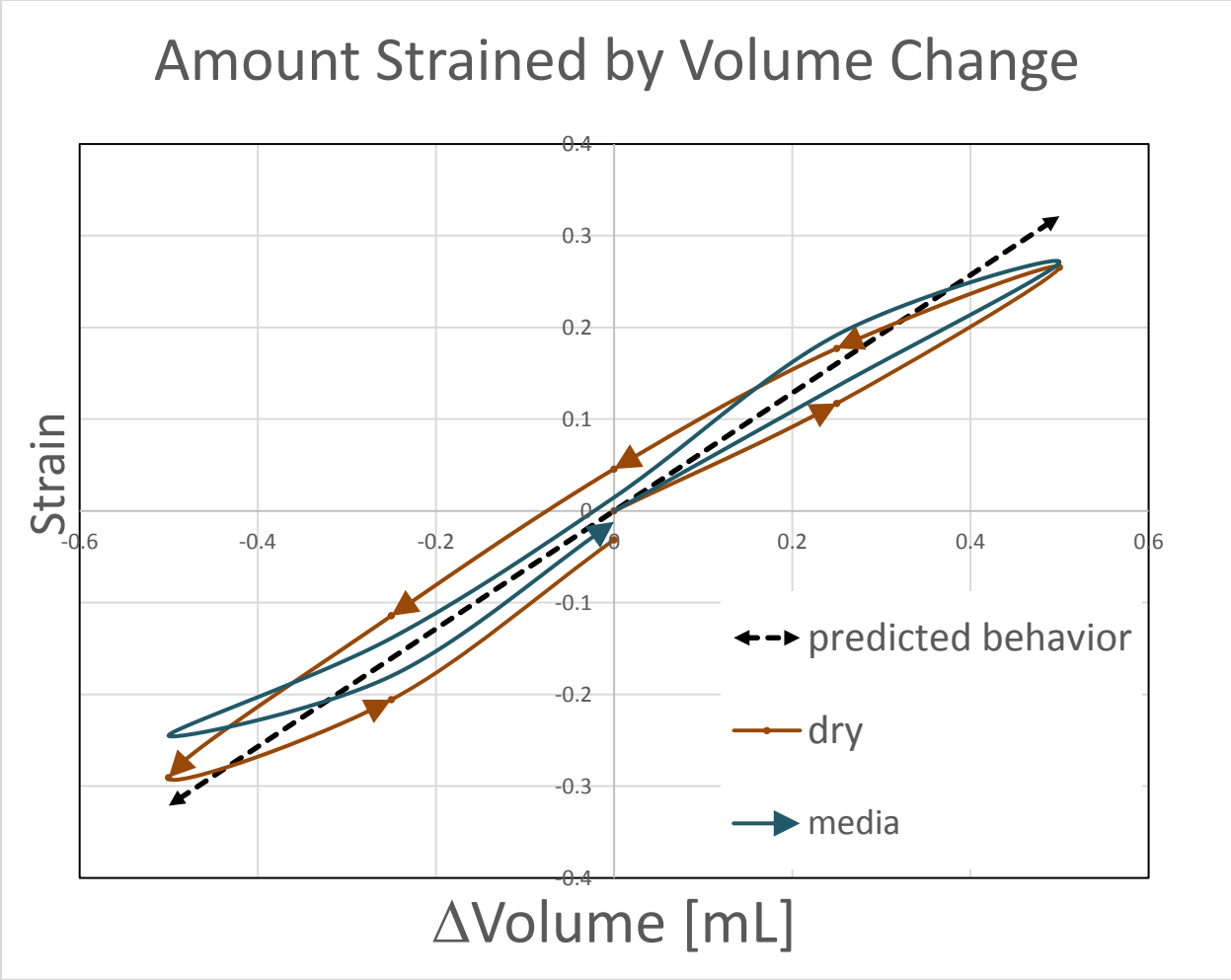
Figure 67. Predicted behavior, experimental behavior (dry) and (with media) for strain applied over volume change.

The device normal operation would range from -5% to 20% strain. As seen in Figure 62, the greater the strain the greater the error. Percent error is calculated by:

$$\frac{|predicted - exact|}{exact} = Percent\ error$$

At 20% strain the predicted volume change is 0.32 mL, and the media value is about 0.35 mL. The maximum error between the predicted behavior and the media test is 8.5% at 20% strain.

6.4 Tissue stimulated results

The gel matrix and C2C12 myoblasts were seeded into each well of the device. From here they were incubated for 4 days to ensure formation before mechanical stimulation. On the fifth day, the constructs were strained and exercised at a rate of 5% positive strain cyclically (1 cycle per minute) for 15 minutes. The strain rate was increased over the course of several days to 5-15% strain, but the rate of strain (1 cycle/minute) was kept constant. After 4 days of exercise the tissues were fixed, embedded, and cut for staining. The stimulated tissues were compared to unstimulated (control) tissue and were histologically compared using H+E and myosin staining.
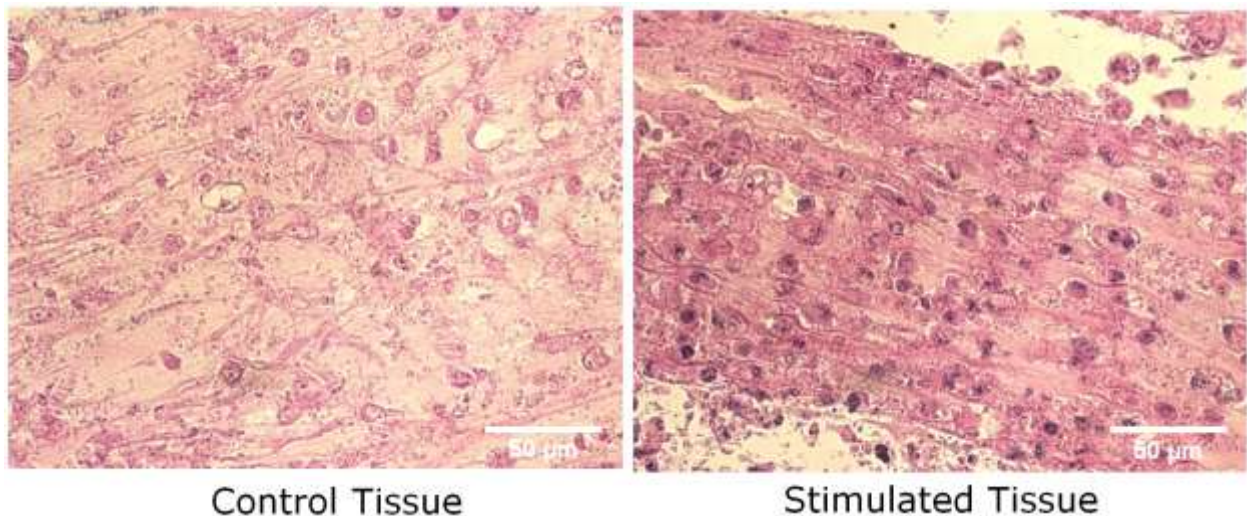
Figure 68. The H+E stain was imaged at 40x magnification of both unstimulated control tissue and experimental stimulated tissue.

The H+E stain in Figure 63 reveals an increase in fiber alignment in the stimulated tissue as well as longer fibers with higher fiber density. There is evidence of multinucleated cells and cytoplasmic fusion in the stimulated tissue. The elliptically-shaped nuclei are indicative of myotubes. In contrast, the fibers in the control tissue are more disorganized and less dense. The color of the stain was not as strong because the cells were not as densely packed. The cells in the control tissue are noticeably less aligned. This suggests that the device had a positive impact on improving muscle formation.

121
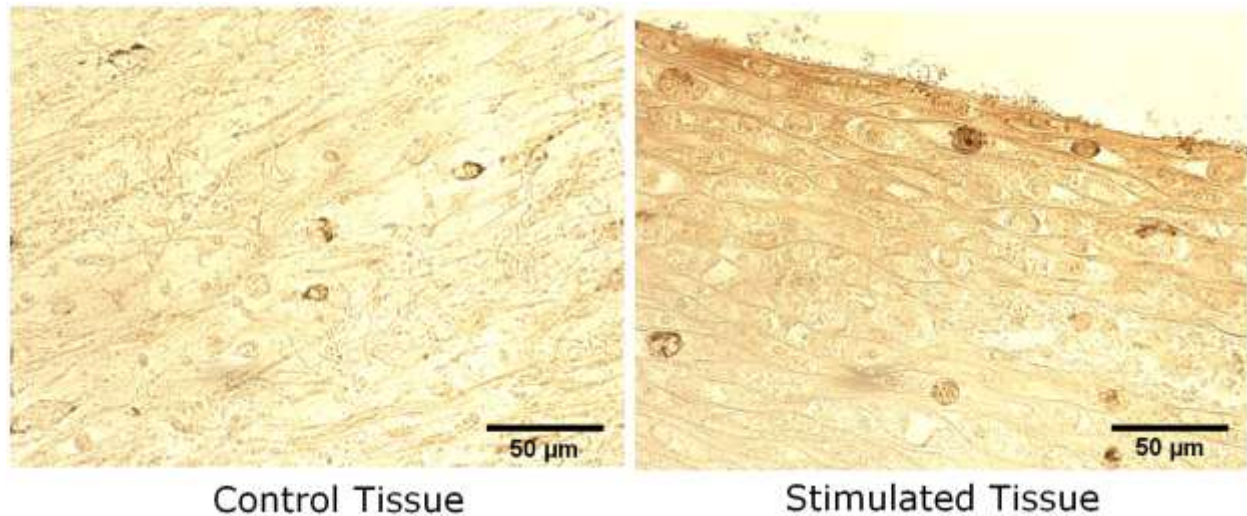
Figure 69. Myosin stain at 40x magnification comparing an unstimulated control tissue with a stimulated experimental tissue.

The brown myosin stain targets the myosin proteins with enzymes, which makes the cells/myotubes appear dark in an image. Figure 64 compares the difference between the stimulated and unstimulated tissues. The stimulated tissue has darker coloring along its edge. These darker cells also have elliptically shaped nuclei and appear to be fused together. These are all characteristics of myotubes and the presence of long strands of myosin. In contrast, the control tissue appears with minimal staining, less alignment, and circular nuclei. The stimulated image shows improved muscle formation and an increased presence of muscle proteins.

Chapter 7: Discussion of Results

The goal of this project was to design an in vitro stimulation system that produced accurate models of in vivo skeletal muscle tissue by focusing on: tissue anchorage, tissue stimulation, and using the minimal functional unit of *in vitro* tissue.

7.1 Mechanical Testing: Analysis of Results

7.1.1 Thermal Expansion of Fluid

The experiment as shown in Figure 61 from section 6.3.1 demonstrated that no thermal expansion of the mineral oil occurred when transitioning from room temperature to 41°C. Therefore,

mineral oil is adequate for use as the working fluid for the team's design, as it will not affect the strain

rate per volume of fluid with the various temperatures of the system (half the tubing in the incubator

conditions of 37°C and the other half of the tubing at room temperature conditions of 21°C).

7.1.2 Amount Strain/Volume Change of Fluid

In Tables 8 and 9, the experiment images can be seen in the dry and media trials, respectively.

The device performed better in the media trial, which is ideal since the device is to be operated with

media present. This increased performance is most likely due to the decreased friction that the fluid

provides between the plates, allowing for a smoother transition between positive and negative strain.

The final device was capable of operation within incubator conditions, and was reusable after

sterilization between experiments. As shown in Figure 62 in section 6.3.2, the device is capable of

uniaxial positive and negative strain, matching both the recommended literature values of -5 to 15%

strain and the user/client request for +/- 50% strain. Strain rates produced by the device are predictable,

with the highest percent error being ~17% at maximum strain of 50%. However, between -5 and 15%

strain the maximum error is 8.5%, indicating that the device will be accurate within the range that

literature values indicate is best for forming muscle tissue.

The percent error in the device's strain per volume change can be reduced in several ways. Since

the tubing that housed the mineral oil was very flexible, the walls of the tubing were able to expand

slightly as the fluid moved through. This expansion of the tubing causes slight error in the displacement

of the syringe, as the fluid movement is not entirely one directional in this case. By replacing the current

tubing with more rigid-walled tubing, this error can be reduced. In addition, more careful administration

of the mineral oil into the tubing and syringes could be used to prevent the formation of bubbles within

the tubing. The bubbles also restrict full movement of the syringe, as they take up volume in the tubing

that should be filled with mineral oil to provide the most uniform fluid within the tubing. Lastly,

changing the operation of the syringe from human operation to operation with a syringe pump that is able to both withdraw and infuse would eliminate human error in precisely moving the syringe to the desired displacements.

7.2 Cell Seeding and Cytotoxicity: Analysis of Results

As specified in the introduction to Chapter 6, the differentiation media for tissue culture was prepared (per 100mL) by extracting 94mL from the cell differentiation media and then adding the volumes of aprotinin and tranexamic acid shown. The roles of aprotinin and tranexamic acid are explained later in Section 7.2.

The cytotoxicity test proved that all device materials in contact with cells (polypropylene, MED610) were cytocompatible in the context of device operation. Polypropylene appeared to have no effect on cell viability compared to a tissue-culture polystyrene control. Though a decrease in cell viability over time was perceptible for the MED610 material, the ANOVA p-value between groups was 0.092 (greater than 0.05). The null hypothesis—that there is no significant difference in cell viability between groups—is therefore validated. To minimize cell death in any case, the recommended device operation procedure (Section 5.6) calls for replacing media in the device every 2 days or less. As Figure 59 illustrates, viability for cells exposed to MED610 up to 2 days is virtually identical to that of the polystyrene-exposed control.

Techniques for self-assembly of *in vitro* skeletal muscle tissues, i.e. without an exogenous scaffold, continue to be developed by several research groups— see Huang et al (2005), Dennis and Kosnik (2000), and Carosio et al (2013). Self-assembled tissues have shown to be functionally similar to native skeletal muscle; however, long periods of time are required for self-assembled muscle to display

a mature phenotype. A co-culture of fibroblasts with myoblasts is typically necessary for self-assembly, to endogenously provide ECM for directing contiguous tissue formation and alignment.

The fibrin gel-assisted assembly method allows the use of a pure myoblast population, since the initial ECM is exogenous. Constructs created via fibrin gel were found by Huang et al (2005) to form rapidly, in about a third of the time required for formation of tissues (of similar dimensions) via self-assembly. Fibrin-seeded tissues also produced greater specific force than self-assembled tissues. Because of the strong binding affinity of fibrin to muscle growth factors, the fibrin gel solution can be mixed with these growth factors to optimize tissue maturation and hypertrophy. Huang et al (2005) proposes that such a system could provide slow, controlled release similar to that in myogenesis, to further direct and stimulate native-muscle-like formation of tissue.

For the tissue culture validation test outlined in Section 6.2, differentiation media was supplemented with aprotinin and tranexamic acid, as specified in the media formulations at the beginning of this section. Aprotinin slows the breakdown of fibrin by inhibiting plasmin, a fibrinolytic protease secreted by differentiating C2C12 cells (Furst et al, 2007). Tranexamic acid is also anti-fibrinolytic, inhibiting the activation of plasmin by competitively binding plasminogen (Furst et al, 2007).

As Figure 60 illustrates, the tissue culture validation test produced dogbone-shaped, contiguous tissue, looped at each end around a post. The mimicry of muscle-bone attachment is validated by the contiguous loops of tissue formed around each post, visible in Figure 60. The cells in fibrin attach to one another and the fibrin exogenous matrix, and contract, inducing active tension in the cell/fibrin construct. With the two posts as anchorage points for the developing tissue, this tension causes the layer to contract upon itself, producing elongated tissue constructs suspended between the posts within 24 hours. The tissue fragments observed at high seeding densities (see Section 6.2) were likely a result of the large number of cells degrading the fibrin gel too rapidly. The construct therefore was broken

down into fragments before cells could form tissues using the exogenous ECM. The lack of any visible tissue formation in the 200,000 cell-seeded well was likely because sufficient numbers of cells were not able to contact other cells and generate the active tension needed to roll up the cell-in-gel layer into the dogbone-shaped construct around the posts.

Clinically, skeletal muscle biopsy samples obtained from humans are muscle fiber bundles of 3-4mm in length, and commonly about 1mm in diameter (Saks et al, 1998). These samples are then used to study contractile properties, metabolic responses, and fiber density, and are typically taken from human soleus, gastrocnemius, tibialis anterior, or quadriceps muscles (Saks et al, 1998). The biopsy sample dimensions therefore provide an existing clinical standard for a "minimal functional unit" of muscle— as a means to accurately study muscle function as in native tissue *in vivo* while minimizing the invasiveness and tissue loss in the patient (Saks et al, 1998). The *in vitro* tissues produced within the device correspondingly fall within this size specification, with a length of about 3.5mm and a diameter of 1.0mm. This correspondence suggests that the tissues the device produces are a sort of minimal functional unit, validating the capability of tissue culture to produce functionally-accurate muscle models with minimal resources, in a high-throughput manner. The technique of seeding cells in fibrin gel also demonstrates rapid formation of tissue constructs, supported by Huang et al (2005). Within 24 hours, a clear dogbone shape emerges as a result of active contraction and tissue anchorage at two points.

The cytotoxicity test showed no substantial drop in percent cell viability over 6 days of incubation with (cell-culture) polystyrene or (cell-culture) polypropylene. Both materials were listed as intended for cell culture on the packaging, and these results confirm the labeling. A slight decrease in percent live cells per image image was observed over time for the cells incubated with MED610-exposed media. However, an Analysis of Variance (ANOVA) returned a p-value > 0.05, suggesting the decrease was not

statistically significant. Any detriment to cell viability caused by material leaching is further minimized by the replacement of media every 48 hours, as in the device operation procedure (Section 5.6).

Chapter 8 – Project Impact

The project not only impacts the world of engineered skeletal muscle, but also extends to many other societal, environmental, and political areas. The gap in research will be bridged with the device as an enabling tool between treatment and research. Beyond the scope of skeletal muscle, this device and its methods could be slightly altered to fit cardiac tissue, cartilage, or smooth muscle. This chapter will analyze the limitations of the project as well as the impact and influence of its usage.

8.1 Benchmarks and Standards for Success – A Comparison to Other Works

The device developed in this project comprises of mechanical stimulation capabilities that vary in comparison to the gold standard Vandenburgh device as outlined in section 2.8.1. Vandenburgh's device achieved -5% to 20% strain, while the device created in this project achieves strain of -50% to 50% strain. By having a larger strain range, the device is able to fulfill the needs of a wider variety of researchers and experiments. The Vandenburgh device supported a maximum of 12 wells, while the team's device supports 96 wells.

The skeletal muscle tissue constructs used for device validation were constructed using a "cell-in-gel" method similar to that used by Vandenburgh et al (1988) and Huang et al (2005). Seeding primary myoblasts in fibrin gels, Huang et al (2005) produced tissue with diameters of 100-500 μm within 10 days, which were functional for 6 weeks in culture. Longitudinal sections stained with hematoxylin, eosin, and anti-myosin-heavy-chain antibody showed areas of contractile machinery organized within discernible z-lines. Andersen et al (2014) found that mechanical stimulation over a span of 24 hours produced fully-aligned myotubes oriented in the same parallel direction. At the end of 10 days, after a 48-hour mechanical stimulation period, the percentage of multinucleated myofibrils

expressing myosin was four times that in the unstimulated control. As a benchmark for in vivo tissue, myofiber diameter for *in vivo* human muscle ranges from 10-100 µm and average length 23.3 µm. In native myotubes, the density of nuclei per sectioned slide of *in vivo* tissue is between 30-57 nuclei/mm^2. (Vandenburgh, 1991).

8.2 Limitations in Data

The project was limited in many regards based upon the resources available to the team. Limiting resources include time, money, and experience. Time limited the amount of tests the team was able to perform. Having a low number of experiments limited statistical significance. With more time, more experiments could be performed to truly prove whether the device produces more accurate models of *in viv*o tissue.

The allowed budget limited the team's ability in using alternative manufacturing processes, to manufacture a multi-functional device. The current device is a pure straining device, because the Objet 3D printer could only print with one rigid biocompatible material at a time. If more money was available, the team could contract to a 3D printer that could print with two different biocompatible materials at once. This would allow the device to have rigid plates and flexible PDMS posts. With flexible posts, the user has the ability to measure deflection in the post and determine the force exerted by the tissue. But the team was limited to the WPI Objet 3D printer. Not having flexible posts limits the potential data to be collected.

8.3 Economics

The influence of this project will impact the everyday living economy of both patients with degenerative muscle diseases and researchers in the field. The device itself costs about $203.89 to make in a 96 well model and it replaces animal model methods, which cost about $90 each, not including food and containment. Animal testing for 96 samples would cost $8640. This drastically increases both higher throughput testing as well as accuracy using human cells over animals. The more affordable research

improves the rate of discovery, which ideally creates more treatments for degenerative muscle diseases and more affordable options. More affordable options would be generated from less expensive research, which would make the treatments more readily available to underprivileged families. Table 9 is a complete bill of materials for operational use of the device.

Table 9: Device Bill of Materials

Item/Material/Labor	Estimated Cost (per device):
Full Device	$203.89
NIPAAm	$87.10/gram
Fibrinogen (bovine)	$170.50/gram
Thrombin (human)	$288.50/150UN
Cell culture agents	$250.00
TOTAL:	**$999.99**

*cell culture agents include: PBS, Trypsin, L-Glutamine, P/S, Adult horse serum, ITS, Fetal bovine serum, DMEM

8.4 Environmental Impact

The materials in this project were selected for their sterility and reusability. The well plates are autoclavable and can be used multiple times. This reduces the quantity of plates that require disposing. This more positively impacts the environment than disposable plates which add to plastic buildup and nonbiodegradable materials. There is also a greater risk in disposable plates for leakage of drugs or cellular debris into the environment from landfills and improper disposal of materials. The reusable plates do not have this problem and their eventual disposal would be incineration so that no biohazardous waste would be leaked into the environment.

There are several environmental factors related to this project that must be analyzed. While plastic is a more economical material to use, it also is non-biodegradable. This could possibly result in more plastic being disposed of improperly and have a negative impact on the environment. In an effort to reduce the impact on the environment the team could include directions on proper disposal of the device if it should be damaged.

8.5 Societal Influence

The device will indirectly enhance the quality of life for many people because of its enhancement of current research techniques. There are very few treatments for degenerative muscle diseases and few ways to test pharmaceuticals for approval. This device would enable researchers an increased rate of discovery as well as a less expensive means of research. Indirectly, this will also make treatment products less expensive because of their cheaper cost to make/discover and improve quality of life.

8.6 Ethical Concern

The purpose of the device is to improve and enhance current research methods and strategies. This will hopefully generate more treatments that are more affordable and widely available. The use of the device is not offensive or unethical; embryonic stem cells for human therapeutic cloning is banned in certain states, but that would only be a restriction on cell line. Certain religious beliefs prohibit the transfer of bodily fluid thereby forbidding blood transfusions and other tissue transference. The ultimate goal of the device is to help improve the human condition through improving the rate of discovery toward a cure for degenerative muscle diseases.

8.7 Manufacturability

The processes to manufacture this device are advantageous to researchers anywhere in the world. The final design was manufactured by a 3D printer and designed in CAD drawings. The popularity of 3D printers is spreading across the world. Thus by simply sending a CAD file of the device, any lab with 3D printing capabilities would have access to the device. By having the design readily available to be manufactured anywhere for skeletal muscle tissue researchers, they can access the device faster and increase the rate at which their labs can discover and test cures to skeletal muscle diseases. 3D printers also reduce plastic waste compared to other manufacturing processes, eliminate the need to transport the device from a manufacturing plant to laboratories, and reduce human error in production.

8.8 Sustainability, Health and Safety Issues

In order to produce a sustainable device, several considerations were made during the design

process. Creating an environmentally-friendly device, both in the process of manufacturing and use, is

one important consideration. Since the device is created out of single material via the precise process of

3D printing, the amount of waste is negligible during production. The device can be autoclaved multiple

times, allowing reusability, minimizing device disposal. Economic sustainability was also incorporated

into the design. The product is designed for multi-functional use in both small, private laboratories and

large pharmaceutical companies. The capacity for high-throughput tissue generation and screening, up

to 96 tissue constructs, is provided. The large volume of tissues testable per use allows for a societal

impact on quality of life, once a drug is created to treat or cure muscular diseases. Compared to live

animal testing, the device improves user safety by eliminating the health hazard of being bitten or

scratched during handling. Additionally, the entire device (including syringe) is lightweight, reducing the

risk of injury from lifting or dropping the device.

Chapter 9: Conclusions and Recommendations

This chapter encompasses the conclusions and recommendations of this Major Qualifying Project.

9.1 Conclusion

The deliverable for this project is a mechanical stimulator of *in vitro* skeletal muscle tissue that

improves modeling *in vivo* skeletal muscle.

The device is able to generate minimal functional units of tissue from myoblast cells *in vitro*,

with tissue shape and anchorage mimicking muscle-bone attachment *in vivo*. Several tissues (up to 96)

can be generated, and then highly- reproducible uniaxial mechanical stimulation can be applied to these

tissues simultaneously. This stimulation can be applied from outside the incubator while preserving

sterility, via a programmable syringe pump, minimizing user effort. The device can therefore allow high-

throughput generation and stimulation in a small form factor that fits in an incubator, while also preserving functionally-accurate muscle modelling.

With a high degree of consistency, the device is able to improve key parameters of in vivo skeletal muscle via mechanical stimulation, including muscle fiber alignment and fiber density. In addition to positive strain, the device is also capable of applying negative strain to tissues. This allows the tissues to relax and recover between strain cycles, minimizing the risk of tissue rupture. The capability for negative strain also allows our device to produce models of muscle atrophy, as absence of passive tension causes losses in muscle mass and strength.

The hydraulic actuation of the device provides a way to stimulate tissues from outside the incubator without heat-sensitive or humidity-sensitive components, while the virtually-zero compressibility of the hydraulic fluid maximizes mechanical responsiveness and sensitivity at the device. Actuation driven by a syringe pump allows for highly-reproducible, controllable stimulation regimens with minimal user effort.

As a consistent means to generate and mechanically stimulate tissues, the device is an enabling platform that promises to disrupt pharmacological research and development for muscle diseases. Providing a functionally-accurate *in vitro* model of mature human skeletal muscle eliminates the need for a (less accurate) live animal model during drug approval screening. A high-throughput design allows drug screening using a large number of tissues at once, minimizing time for drug screening and improving the ease with which drug effects can be directly observed. The 96-well format also leaves open the possibility of compartmentalization, so that different drugs may possibly be tested in the same device at any one time.

The device offers a higher functionality than similar devices on the market that mechanically stimulate *in vitro* skeletal muscle tissue. A simple, lean design minimizes manufacturing and operating

costs relative to other devices. The device's similarity to 96-well plates, which are common and familiar to pharmacological laboratories, makes general device operation intuitive. This design familiarity also minimizes the adaptations necessary for existing manufacturers of 96-well plates to manufacture the device.

9.2 Recommendations

Due to the limitations of the design stated in Section 5.7 and problems seen during the testing process, there are eight main recommendations the team suggests for future improvements of this design.

Recommendations for Tissue Development:

- Perform more stimulation experiments and statistically validate results

- Optimize tissue exercise regime

- Adapt to engineered tissue by cell self-assembly

- Optimize media composition

Recommendations for Device Construction and Future Components:

- Replace MED610

- Replace post to PDMS

- Use more rigid tubing to reduce error

- Incorporate electrical stimulation component

Based from the results in this project in terms of stimulated tissue growth, the device shows great promise towards the overall goal. However, due to time constraints not as many tests were able to be performed to statistically prove the device produces consistent results. The team suggests performing more testing with the device to produce more data that supports the device function. The teams experiments show the device can produce skeletal muscle tissue with higher fiber alignment and

greater fiber density by mechanical stimulation. The goal of this recommendation is to statistically prove consistent device function.

The second recommendation for tissue development is to optimize the exercise regime of the developing tissues to produce the best tissue models. In literature, many researchers have found their own optimal strain amount, strain rate, and frequency. However, those optimal numbers pertain to their specific methods of mechanical stimulation. The goal of this suggestion is to perform many experiments with different strain magnitudes, rates, and frequency and compare results to find which combination proves the best model of in vivo tissue or best models of various muscular disease or atrophy. This information can later be used by pharmaceutical companies when screening drugs.

The third recommendation for tissue development is to adapt the cell seeding protocol for engineered tissue to a cell self-assembly method. Currently, a fibrinogen/thrombin gel method is used in the cell seeding processes to create an exogenous ECM. Self-assembly of engineered tissue is a method to grow tissue that better mimics *in vivo* development. The cells produce their own ECM and develop contiguous tissue around anchorage points mimicking native skeletal muscle tissue attachment to bone. Also, there is a much greater fiber density in the self-assembly method. This would be a better model of in vivo tissue.

The fourth recommendation is to optimize media composition during tissue development. By improving media composition tissue maturation, hypertrophy, and fiber size can improve. These all lead to more accurate models of *in vivo* human skeletal muscle tissue.

The fifth recommendation is to replace the prototyping material (MED610) with another more durable material that can be used for cell culture. MED610 is a resin-plastic used in the Objet260 3D printer and is what the team had available to manufacture the device. This is a known biocompatible dental material. However, after 5 autoclave cycles the plastic became porous, deformed in shaped, and began to leach more and more particles into the media. Deformation only occurred in the device where

wall thickness was 1 mm. Along with changing the material of the device, it is suggested to increase wall thickness to a minimum of 2 mm. Suggested materials include titanium, polystyrene (not autoclave-able, but makes the device cheap and disposable), polycarbonate, or polypropylene. Each material has pros and cons.

The sixth recommendation is to replace the devices rigid post with flexible PDMS plastic post. Currently the device is a strain only device. With flexible PDMS post the ability to measure force applied to the tissue becomes possible by measuring the deflection in the post. The material properties of PDMS are well defined. Using the relationships between deformation and force of PDMS and measuring the angle at which the post deforms during stimulation or culturing, force can be calculated. Having PDMS post instead of rigid post allows for the measurement of force in the device, information important to know in order to match in vivo parameters.

The seventh recommendation is to use more rigid tubing in the syringe pump system to improve accuracy. As discussed in section 7.1, the tubing is a large contributor to the error in device straining of tissues. As pressure increases or decreases the tube expands or contracts, altering the volume change that directly corresponds to percent strain of the tissues. More rigid tubing would prevent this variance and make the straining processes more controlled improving accuracy.

The final recommendation is to add the electrical stimulation component to this existing device. Due to time and budget constraints the electrical components were not looked into further than potential designs. The electrical stimulation component is a key part in mimicking tetanic signaling in vitro. All these recommendations will lead to a better in vitro model of in vivo skeletal muscle tissue.

References:

"Amyotrophic Lateral Sclerosis (ALS) Fact Sheet." *National Institute of Neurological Disorders and Stroke*. NINDS, June 2013. Web. 21 Sept. 2014.

Andersen, J. I., Juhl, M., Nielsen, T., Emmersen, J., Fink, T., Zachar, V., & Pennisi, C. P. (2014). Uniaxial cyclic strain enhances adipose-derived stem cell fusion with skeletal myocytes. Biochemical and biophysical research communications, 450(2), 1083-1088.

Bach, AD, JP Beier, J. SternStaeter, and RE Horch. (2004). "Skeletal Muscle Tissue Engineering." Journal of Cellular and Molecular Medicine 8 (4): 413-422.

Brian, W., Bursac, N. (2008). Tissue engineering of functional skeletal muscle: Challenges and recent advances. *IEEE Eng Med Biol Mag, 27*, 109-113.

Bock, R. "NIH study uncovers details of early stages in muscle formation and regeneration." *National Institute of Neurological Disorders and Stroke*. NINDS, May 2013. Web. 21 Sept. 2014.

Boldrin, L., Muntoni, F., & Morgan, J. E. (2010). Are human and mouse satellite cells really the same? *Journal of Histochemistry & Cytochemistry*, *58*(11), 941-955.

Buckingham, Margaret, Lola Bajard, Ted Chang, Philippe Daubas, Juliette Hadchouel, Sigolène Meilhac, Didier Montarras, Didier Rocancourt, and Frédéric Relaix. 2003. "The Formation of Skeletal Muscle: From Somite to Limb." Journal of Anatomy 202 (1): 59-68. doi:10.1046/j.1469-7580.2003.00139.x.

Burattini, S., Ferri, P., Battistelli, M., Curci, R., Luchetti, F., & Falcieri, E. (2009). C2C12 murine myoblasts as a model of skeletal muscle development: morpho-functional characterization. *European Journal of Histochemistry*, *48*(3), 223-234.

Burks, T.N., Cohn, R.D. "Role of TGF-β signaling in inherited and acquired myopathies" Skeletal Muscle. 2011. May 4; 1(1), 1-19.

Burns, E., Krier, K., Lebel, M., & Peppel, M. (2008). Skeletal muscle tissue engineering. Retrieved September 10, 2014, from <http://chen2820.pbworks.com/w/page/11951479/Skeletal muscle tissue engineering>

Campellone, Joseph V., and David Zieve. "Multiple Sclerosis." *Multiple Sclerosis*. U.S. National Library of Medicine, 25 Sept. 2013. Web. 21 Sept. 2014.

Campellone, Joseph V., MD, and David Zieve, MD. "Muscular Dystrophy: MedlinePlus Medical Encyclopedia." *U.S National Library of Medicine*. U.S. National Library of Medicine, 24 Feb. 2014. Web. 21 Sept. 2014. http://www.nlm.nih.gov/medlineplus/ency/article/001190.htm

Carosio, S., Barberi, L., Rizzuto, E., Nicoletti, C., Del Prete, Z., & Musarò, A. (2013). Generation of ex vivo-vascularized muscle engineered tissue (X-MET).*Scientific reports*, *3*.

Chakravarthy, M. V., Abraha, T. W., Schwartz, R. J., Fiorotto, M. L., & Booth, F. W. (2000). Insulin-like Growth Factor-I Extends in VitroReplicative Life Span of Skeletal Muscle Satellite Cells by Enhancing

G1/S Cell Cycle Progression via the Activation of Phosphatidylinositol 3'-Kinase/Akt Signaling Pathway. *Journal of Biological Chemistry*, *275*(46), 35942-35952.

Christ, G. (2013). *U.S. Patent No. 20130197640.* Washington, DC: U.S.

"Data & Statistics." *Centers for Disease Control and Prevention*. Centers for Disease Control and Prevention, 18 Sept. 2014. Web.

Dennis, R. (2001). *U.S. Patent No. 6114164.* Washington, DC: U.S.

Dennis, R. G., & Kosnik II, P. E. (2000). Excitability and isometric contractile properties of mammalian skeletal muscle constructs engineered in vitro. *In Vitro Cellular & Developmental Biology-Animal*, *36*(5), 327-335.

Eagle, M., Baudouin, S. V., Chandler, C., Giddings, D. R., Bullock, R., & Bushby, K. (2002). Survival in Duchenne muscular dystrophy: improvements in life expectancy since 1967 and the impact of home nocturnal ventilation. *Neuromuscular Disorders*, *12*(10), 926-929.

Emery, Alan E. M. *Muscular Dystrophy: The Facts.* Oxford: Oxford University Press, 1994. Web.

Generation of ex vivo-vascularized muscle engineered tissue (X-MET).*Scientific reports*, *3*.

Gilbert SF. Developmental Biology. 6th edition. Sunderland (MA): Sinauer Associates; 2000. Myogenesis: The Development of Muscle. Available from: http://www.ncbi.nlm.nih.gov/books/NBK10006/

Gilles AR, Lieber RL. Structure and function of the skeletal muscle extracellular matrix. *Muscle Nerve.* 2011;44:318-331.

Goudenege, S., Pisani, D. F., Wdziekonski, B., Di Santo, J. P., Bagnis, C., Dani, C., & Dechesne, C. A. (2009). Enhancement of Myogenic and Muscle Repair Capacities of Human Adipose–derived Stem Cells With Forced Expression of MyoD. *Molecular Therapy*, *17*(6), 1064-1072.

Grabowska, I., Szeliga, A., Moraczewski, J., Czaplicka, I., & Brzóska, E. (2011). Comparison of satellite cell-derived myoblasts and C2C12 differentiation in two-and three-dimensional cultures: changes in adhesion protein expression.*Cell biology international*, *35*(2), 125-133.

Grefte, S., A. M. Kuijpers-Jagtman, R. Torensma, and J. W. Von den Hoff. 2007. "Skeletal Muscle Development and Regeneration." Stem Cells and Development 16 (5): 857-868. doi:10.1089/scd.2007.0058.

Guilak et al. (2003). Functional Tissue Engineering. Springer-Verlag New York, Inc.

Gwyther, T., Hu, J., Billiar, K., Rolle, M. (2011). Directed cellular self-assembly to fabricate cell-derived tissue rings for biomechanical analysis and tissue engineering. *Journal of Visualized Experiments, 57*, 3366.

Herman, I. M., Crisona, N. J., & Pollard, T. D. (1981). Relation between cell activity and the distribution of cytoplasmic actin and myosin. *The Journal of cell biology*, *90*(1), 84-91.

Kosnik, P. E., Faulkner, J. A., & Dennis, R. G. (2001). Functional development of engineered skeletal muscle from adult and neonatal rats. *Tissue engineering*,*7*(5), 573-584.

Laterreur, V., Ruel, J., Auger, F. A., Vallières, K., Tremblay, C., Lacroix, D., ... & Germain, L. (2014). Comparison of the direct burst pressure and the ring tensile test methods for mechanical characterization of tissue-engineered vascular substitutes. Journal of the mechanical behavior of biomedical materials, 34, 253-263.

Lewis, M. R. (1915). Rhythmical contraction of the skeletal muscle tissue observed in tissue cultures. *Am. J. Physiol*, *38*, 153-161.

Li, M., Dickinson, C. E., Finkelstein, E. B., Neville, C. M., & Sundback, C. A. (2011). The role of fibroblasts in self-assembled skeletal muscle. *Tissue Engineering Part A*, *17*(21-22), 2641-2650.

MacArthur BD, Oreffo RO. 2005. "Bridging the Gap." Nature (433).

Martin-Piedra, M., Garzon, I., Oliveira, A., Alfonso-Rodriguez, C., Sanchez-Quevedo, M., Campos, A., Alaminos, M. (2013). Average cell viability levels of human dental pulp stem cells: an accurate combinational index for quality control in tissue engineering. *Cryotherapy, 15,* 507-518.

"Myasthenia Gravis Fact Sheet," NINDS. Published September 2010. NIH Publication No. 10-768. Web.

Okano T. & Matsuda T. (1998) Tissue engineered skeletal muscle: preparation of highly dense, highly oriented hybrid muscular tissues. Cell Transplant 7, 71–82

Perniconi, B., & Coletti, D. (2014). Skeletal muscle tissue engineering: best bet or black beast?. *Frontiers in physiology*, *5*.

Powell, C., Smiley, B., Mills, J., Vandenburgh, H. (2002). Mechanical stimulation improves tissue-engineered human skeletal muscle. *American Journal of Physiology-Cell Physiology, 283,* 1557-1565.

Radisic, M. (2005). *U.S. Patent No. 20050112759.* Washington, DC: U.S.

Roberts, R. G. (2001). Dystrophins and dystrobrevins. *Genome Biol*, *2*(4), 1-7.

Sabourin, L. A., Girgis-Gabardo, A., Seale, P., Asakura, A., & Rudnicki, M. A. (1999). Reduced differentiation potential of primary MyoD−/− myogenic cells derived from adult skeletal muscle. *The Journal of cell biology*, *144*(4), 631-643.

Saks, V. A., Veksler, V. I., Kuznetsov, A. V., Kay, L., Sikk, P., Tiivel, T., ... & Kunz, W. S. (1998). Permeabilized cell and skinned fiber techniques in studies of mitochondrial function in vivo. In *Bioenergetics of the Cell: Quantitative Aspects* (pp. 81-100). Springer US.

Shansky J., Del Tatto M., Chromiak J. & Vandenburgh H. (1997) A simplified method for tissue engineering skeletal muscle organoids in vitro. In Vitro Cell Dev. Biol. Anim 33, 659–661.

Shier, David, Jackie Butler, and RickiLewis.Hole's Essentials of Human Anatomy & Physiology. Boston: McGraw-Hill Higher Education, 2009. Print.

Smith, C., Kruger, M. J., Smith, R. M., & Myburgh, K. H. (2008). The inflammatory response to skeletal muscle injury. *Sports medicine*, *38*(11), 947-969.

Silverthorn, D.U. (2010). *Human Physiology: An Integrated Approach.* Pearson. p. 398. ISBN 978-0-321-55980-7.

St. John, Tina M. "Degenerative Muscle Disease Symptoms." *LIVESTRONG.com*. August 17, 2013. Web.

Strober, W. (2001). Trypan blue exclusion test of cell viability. *Current protocols in immunology*, A-3B.

Strohman RC, Bayne E, Spector D, Obinata T, Micou-Eastwood J, and Maniotis A (1990). Myogenesis and histogenesis of skeletal muscle on flexible membranes in vitro. *In Vitro Cell Dev Biol* **26**: 201–208.

Totten, G. E. (2011). *Handbook of hydraulic fluid technology*. CRC Press.

Van Wachem P. B., van Luyn M. J. & da Costa M. L. (1996). Myoblast seeding in a collagen matrix evaluated in vitro. J. Biomed. Mater. Res. 30, 353–360.

Vandenburgh, H., Shansky, J., Benesch-Lee, F., Skelly, K., Spinazzola, J. M., Saponjian, Y., & Tseng, B. S. (2009). Automated drug screening with contractile muscle tissue engineered from dystrophic myoblasts. *The FASEB Journal*, *23*(10), 3325-3334.

Vandenburgh, H., Shansky, J., Benesch-Lee, F., Barbata, V., Reid, J., Thorrez, L., ... & Crawford, G. (2008). Drug-screening platform based on the contractility of tissue-engineered muscle. *Muscle & nerve*, *37*(4), 438-447.

Vandenburgh, H. (1992). *U.S. Patent No. 5153136.*Washington, DC: U.S.

Vandenburgh H. *et al (1996).* Tissue-engineered skeletal muscle organoids for reversible gene therapy.Hum. Gene Ther. 7, 2195–2200.

Vandenburgh, H. H., Hatfaludy, S., Karlisch, P., & Shansky, J. (1991). Mechanically induced alterations in cultured skeletal muscle growth. Journal of biomechanics, 24, 91-99.

Vandenburgh, H. H., Karlisch, P., & Farr, L. (1988). Maintenance of highly contractile tissue-cultured avian skeletal myotubes in collagen gel. *In vitro cellular & developmental biology*, *24*(3), 166-174.

von der Mark, H., Dürr, J., Sonnenberg, A., von der Mark, K., Deutzmann, R., & Goodman, S. L. (1991). Skeletal myoblasts utilize a novel beta 1-series integrin and not alpha 6 beta 1 for binding to the E8 and T8 fragments of laminin. *Journal of Biological Chemistry*, *266*(35), 23593-23601.

WPI Academic Resource and Computing. (2013). Rapid prototyping guidelines. Web.

Zhao, Y. (2009). Investigating electrical field-affected skeletal myogenesis using a microfabricated electrode array. Sensors and Actuators A: Physical, 154(2), 281-287.

McKeehen, J. N., Novotny, S. A., Baltgalvis, K. A., Call, J. A., Nuckley, D. J., & Lowe, D. A. (2013). Adaptations of mouse skeletal muscle to low intensity vibration training. *Medicine and science in sports and exercise*, *45*(6), 1051.

Jenkyn, T. R., Ehman, R. L., & An, K. N. (2003). Noninvasive muscle tension measurement using the novel technique of magnetic resonance elastography (MRE). *Journal of biomechanics*, *36*(12), 1917-1921.

Blottner, D., Salanova, M., Püttmann, B., Schiffl, G., Felsenberg, D., Buehring, B., & Rittweger, J. (2006). Human skeletal muscle structure and function preserved by vibration muscle exercise following 55 days of bed rest. *European journal of applied physiology*, *97*(3), 261-271.

Humphries, B., Warman, G., Purton, J., Doyle, T. L., & Dugan, E. (2004). The influence of vibration on muscle activation and rate of force development during maximal isometric contractions. *Journal of sports science & medicine*, *3*(1), 16.

Bosco, C., Colli, R., Introini, E., Cardinale, M., Tsarpela, O., Madella, A., ... & Viru, A. (1999). Adaptive respsonses of human skeletal muscle to vibration exposure. *CLINICAL PHYSIOLOGY-OXFORD-*, *19*, 183-187.

Bosco, C., Cardinale, M., & Tsarpela, O. (1998). Influence of vibration on mechanical power and electromyogram activity in human arm flexor muscles. *European journal of applied physiology and occupational physiology*, *79*(4), 306-311.

Roberts, D. (2012). The Limits of Vibration Frequency for Miniature Vibration Motors. *Precision MicroDrives. Web.*

Levenberg, S., J. Rouwkema, M. Macdonald, E.S. Garfein, D.S. Kohane, D.C. Darland, R. Marini, C.A. van Blitterswijk, R.C. Mulligan, P.A. D'Amore, R. Langer R: Engineering vascularized skeletal muscle tissue. Nat Biotechnol, 23, 879-84 (2005)

Scime, A., Caron, A. Z., & Grenier, G. (2009). Advances in myogenic cell transplantation and skeletal muscle tissue engineering. *Front Biosci*, *14*, 3012-3023.

Ross, J. J., & Tranquillo, R. T. (2003). ECM gene expression correlates with in vitro tissue growth and development in fibrin gel remodeled by neonatal smooth muscle cells. *Matrix biology*, *22*(6), 477-490.

Huang, Y. C., Dennis, R. G., Larkin, L., & Baar, K. (2005). Rapid formation of functional muscle in vitro using fibrin gels. *Journal of Applied Physiology*, *98*(2), 706-713.

Coleman, M. E., DeMayo, F., Yin, K. C., Lee, H. M., Geske, R., Montgomery, C., & Schwartz, R. J. (1995). Myogenic vector expression of insulin-like growth factor I stimulates muscle cell differentiation and myofiber hypertrophy in transgenic mice. *Journal of Biological Chemistry*, *270*(20), 12109-12116.

Lian, S., Xiao, Y., Bian, Q., Xia, Y., Guo, C., Wang, S., & Lang, M. (2012). Injectable hydrogel as stem cell scaffolds from the thermosensitive terpolymer of NIPAAm/AAc/HEMAPCL. *International journal of nanomedicine*, *7*, 4893.

Appendix

Preliminary Experiment: Electric and Vibratory Stimuli

This experiment compared the effects of vibratory and electrical probe stimulation with a control of non-stimulated cells. The goal was to determine if the probe stimulation method contaminated the constructs or if the vibration method deteriorates the tissue constructs. The experiment was performed on C2C12 ring constructs seeded at a rate of 400,000 cells per 55 µL. The tissues were given 2 days to form in an agarose mold before commencement of stimulation. The different experimental groups were separated into different culture plates where each group had 4 C2C12 ring tissue constructs. From days 3-5, the rings were stimulated once a day using the following regiments:

Vibration Stimulation:

The coin type vibration motor was selected for its size and variable speeds. The motor itself, shown in Figure 70, was advertised on Amazon.com as a "Vibrating Motor for Cell Phone Toys". The DC micro-coin motor has the following specifications:

Voltage	DC 3V
Rated Current	0.09A
Speed	12000 RPM
Speed Tolerance	Â±2500 RPM
Body Size	10 x 3.6 mm/0.39 in x 0.14 in (D*T)
Cable Length	10 mm / 0.39 in
Weight	5g

Figure 70: DC Micro Coin Type Vibrating Motor for Cell Phone Toys

According to Roberts (2012), for DC vibration motors, vibration frequency is given by:

$$f\ (Hz) = \frac{Motor\ Speed\ (RPM)}{60}$$

The frequency of the vibration motor is listed by the manufacturer as 12000 RPM, with an error margin of 2500 RPM. Therefore the frequency for the motor is defined by:

$$\frac{(12000 \pm 2500)\ RPM}{60} = 200 \pm 42\ Hz$$

From the literature review, there have been tested vibration experiments using frequencies between 100-200 Hz (Bosco et al, 1998). Therefore, by running the vibration experiments at a lower voltage, the frequency will be decreased into the range tested in the Bosco study. Voltage is linearly proportional to vibration frequency (Roberts, 2012), so at 2V, the voltage the team used for the preliminary tests:

$$\frac{2V}{3V} = \frac{f}{200 \pm 42\ Hz}$$

$$f = 133 \pm 28\ Hz$$

The Bosco regiment for stimulation was five repetitions of one full minute of vibration and one full minute of rest (Bosco et al, 1998). The coin type vibration motor was attached to a DC power supply

143

which ran 2 volts of power with 0.062 Amps. The coin motor was placed under the cell culture plate
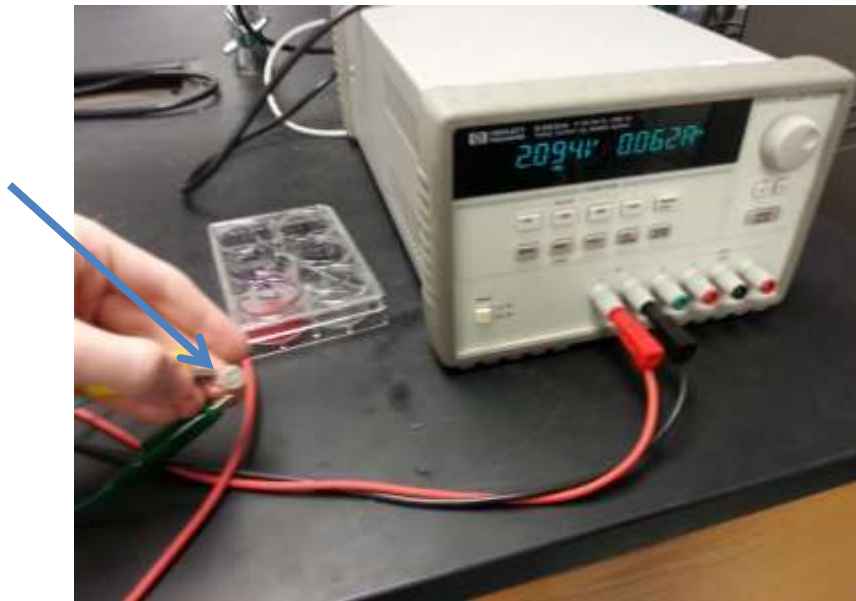
containing 4 formed tissues.

Figure 71: Setup for vibratory stimulation. Vibration motor indicated by blue arrow.

Electrodes

As stated in section 2.8.3, electrical stimulation is often used in tissue formation as a

supplementary means of ensuring tissue maturation. The electrical signal is a replacement for the

chemical (tetanic) nervous stimulation *in vivo* to perform contraction. To validate that electrical

stimulation does in fact improve tissue formation, an electrical stimulation method through use of

probes was used for experimentation on the tissue rings using a DC power source. This process was

carried out with a 4 mA current with 0.5 volts applied to the tissue for 10 minutes in duration. Each cycle

was 2 Hz, the probes being immersed in the media for one second, then the probes were removed from

the media for one second. The rings were then incubated for 24 hours before the process was repeated

twice more, daily.

Whenever the experimental tissue plates were removed from the incubator, the control plate

was as well so that the conditions of the tissues were as similar as possible. Unfortunately, the tissue

144

ring constructs did not form as predicted. As seen in the table below, the C2C12 cells remained flattened on the bottom of the well, rather than constricting together around the post. This seems to suggest a loss of myogenic potential and a lack of tissue formation. Therefore, the only conducive result is that the methods of stimulation (external vibration and electrical probe) were not cytotoxic, did not cause visible contamination, and were repeatable. The two of the control rings seemed to rupture, however, because they did not contract into a ball of tissue it appears as they the tissue was not fully formed/connected. Initially it appeared as though the vibration motor aided in creating ring formation that was better rounded; however, the lack of progression in ring development suggests that this only resulted in equally-dispersed cells rather than promote ring formation. Images of the rings after 5 days of formation and 3 days of stimulus are presented below:
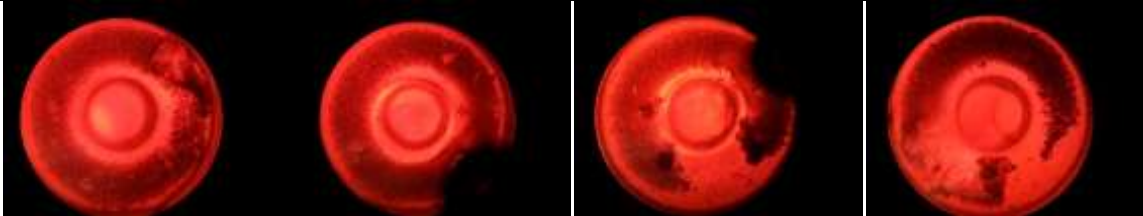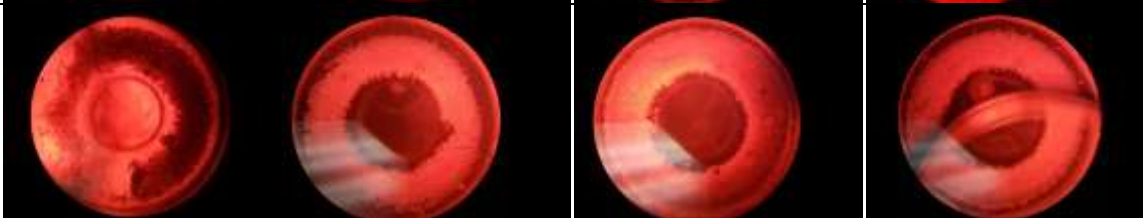
Group	5 Day old rings (24 h after last stimulus)
Control [1-4]	
Electric [1-4]	
Vibrate [1-4]	

Figure 72. Preliminary Electrical Stimulation Experiments